Stabilizing Renewable Power Generation System Incorporating Hybrid Energy Storage

Thesis

Submitted by

Pinaki Dhar

Doctor of Philosophy (Engineering)

Department of Power Engineering
Faculty Council of Engineering & Technology
Jadavpur University
Kolkata – 700032, India

2024

JADAVPUR UNIVERSITY
FACULTY OF ENGINEERING AND TECHNOLOGY

INDEX NO. : 35/18/E

1. Title of the Thesis:	Stabilizing Renewable Power Generation System Incorporating Hybrid Energy Storage
2. Name, Designation & Institution of the Supervisor:	Prof. Niladri Chakraborty Professor Department of Power Engineering Jadavpur University Salt Lake Campus, Block – LB, Plot – 8, Sector III, Salt Lake City Kolkata – 700106 West Bengal, India

3.List of Publications:

Pinaki Dhar, Niladri Chakraborty. "Optimal techno-economic analysis of a renewable based hybrid microgrid incorporating gravity energy storage system in Indian perspective using whale optimization algorithm." *International Transactions on Electrical Energy Systems* 31.9 (2021): e13025. DOI: **10.1002/2050-7038.13025**

Pinaki Dhar, Niladri Chakraborty. "A dual mode wind turbine operation with hybrid energy storage system for electricity generation at constant voltage in an islanded microgrid." *International Journal of Energy Research* 45.13 (2021): 18885-18902. DOI: **10.1002/er.6994**

Pinaki Dhar, Niladri Chakraborty. "Operation of two mechanically driven gravity energy storage systems using one wind turbine for uninterrupted energy supply in an isolated microgrid." *International Journal of Energy Research* 46.13 (2022): 18866-18878. DOI: **10.1002/er.8446**

4. List of Patents: NIL

5. List of Presentations in National/ International/ Conferences/ Workshops:

Pinaki Dhar, Niladri Chakraborty. "Standalone renewable based microgrid for rural areas of North East India with optional grid sales capability" (Published In Conference On *Emerging Trends In Energy And Electrical Systems – 2019*, Assam Engineering College Guwahati)

JADAVPUR UNIVERSITY

FACULTY OF ENGINEERING AND TECHNOLOGY

Statement of Originality

I, ***Shri Pinaki Dhar****, registered on* ***14th June, 2018*** *do hereby declare that this thesis entitled* ***"Stabilizing Renewable Power Generation System Incorporating Hybrid Energy Storage"*** *contains literature survey and original research work done by the undersigned candidate as part of his Doctoral studies.*

All information in this thesis have been obtained and presented according to the existing academic rules and ethical conduct. I declare that, as per the requirements of these rules and conduct, I have fully cited and referred all materials and results that are not original to this work.

I also declare that I have checked this thesis as per the "Policy on Anti Plagiarism, Jadavpur University, 2019", and the level of similarity as checked by iThenticate software is 4 *%.*

Signature of the Candidate:

Pinaki Dhar.

Pinaki Dhar
Date: 25/11/2025

Certified by Supervisor:
(Signature with date & seal)

25/11/25

Prof. Niladri Chakraborty
Professor
Dept. of Power Engineering,
Jadavpur University,
Salt Lake Campus,
Kolkata- 700106.
India

Prof. Niladri Chakraborty, DIC (Imperial), PhD(London)
Department of Power Engineering
Jadavpur University Salt Lake Campus
Kolkata - 700 106

JADAVPUR UNIVERSITY
FACULTY OF ENGINEERING AND TECHNOLOGY

Certificate from the Supervisor

This is to certify that the thesis entitled ***"Stabilizing Renewable Power Generation System Incorporating Hybrid Energy Storage"*** *submitted by* ***Shri Pinaki Dhar****, who got his name registered on 14th June, 2018 for the award of* ***Ph.D. (Engineering)*** *Degree of Jadavpur University is absolutely based upon his own work under the supervision of* ***Prof. Niladri Chakraborty****, Professor, Department of Power Engineering, Jadavpur University and that neither his thesis nor any part of the thesis has been submitted for any degree/diploma or any other academic award anywhere before.*

Signature of the Supervisor with date & seal

25/11/21

Prof. Niladri Chakraborty
Professor
Dept. of Power Engineering,
Jadavpur University, Salt Lake Campus,
Kolkata- 700106, India

Prof. Niladri Chakraborty, DIC (Imperial), PhD(London)
Department of Power Engineering
Jadavpur University Salt Lake Campus
Kolkata - 700 106

DEDICATED

TO

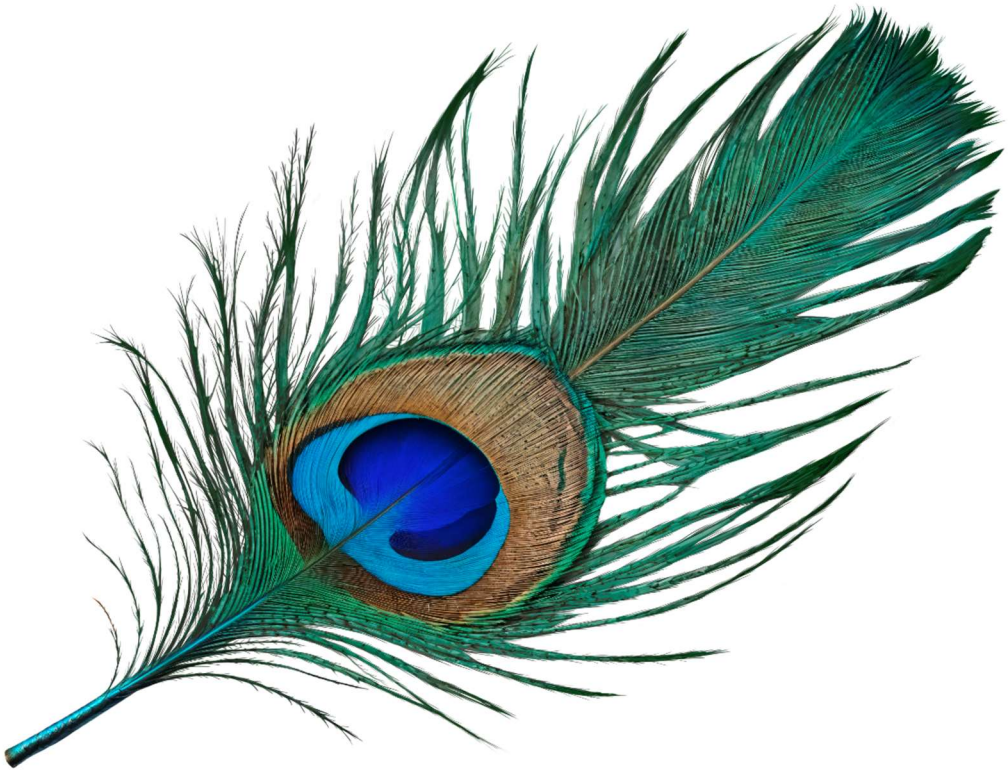

ACKNOWLEDGEMENT

I would like to express my sincere gratitude to Council of Scientific & Industrial Research (CSIR), Government of India, for funding me as Senior Research Fellow (SRF – Direct).

I am and shall always remain indebted to Almighty God for helping me develop the thought process required to design both the novel Dual Mode Wind Turbine System and Wind Turbine Driven Dual Gravity Energy Storage System.

Though the world has suffered a lot from COVID-19 and I have also lost some of my beloved ones but I must acknowledge the presence of lockdown period in my life that helped me to work for almost day and night, with full concentration, being detached from the regular dramas and hurdles of both personal and professional life.

I am thankful to Ms. Alexandra Elbakyan for her website Sci-Hub that provided free scientific literatures at the time of lockdown. Without this support it won't be possible for me to utilise that depressing phase so fruitfully.

I am thankful to my supervisor Prof. Niladri Chakraborty for providing all the facilities required during this journey.

I am immensely indebted to Prof. Amitava Datta and Prof. Ranjan Ganguly for their invaluable indirect input towards my learning process.

I would also like to express immense gratitude to my beloved wife, Ms. Mayurakshi Mondal, who inculcated within me the longing of doing PhD since our Graduation days and always stand by me in the thick and thin of life.

I am also very thankful to my father-in-law Mr. Dhiraj Mondal, who has always encouraged me to complete my PhD work and carry on my research work.

Last but not the least I would like to thank all those persons in my life who had tried to pull me down throughout this journey. Their negative behaviours had always developed more and more positive attitude in me.

I am also thankful to my parents and lab mates.

Pinaki Dhar 25/11/2025

Pinaki Dhar

Department of Power Engineering
Jadavpur University, Salt Lake Campus
Sector –III, Block –LB, Kolkata –700 106
25th November, ~~2024~~ 2025

ABSTRACT

The increase in pollution and decrease in fossil fuel reserve leads us to a conclusion of replacing thermal energy with steady and continuous renewable / non-conventional energy. The researches presented in this thesis aim to contribute to the advancement of sustainable energy solutions and promote the adoption of green technologies in the field of microgrid systems, completely eliminating the presence of fossil fuel in terms of eliminating diesel generator, as a backup storage.

The novelties implemented in the flow of research firstly, lie in the innovative design modifications made to a wind turbine system. The wind turbine has been adapted to alternately charge one Pumped Storage Hydro (PSH) system and one Gravity Energy Storage System (GESS). This modification ensures a continuous and stable supply of renewable-based electricity, by utilizing both storage systems effectively. Secondly, the wind turbine has been further enhanced to simultaneously charge and discharge two GESSs. This feature enables uninterrupted renewable-based electricity supply with lower land requirement. This design modification is crucial for ensuring a reliable and consistent power supply from renewable sources to the places with land scarcity and unable to establish a PSH. Lastly, a system design has been developed to ensure continuous operation of the wind turbine system. This includes the integration of various components to optimize the performance and efficiency of the system, ultimately leading to a reliable and sustainable source of electricity along with its LCOE (Levelized cost of energy), that is at par with the domestic unit electricity price of the place, established by the state government.

Overall, the novelties of this work showcase the potential for enhancing the capabilities of wind turbine systems to provide continuous and stable renewable-based electricity supply. These advancements have the potential to significantly contribute to the transition towards a more sustainable energy future.

LIST OF ABBREVIATIONS

ABBRIVIATIONS	FULL FORM
α	Temperature coefficient of solar modules
β	Coefficient vector
γ	Coefficient vector
μ_p	Power co-efficient of WT
ρ_{air}	Air Density
$\rho_{material}$	Density of Material
ρ^{SW}	Density of Suspended Weight of GESS
ρ_{water}	Density of Water
ρ_W	Density of the material
ρ_{wire}	Density of the material of rope
η_{Alt}	Efficiency of Alternator
η_{BG}	Efficiency of Biomass Generator
η_{Gear}^{Ch}	Gear efficiency
η_{VRFB}^{ch}	Charging efficiency of VRFB
η_{CP}	Efficiency of CP
η_{VRFB}^{dch}	Discharging efficiency of VRFB
η_{Gear}^{dch}	Efficiency of gear assembly
η_{DC-inv}	Efficiency of DC motor – inverter assembly
η^{GESS}	Roundtrip Efficiency of GESS
η_{Li-ion}^{ch}	Charging Efficiency of Lithium-ion battery
η_{Li-ion}^{dch}	Discharging Efficiency of Lithium-ion battery
η_{Gen}	Efficiency of WT generator
η_T	Efficiency of the Transmission System
η_{Trans}	Efficiency of the Transmission System

η_{WT}	Efficiency of WT
η_{wt}	Efficiency of Water Turbine
η_{WTG}	Efficiency of Water Turbine
$\overline{\sigma}_{W}$	Tensile Strength of rope
$\overline{\sigma}_{wire}$	Tensile Strength of rope
ω	Angular Velocity
ω_{R}	Motor speed during regenerative braking
ω_{R}^{0}	No-load speed of the motor
a	Acceleration
$\overline{a}$	Maximum Acceleration
$\overline{A}$	Maximum Acceleration
A_{UR}	The Area of UR
A_{W}	The minimum cross-sectional area of the rope
A_{Wire}	Cross-sectional area of the rope
b	A constant to provide the spiral shape
BMG	Biomass Generator
$C_{Biomass\_fuel}^{Annual}$	Annual fuel cost of Biomass generator
$C_{Capital}^{Annual}$	Annualized Capital Cost
$C_{O\&M}^{Annual}$	Annual operation and maintenance cost of equipment
$C_{Capital}^{Biomass}$	Installation Cost of Biomass Generator
$C_{Fuel}^{Biomass}$	Cost of per kg of Biomass
$C_{Per\_KW}^{Biomass}$	Installed Capacity of Biomass Generator
C_{BM}	Calorific value of Biomass
$C_{O\&M}^{Biomass}$	Annual O&M cost per kW of Biomass generator
$C_{O\&M}^{inv}$	Annual O&M cost per kW of inverter
$C_{Capital}^{Solar}$	Capital Cost of solar PV
$C_{O\&M}^{Solar}$	Annual O&M cost per kW of solar PV
$C_{Per\_KW}^{Solar}$	Cost of solar panel, inverter and allied services per kW

CP	Centrifugal Pump
CRF	Capacity Utilization Factor
DD	Direct drive
DFIG	Doubly fed induction generator
D^{GESS}	Usable depth of the GESS
$D_{Released}^{GESS}$	Weight released from the height
D_{GESS}^{Max}	Maximum usable depth of the GESS
d^{SW}	Diameter of Suspended Weight of GESS
D^{T}	Depth of Vertical Tunnel
D_{VT}	Vertical tunnel depth of the GESS
DWMT	Dual mode wind turbine
$E_{Biomass}^{Annual}$	Annual Energy Production per kW from Biomass generator
E^{GESS}	Energy Storage Capacity of GESS
E_{GESS}^{Gen}	Energy generated by GESS at any interval
$E_{GESS}^{Gen\ Max}$	Possible maximum energy generation from a GESS
E_{GESS}^{max}	Maximum Energy Storage Capacity of GESS
ER	Rotating mechanical part, connecting mechanical transmission system with alternator
E_R	Emf of the motor during regenerative braking
E_{Li-ion}^{rated}	Rated energy of the Li-ion battery
E_{VRFB}^{rated}	Rated energy storage of the VRFB
ESD	Energy Storage Device
F 1	Fixed mechanical connection with brush between ‘M 1’ and ‘M 2’
F 2	Fixed mechanical connection with brush between ‘M 3’ and ‘M 4’
F^{M}	Force required to pull the Suspended Weight against Gravity
F_{MC}	Force supplied by the mode changer
F_{MCS}	Force required to expand the spring
g	Gravitational Acceleration
H^{SW}	Height of Suspended Weight of GESS

GaAs	Gallium Arsenide
GESS	Gravity Energy Storage System
G_i^H	hourly solar irradiance at 'i^{th}' hour
G^{NOCT}	Solar Irradiance at NOCT
GoI	Government of India
G^{STC}	Solar Irradiance at STC
H_{BG}	Maximum Operation Time of a Biomass Generator in a day
H_{CSW}	Perpendicular length of cylindrical suspended weight of a GESS
HOMER	Hybrid Optimization of Multiple Energy Resources
H_{UR}^n	Water level at UR at the starting of any interval $'n'$
H_{UR}^{n-1}	Water level at the starting of $'n-1'$ interval
H_{UR}^{Rated}	Rated height of UR
H_{MH}^{Rated}	Rated height from where water gets released
H_{UR}^{Max}	Maximum height of UR
I_A	Armature current
IEA	International Energy Agency
IEX	Indian Energy Exchange
INDC	Intended Nationally Determined Contribution
I-PMS	Improved power management strategy
I_R	Current during regenerative braking
J	Rotational Inertia of Motor associated with GESS
k	Spring Constant
K_m	Motor torque constant
l	A random number in [-1,1]
LCOE	Levelized cost of energy
L_{MCS}	Length of Spring
LR	Lower Reservoir
L_S	Length of Spring

L_W	Length of Rope
L_{wire}	Length of Rope
M 1	Charging side rotating mechanical connection between WT mechanical transmission and GESS 1
M 2	Charging side rotating mechanical connection between WT mechanical transmission and GESS 2
M 3	Generating side rotating mechanical connection between GESS 1 and DC motor
M 4	Generating side rotating mechanical connection between GESS 2 and DC motor
M_{BM}	Tons of Biomass available per year in the study area
M_C	Mass of the charging side assembly including mass of gears etc.
MCA	Mode Changer Assembly
MCE	Mode changer electromagnet and magnetic material strip
MCS	Mode changer spring with hook
MCW 1	Mode changer weight (suspended) above 'M 2'
MCW 2	Mode changer weight (suspended) above 'M 4'
M_{CSW}	Mass of cylindrical suspended weight of a GESS
M_G	Mass of the generating side assembly including mass of gears etc.
MLUCA	Multi-objective line-up competition algorithm
M_{MCW}	Mass of Suspended Weight
MNRE	Ministry of New and Renewable Energy
MR	Rotating mechanical part, connecting mechanical transmission system with CP
M^{SW}	Mass of Suspended Weight of GESS
M_W	Mass of the rope
M_{wire}	Mass of the rope
NOCT	Nominal Operating Cell Temperature
N_{PV}^{P}	Number of solar panels in Parallel
N_{PV}^{S}	Number of solar panels in Series
N_{Panel}^{Solar}	Total number of installed solar panel
p	Probability

P_{Gen}^{air}	Generator Output from WT
$P^{Biomass}$	Installed Capacity of Biomass Generator
$P_{Installed}^{Biomass}$	Installed Capacity of Biomass Generator
P_{DMWT}^{Elec}	Electrical Power output from DMWT
P_{PSH}^{Gen}	Generated output of PSH
P_{BG}^{H}	Hourly generation from Biomass Generator
P_{S}^{H}	Power Output of Solar PV at maximum power point
P_{Li-ion}^{i}	Dispatched Power in 'i^{th}' interval
P_{CP}^{in}	Input power of CP
P_{GESS}^{in}	Input mechanical power to GESS
$P_{Installed}^{inv}$	Installed Capacity of Inverter
P_{BG}^{max}	Maximum installation capacity of Biomass Generator
P_{VRFB}^{n}	Dispatched power of VRFB in $'n^{th}{}'$ interval
P_{T}^{O}	Output Power produced from the Transmission System
P_{Trans}^{O}	The output produced from the mechanical transmission system
P_{O}	Output Power
P-PSH	Piston-based PSH
P_{R}	Power generated from DC motor during regenerative braking
PSH	Pumped Storage Hydroelectric
P_{DMWT}^{Shaft}	Generated mechanical power at the shaft of DMWT
$P_{Installed}^{Solar}$	Installed Capacity of Solar PV
$P_{m}{}^{SS}$	Steady State Power of Motor associated with GESS
P_{WT}^{Shaft}	Generated power at the shaft of the WT
P_{STC}^{Solar}	Solar panel output at STC
P_{S}^{STC}	power generated from single solar panel at STC
PV	Photovoltaic
PWM	Pulse Width Modulation
P_{Output}^{WTG}	WT Generator Output

Q_{PSH}^{dis}	The volume of water discharged into UR
$Q_{PSH}^{dis^n}$	Water discharge into UR at $'n'$ interval
$Q_{PSH}^{dis^{n-1}}$	Water discharge into UR at $'n-1'$ interval
$Q_{PSH}^{overflow}$	Water overflown from UR
$Q_{PSH}^{release}$	Flow Rate of water that gets released from a height
$Q_{PSH}^{release^n}$	Water released from the UR for power generation through turbine-generator at $'n'$ interval
$Q_{PSH}^{release^{n-1}}$	Water released from the UR for power generation through turbine-generator at $'n-1'$ interval
R_a	Rotor armature resistance
R_{CSW}	Radius of cylindrical suspended weight of a GESS
R_{DMWT}	The rotor radius of the DMWT
R_{Load}	Resistive Load
R_s	Traction Sheave of Motor associated with GESS
R_{WT}	Rotor Radius of WT
Si	Silicon
SOC	State-of-Charge of Battery
SOC_{ch}^{i}	Charging SOC at 'i^{th}' interval
SOC_{dch}^{i}	Discharging SOC at 'i^{th}' interval
SOC_{ch}^{n}	Charging SOC at 'n^{th}' interval
SOC_{dch}^{n}	Discharging SOC at 'n^{th}' interval
$SOC^{(n-1)}$	SOC of Battery at '$(n - 1)^{th}$' interval
SP 1	Mode changer spring with brush connected to 'M 1'
SP 2	Mode changer spring with brush connected to 'M 3'
STC	Standard Test Conditions
T	Duration of the Time Period
T_B	Braking torque
T_c	Cell temperature of Solar Module
T^m	Torque of Motor associated with GESS
T_a^{NOCT}	Ambient Air Temperature at NOCT

T_c^{STC}	Nominal cell temperature at STC
TSR	Tip Speed Ratio of WT
UR	Upper Reservoir
v	Velocity
V_{air}	Wind Speed
V_{air}^{cin}	Cut in speed of WT
V_{Air}^{c-in}	Cut in speed of WT
V_{air}^{cout}	Cut out speed of WT
V_{Air}^{c-out}	Cut out speed of WT
V_{CSW}	Volume of cylindrical suspended weight of a GESS
V_o	Output Voltage
V_t	Terminal Voltage of the motor
VRFB	Vanadium Redox Flow Battery
V^{SW}	Volume of Suspended Weight of GESS
w	Random number
$W_{Fuel}^{Biomass}$	Weight of Biomass required to generate each kW of energy
WEO	World Energy Outlook
WOA	Whale Optimization Algorithm
WT	wind turbine
Y_B	Location vector
Y_C	Current position vector
Y_{rand}	Randomly selected position vector

Table of Contents

LIST OF FIGURES

LIST OF TABLES

CHAPTER 1

1. Introduction

The concept of complete replacement of conventional power generating system lies on the stabilization of renewable-based power generation. Worldwide scenario of power generation is mainly dependent upon fossil fuel, which is close to its extinction. World Energy Outlook (WEO) 2018 of International Energy Agency (IEA) estimates an increment of global primary energy demand by 25% within 2017 to 2040, whereas in case of India the demand is projected to be more than double [1]. Global demand of electricity is most likely to increase by 60% in between 2017 to 2040, whereas for the developing countries the number is predicted to be nearly 90% [1]. According to a report of IEA, India is expected to have a yearly energy consumption growth rate of 5% to support the anticipated economic growth rate over 8% through 2023 [2]. This depicts a growth rate of less than 4% of coal-based power generation [2]. Although the coal-based power generating growth rate is envisioned to decrease from the 6% rate of the last decade [2] due to renewable penetration, but a lot more renewable-based power generation is required to at least stop the increment in coal-based power generation. Apart from extinction, fossil fuel-based electricity generation leaves the footprint of carbon as byproduct, which is the root cause of global warming. To address this global warming issue, Indian Government has made an international commitment – INDC (Intended Nationally Determined Contribution) in Paris Agreement on Climate Change, 2015 to make 40% of its collective power installed capacity from clean renewable resources and diminish the emission intensity by 33-35% per unit GDP over the 2005 level by the year of 2030 [3]. According to a 2017 press release by Ministry of New and Renewable Energy (MNRE), Government of India (GoI), India has a share of around 18.37% of renewable power (i.e. 60.98 GW) in respect to the total installed capacity (i.e. 331.95 GW) as on 31st October 2017, which is much lower than the estimated renewable energy potential of around 1096 GW [4]. Sector-wise renewable potentials are as follows: Wind – 302 GW (at 100-meter mast height); Bio-energy – 25 GW; Small Hydro – 21 GW; and 750 GW of solar power, assuming 3% wasteland [4]. These data show a strong potential of renewable growth with a drawback of its intermittent nature. In this context, a micro-grid with a number of renewable power plants and efficient storages can be an effective option for continuous and reliable power supply [5]. Hybridization of such micro-grids with the conventional grid can also help in reduction of CO_2 emission level [6].

1.1. The standard Electricity Grid System

The electrical energy grid system may broadly be categorized into two sections *i.e.* central grid system and microgrid system. A conventional grid system consists of a number of large conventional and renewable generators. They generally serve a huge amount of load. Whereas, a microgrid consists of small generators and they serve a small amount of load (e.g. load of a cluster of villages or small urban areas etc.

1.1.1. Central Grid

Central grid is a high voltage power transmission network that handles the power supply between power generating stations and load centers through sub-stations. In Indian context, National grid serves the purpose of central grid system, where, the power generating stations are mainly of conventional type.

1.1.2. Microgrid

A microgrid is an energy grid operates locally for a small load demand [7]. They may either be a conventional grid connected or an isolated / islanded one. However, a microgrid has full control capability on its energy generation or delivery strategy [7]. A microgrid depending on presence of generators may be categorized into two subsections.

1.1.2.1. Conventional Energy-based Microgrid

Conventional energy based microgrids are fossil fuel dependent. This type of microgrid is generally fired using diesel generator alone without any renewable resources present in the system, as coal-based power plants are generally commissioned with large generation capacity that does not fit with microgrid load capacity. These microgrid are prone to pollution as diesel is the source of energy, however they are extremely stable in operation. Xiao *et al*. presented a sizing method of for energy storage and diesel generator in a microgrid using discrete Fourier transform [8]. Krishnamurthy et.al has presented a diesel engine driven wound field synchronous generator for a microgrid operation. The operation and control strategy are also determined in the article [9].

1.1.2.2. Renewable Energy-based Microgrid

Renewable energy generator are the primary resources in this type of microgrid. They may either be grid connected or isolated ones. In the grid connected microgrid, the conventional grid or diesel generators acts as a back up to handle any disturbances beyond the control of the microgrid. Renewable energy powered isolated microgrid may have a number of structures. There may be a single or multiple type of renewable resources present in the microgrid. They may also include one or different type of storage system for back up.

1.1.2.3. Hybrid Resources-based Microgrid

Hybrid resource based microgrids deal with a blend of conventional and non-conventional / renewable resources. Generally, the conventional generators i.e. diesel generators are kept as back-up to handle any anomaly or are used to supply the peak demand.

There are several literatures available with this configuration. Adaramola *et.al.* have described a Solar PV – diesel generator-based hybrid microgrid for a daily average load of 1 kW in Northern Nigeria to provide stable energy in a cost-effective way [10]. Ghenai *et.al.* have modelled a cost-optimized microgrid structure using solar PV and diesel generator [11]. They have also included a battery bank for uncertainty handling and determined the minimum Levelized cost of energy (LCOE) as 0.286 $/kWh [11]. Usman *et al.* have presented a hybrid solar PV, diesel generator, battery bank based microgrid duly connected with the grid. Authors have shown different combinations of resources to identify best possible combination technically as well as economically [12]. Ammar *et al.* have presented a review of previously published literatures incorporating solar PV and diesel generator hybrid microgrid [13]. Authors have also tabulated the cost and emission effectiveness of such a hybrid structure presented in different literatures. To decrease the usage of diesel generator several researchers have incorporated a battery back-up along with solar PV – diesel generator based microgrid system. Chaudhary *et al.* have reported a solar PV- battery-diesel generator based microgrid system for an islanded area in tropical Australia [14]. Wu *et al.* has presented a microgrid incorporating Solar PV-battery and diesel generator for load dispatch in a remote location. The system also incorporates a reverse osmosis desalination plant for drinking water supply. The microgrid operation is optimized to meet the lowest cost of energy using Tabu search algorithm [15]. Jeyaprabha *et.al.* have presented an optimal sizing and tilt angle operation of a solar PV array in a microgrid, also incorporating a diesel generator and battery bank for optimal load delivery. The PV array tilting function is performed considering reduction of diesel generator usage. A dump load is also used in this study. The optimal tilt angle is derived for a number of cities of India [16]. A simplified model of Solar PV-battery-diesel generator based microgrid is presented in literature. Ameen *et.al.* have presented this model to predict the operation of such a microgrid throughout a specific time period. Load following and cycle charging dispatch is used to control the system operation for sizing and performance analysis [17]. Ghenai *et.al.* have presented a comparison between an on grid and off grid Solar PV powered desalination plant. A battery bank is also considered for off-grid operation purpose [18]. Lai *et al.* have proposed a solar PV based microgrid incorporation energy storage system to scatter a load in a microgrid. They have proposed a novel energy delivery cost calculation method namely Levelized cost of delivery for energy storage systems. The method of cost calculation is compared using Solar PV powered Li-ion and Vanadium redox flow battery system [19]. Akter *et al.* has studied a comprehensive economical evaluation on grid independence with solar PV – battery structure for a residential building in Australia. They successfully evaluated the comparative self-sustainability on different conditions in presence of Solar PV and Solar PV – Battery structure

[20]. Debnath et al. have proposed a novel Transformer coupled dual-input converter for maximum tracking of solar PV and battery charge controller while stabilizing the voltage output from Solar PV. The proposed system works simultaneously reducing the battery overcharging along with increasing the overall system efficiency [21]. An economic evaluation of profit sharing between the owner of solar PV- battery installation and consumers in an apartment building is formulated in literature. The proposed scheme also evaluates social welfare of consumers along with cost evaluation for the model under consideration [22].

Apart from Solar PV – battery/diesel/energy storage schemes notable works on wind energy based microgrid have also been presented by several researchers, where wind is the sole source of renewable energy, diesel generator and battery banks are used as back up.

Guo *et al.* has studied an optimal battery energy storage operation in a Wind – diesel islanded microgrid. This study is based on economic, environment and stability aspects. Energy randomness, component failure rate and power flow constraints have been taken into account to ascertain the viability of the proposed model [23]. An application and control strategy of battery energy storage for frequency regulation and peak shaving in a wind-diesel system is formulated in literature. The system is designed to withstand wind speed fluctuations to provide smooth output. A dump load is also used to stabilize the same [24]. A similar study is performed for stability and reliability analysis of a wind-diesel isolated system. An Ni-MH battery is used for backup [25]. In another study a novel hydro-pneumatic storage for wind-diesel system is proposed. The literature shows viability of a compressed air storage in hybridization with the hydro-pneumatic storage for a microgrid. The study has found out significant reduction of compressed air storage along with fuel consumption. With reliable operation, the system also enhances renewable energy penetration in the microgrid [26]. Hong *et al.* has optimized the sizing of an energy storage in wind-diesel environment. Load growth uncertainty is considered in designing the microgrid system and the system is optimized using two stage stochastic optimization framework for optimal sizing of the energy storage [27]. Khalid *et al.* have presented a novel pricing framework for grid connected microgrid with battery storage system. An optimal operation strategy is formulated considering energy price variability and load forecasting for profit maximization [28].

Discarding the diesel generator; to provide completely clean energy, one or more battery system can be incorporated with wind energy for an establishment of steady microgrid system. This structure provides comparatively stable energy output with zero emission. Fathima *et al.* have presented a review of different combinations of wind – battery storage combinations available in literatures. The main focus authors have presented is combining different battery technologies used with wind turbine for any microgrid [29]. Ibrahim *et al*. has presented an application of compressed air energy storage in integration with a microgrid. A comparison with distributed application is also drawn. With high economic advantage, fast response and low environmental impact, the compressed air energy storage seems to be a viable alternative [30]. Zhang *et al.* has presented a concept of decreasing wind energy curtailment using hydrogen energy storage. The effect of electrolyser power and hydrogen price have been taken into consideration for payback period

calculation [31]. In literature, a novel low pressure compressed energy storage system is formulated for wind energy storage application. The system is of a smaller size and can easily be implemented in both microgrid and grid connected scenarios. A system operation evaluation in microgrid is also presented in the article [32]. Mesbahi *et al.* have provided an improved structure of stand-alone wind turbine using doubly fed induction generator and permanent magnet induction motor. A Li-ion battery is used to provide voltage support to the microgrid. A back-to-back PWM converter is used to regularize the output [33]. Nguyen *et al.* have provided a cost-effective battery sizing method for grid connected wind turbine [34]. Luo *et al.* have proposed a coordinate operational dispatch method for wind turbine – battery combination. This method reduces wind speed forecasting errors and increases battery life. This method also helps in determining the optimal size of battery storage in a system [35].

So far, the discussion is focused on application of only one type of renewable resource as a sole energy generating source in a microgrid. However, this type of microgrid without an efficient energy storage is somewhat unpredictable or may face severe problems due to inherent fluctuating character of renewable resources.

This intermittency issue can be tackled with an efficient energy storage or efficient operation design of one or more energy storages or creating a hybrid microgrid with more than one renewable resource along with ample amount of energy storages for stable power output. Considering these themes different authors have designed / proposed different hybrid systems for standalone microgrid. However, some of them are equally applicable in grid connected environment also. Rashid *et al.* has proposed an optimal design of a solar PV – wind –diesel based microgrid for a coastal region of Bangladesh. They have shown that with an effective combination of renewable resources with back-up can compete with conventional resources [36]. Olatomiwa *et al.* has provided an alternative to diesel powered mobile base transceiver station using hybrid renewable resources. The authors have compared PV – diesel – battery configuration with PV- wind – diesel – battery system and concluded that the PV – wind – diesel – battery system is much more cost effective than the PV – diesel – battery one. The have used HOMER to find the optimal usage of different resources of the hybrid microgrid [37]. Kusakana *et al.* have performed a comparative analysis of two control strategies; diesel generator ‘continuous’ and ‘on/off’ operation in a solar PV – diesel – wind – battery configuration for optimal power delivery with minimum cost in a microgrid. Considering non-linear curve of load demand and diesel generator fuel consumption, the system provides significant fuel saving [38]. Bianchini *et al.* has presented a cost optimized hybrid microgrid using PV – wind – diesel hybrid system for a remote location. Replacing complete diesel operated system by renewable resources including a battery shows significant reduction in cost and pollution. The article also provides sizing optimization of different resources for better usability [39]. A PV-wind – diesel hybrid microgrid is presented in literature. This microgrid has potential to provide energy autonomy for two continuous days for 10 people. 3 Nos. of 1kW wind turbine, 54 solar panel with 120 W power each is used for the same [40]. Maleki *et al.* have provided an optimal sizing analysis of a PV – wind-diesel system with battery and fuel cell storage to provide energy to a standalone system. The optimality of the presented system is

determined using Harmony search algorithm for better convergence [41]. Diab *et al.* have performed a techno-economic study of hybrid renewable microgrid for commercial purpose. The authors have designed a PV- wind-diesel-battery system for operating a factory in Egypt. They have used 60 kW PV, 100kW Wind, 40kW diesel generator, 50kW converter and 600 batteries to achieve an environment friendly factory [42]. Shi *et al.* have performed a techno-economic analysis of a PV-wind-diesel based microgrid using multi-objective line-up competition algorithm (MLUCA). They have also designed an improved power management strategy (I-PMS) for better handling of energy requirement in the microgrid, where battery is the main back up and diesel generator kept aside for extreme emergency purpose [43]. A different approach of using a hybrid microgrid is published in literature. Where a PV-wind-diesel-battery system is designed considering cost competitiveness, improvement of human development index and job creation. A multiobjective evolutionary algorithm is used to perform the optimization of these objectives [44]. Mamaghani *et al.* have performed a techno-economic analysis of a PV-wind-diesel hybrid microgrid considering the cost of energy as the indicator. They have performed different combination study to achieve the most cost-effective structure for the system [45]. A Stochastic-heuristic method is used in literature to find the PV-diesel-wind-battery hybrid system in a microgrid. Different uncertain conditions related to the renewable resources have been taken into account while performing the optimal sizing and operation strategy for the said system [46]. Ramli *et al.* have used multi-objective self-adaptive differential evolution algorithm for optimal sizing of a PV-wind-diesel hybrid standalone system. The system shows cost effectiveness and high renewable energy penetration to the microgrid in an optimal fashion [47]. Maatallah *et al*. have reported a techno-economic analysis of PV –wind – diesel hybrid system with battery storage for clean energy production. The system is optimized to achieve the best result for the selected location in Africa. The Net present cost, Levelized cost of energy, emission and excess generation from renewable resources are taken into account. A comparison between a grid connected system and isolated one is also determined [48]. Khan *et al.* have presented a comparison of different hybrid system configurations such as PV-wind-diesel-battery, PV-diesel-battery, wind-diesel-battery, PV-wind-battery etc. for telecommunication application. The most techno-economically feasible combination is determined using solar, wind data from different cities in Punjab [49]. Hossain et.al. have performed a feasibility study of PV-wind-diesel-battery hybrid system for a larger load than a general microgrid. The system has been optimized for lowest net present cost and cost of energy. They have also found that a similar system with only diesel generator emits much more greenhouse gas as compared to the hybrid system [50]. Maleki *et al.* has presented an optimal sizing of PV-wind-battery system in a microgrid. They have used Harmony search algorithm to optimize the annual cost and emission of the system. The hybrid system has also been compared with diesel only generation for the same microgrid [51]. Tazvinga *et al.* have presented an energy dispatch strategy in a microgrid using PV-wind-diesel-battery system. Solar and wind uncertainties have been taken into account to determine the stability of the system under disturbance [52]. Zhao *et al.* have represented an optimal feasibility study on PV-wind-diesel-battery system in a microgrid. The system is a standalone one and it has been optimized using improved fruitfly

algorithm [53]. Kazem *et al.* have provided a techno-economic feasibility analysis of a PV-wind-diesel-battery hybrid system in a microgrid. The cost and emission of the system is duly optimized using HOMER [54]. Bouchebbat *et al.* have presented a novel control strategy for PV-wind-diesel-battery hybrid system in a microgrid. The control strategy based upon multi-input single-output method. A modified multi-objective genetic algorithm is used in optimizing the system [55]. Merabet *et al.* have presented a futuristic approach on a PV-wind-battery based microgrid. They have developed a control algorithm for power compatibility and energy management between resources. The system is self-operational and has an open architecture platform for different operation conditions [56]. Katsigiannis *et al.* have presented technical analysis of an autonomous microgrid using wind-diesel-battery hybrid system for island in Greek. The application of Sodium Sulphur battery is presented in the article [57].

1.2. Different Renewable Resources

There are different types of renewable resources like solar, wind, biomass, geothermal, tidal, hydro etc., which are used to harness energy. Mainly solar, wind, biomass and hydro are used as renewable resources in India.

1.2.1. Wind

Wind is formed due to the Earth's atmospheric pressure difference which occurs due to temperature difference and the rotation of Earth. This energy is being used for centuries to generate electricity. And through research over the wind turbines for decades, wind energy has become one of the most promising advanced renewable-based power generating technology. Polinder *et al.* have discussed about the trends in wind turbine generator systems [58]. They have discussed about the researches on constant speed system consisting of squirrel-cage induction generator, and the three variable speed systems comprises with doubly fed induction generator (DFIG), with fully rated converter and gearbox, and direct drive (DD). They have also reviewed the possible future generator systems and the different transmission systems [58]. Work on designing the optimal shape of blade and its composite material has also been done by researchers [59]. Njiri *et al.* have reviewed several control strategies of the wind turbine systems used in both high and low wind speed regions [60].

In wind energy, India globally holds the 4th position regarding installed capacity (32.7 GW in 2017) of wind energy after China, USA and Germany, which is much lower than the estimated potential of 302 GW [4]. The potential can also reach upto 600 GW if the turbine hub is installed at 120 m instead of 100 m [4], which leads to an ocean of opportunity towards the wind-based renewable energy.

1.2.2. Solar PV

Solar energy can be directly converted into electricity through solar photovoltaic (PV) cells, which is made up of semiconductor material. The photons of sunlight provide energy to the electrons of PV cells to move freely, thus, produces electricity. Monocrystalline silicon, polycrystalline silicon, and thin film are three different types of PV cells that dominates the globe commercially. Hudedmani *et al.* have documented the pros and cons of these materials and also discussed about various losses that affects the solar cell efficiency, like - non-absorption of long wavelengths, thermalization of excess energy of photons, total reflection of solar wavelengths, incomplete absorption of photons due to the finite thickness of solar cell, recombination, shading etc. [61]. Further, they have also presented various methods that improve solar flux collection [61]. Dhass *et al.* have analyzed the performance of different PV materials (such as silicon, germanium, indium phosphide, cadmium telluride and gallium arsenide) [62]. GaAs (gallium arsenide) presented best performance while comparing with other materials followed by Si (silicon) [62].

Apart from solar photovoltaic cell, electricity can also be generated through solar thermal power plant. In solar thermal power plants, solar radiation is concentrated through mirrors in a radiation collector where heat bearing medium absorbs the heat and follow the conventional way to generate electricity through turbine generator set. Reddy et al. have presented the global scenario of solar thermal based power plants considering different solar concentrator technologies like parabolic trough, parabolic dish and central power tower [63]. Further they have concluded that the plants using parabolic dish concentrator followed by Stirling engine generates electricity at lower unit cost.

Both solar photovoltaic and solar thermal have the potential to provide green electricity but solar PV systems have advantages to contribute to low-power demand systems like, stand-alone or islanded system and building-integrated grid-connected system. Whereas, solar thermal power plants are best fitted in large scale grid-connected systems, as, it requires a vast amount of land and investment for electricity generation. But for both the systems a storage system is required as sunlight is not available for the whole day.

1.2.3. Biomass

Biomass is organic substance that comes from living organism like plants and animals. The most common biomass that are used as feedstock for energy generation are plants, wood, agricultural waste and residue, forest waste, animal waste and municipal solid waste. Plants used for biomass energy keep the environment carbon neutral as they intake carbon dioxide from air for photosynthesis and return the carbon dioxide to atmosphere in the process of generating energy. Biomass feedstock can be used to produce syngas/producer gas, biogas, bio-diesel and hydrogen as primary energy. Bio-diesel and hydrogen are generally used as transportation fuel, whereas, syngas and biogas are used to generate electricity.

Biomass gasification is a process where biomass is partially oxidized and the biomass breaks down into carbon monoxide, hydrogen, carbon dioxide, light hydrocarbon - methane and heavy hydrocarbon – tar. If the gasification takes place in air medium then nitrogen gets added up with carbon monoxide, hydrogen and carbon dioxide. This gas mixture generated through gasification is termed as syngas or producer gas [64]. Syngas mainly has hydrogen and carbon monoxide as combustible components.
Biogas is produced through anerobic digestion of organic matter like animal waste or food scrap. Biogas is mainly a combination of methane and carbon dioxide along with the presence of negligible amount of nitrogen, hydrogen, hydrogen sulphide and ammonia [65].

1.2.4. Hydro

Hydro power plant is also considered as renewable energy resource as it depends on water cycle, driven by sun. There are three different types of hydropower plant according to their construction: impoundment, run-of-river and pumped storage. Impoundment is the most common type of hydroelectric power plant, where a dam is erected to store river water, then the stored water is sent to turbine through penstock to rotate it and generate power. The turbine is connected with generator; hence, electricity gets generated. In run-of-river type hydroelectric power plant, no dam is constructed only a canal/penstock is built and the natural elevation is used to generate electricity. Pumped storage hydroelectric (PSH) power plant functions as a storage system, where, solar or wind energy is used to pump water from lower reservoir to upper reservoir and at the time of high demand the water from higher reservoir is released towards lower reservoir to generate electricity. As it is well-known, that renewable energy is intermittent in nature, therefore an amalgamation of energy storage system is required with the renewable-based power generating systems for continuous flow of electricity.

1.2.5. Geothermal

Geothermal energy is a natural resource of heat energy harnessed from the internal heat of earth. The temperature below the earth surface rises at a rate of around 30°C per km for the first 10 km of earth crust [66]. This internal storage of heat manifests on earth surface as volcanoes, geysers, hot springs and mud pots. Geothermal energy is commercially used as heat pumps and electric power plants. Moya *et al.* have reviewed on different aspects of geothermal energy development, assessed power plant technology and direct heat applications based on geothermal energy [67]. Anderson *et al.* have discussed the trends and potential role of geothermal energy for a sustainable future.

1.2.6. Tidal

Tidal energy is a form of energy produced by the usual rise and fall of tides caused due to the gravitational interaction between the Earth, the Sun, and the Moon. This tidal energy is converted to electricity using various technology. Chowdhury *et al.* have depicted the trends and future prospects of tidal energy in their work [68]. Johnstone *et al.* have worked on techno-economic analysis of tidal energy technology generating electricity [69].

Apart from geothermal energy source all the other renewable resources discussed in section 1.2 are intermittent in nature depending upon the earth's spin around its own axis (i.e. the occurrence day and night), revolution around the sun (i.e. occurrence of seasonal variation) and moon's presence (i.e. occurrence of high tide and low tide). To eliminate this intermittent nature of renewable energy resources incorporation of energy storage system in the renewable system is essential.

1.3. Energy Storage Systems

Energy storage systems use the technology to store excess generated energy and use it in the time of crisis / peak demand. There are various energy storage technologies available, which can be broadly classified as: Electro-chemical (Lithium-ion battery, Lead-acid battery, flow battery, Lithium polymer battery etc.), Mechanical (Pumped storage hydroelectric system, Compressed air storage, Gravity energy storage and Flywheel energy storage), Electrical (Super conducting magnetic energy storage and super capacitor), Thermal (molten salt, phase change materials etc.) and Chemical (Hydrogen fuel cell, Solid-oxide fuel cell etc.). From the vast field of energy storages some are discussed below:

1.3.1. Electro-Chemical Energy Storage

Batteries are the oldest form of electricity storage system [70] where electricity is stored as chemical energy. A battery is comprised of one or more electrochemical cells consisting of a liquid, paste, or solid electrolyte along with a positive electrode i.e. anode and a negative electrode i.e. cathode [71]. Throughout discharge, electrochemical reactions occur at the two electrodes creating a flow of electrons through an external circuit. The reactions are reversible, allowing the battery to get charged through the application of an external voltage across the electrodes.

1.3.1.1. Lead-acid Battery

It is the oldest (invented in 1859) and most widely used battery [71]. It has a low cost ($ 300 – 600 / kWh) with high reliability and efficiency (70 – 90%) [71]. But it has short cycle life (500 – 1000 cycles) and low energy density (30- 50 Wh/kg) [71]. The electrodes of lead-acid batteries are made up of lead whereas, sulphuric acid is the electrolyte, which makes it a hazardous battery.

1.3.1.2. Lithium-ion Battery

The cathode used in this type of battery is a lithiated metal oxide ($LiMO_2$, $LiCoO_2$, $LiNiO_2$ etc.) and the anode is fabricated of graphitic carbon along with a layering structure [71]. The electrolyte is made-up of lithium salts (such as LiPF6), further, dissolved in organic carbonates [71]. Although the cycle life of this battery is 4 times higher than lead-acid battery but the initial cost of this type of battery is around 630 $/kWh, with an additional recurring cost of 600 $/kWh required for replacement within every 10.5-12.5 years [72].

1.3.1.3. Vanadium Redox Flow Battery

Amongst other technologies, vanadium redox flow battery (VRFB) is considered to be one of the most promising options for renewable applications due to its high energy efficiency of around 85% [71], long cycle life and low maintenance cost [73]. Though it has lower energy density [71] than lead-acid and lithium-ion batteries but it has a long lifetime of around 24 years [73]. VRFB is comprised of two electrolytic cells linked with two electrolytic tanks carrying vanadium redox couples in sulfuric acid electrolyte, separated by a proton exchange membrane. The positive tank is comprised of V5+ and V4+ ions, while, the negative tank is covered with V3+ and V2+ ions [74]. The most interesting part of this battery is that its energy storage capacity and power capacity can easily be increased by respectively increasing the size of the tank and the number of cells [74].

1.3.1.4. Lithium Polymer battery

The usage of carbonic acid esters and organic ethers-based electrolytes in commercially available lithium-ion batteries creates a serious safety issue as the electrolytes have flammability and leakage concerns [75]. To handle these issues solid electrolytes have been introduced. Polymer electrolyte-based lithium battery is known as lithium polymer battery. Along with safety this kind of battery has also high energy density and long cycle life [75].

1.3.2. Mechanical Energy Storage

In mechanical energy storage system, energy is stored in the form of kinetic or potential energy by compression, acceleration or displacement (against gravity) of any suitable medium. At the time of requirement, the kinetic or potential energy can be retrieved through the reversal of the process.

1.3.2.1. Pump Storage Hydroelectric System

It is a matured technology used to store a large amount of energy for a long period of time with high efficiency at a relatively low capital cost per unit energy [71]. In this technology water (hydraulic potential energy) is stored at higher elevation through pumping at the time of off-peak period. Whereas, at peak period the stored water is released towards a reservoir at lower elevation via a turbine generator set. Hence, electricity gets generated.

1.3.2.2. Compressed Air Storage

Compressed air storage system works as a part of conventional gas turbine generation system. It separates the expansion and compression cycles of a gas turbine into two different processes and stores energy as elastic potential energy of the compressed air [71]. During low demand period, energy is stored by compressing the air, typically at 4 – 8 MPa, into an air tight space. At the time of high demand, compressed air is drawn from the storage space, heated up followed by expansion through a high-pressure turbine, which arrests some of the energy of the compressed air. Then the air is mixed with fuel and combusted. The combustion exhaust gets expanded through a low-pressure turbine. Both the high pressure and low-pressure turbines are coupled to a generator to produce electricity.

1.3.2.3. Gravity Energy Storage System

Gravity Energy Storage System (GESS) is relatively newer energy storage technology which has the capability to supply electricity at a stable voltage. Here, electricity is generated from gravitational energy. There are several types of gravity energy storage system available, but they are mainly at pilot project stage or under development condition. Gravitricity [76] is a kind of gravity-based storage, where, a mass is suspended by a rope from an altitude and over the vertical raising and lowering the respective charging and discharging takes place. There is also another technology known as piston-based PSH (P-PSH), which is basically a closed loop PSH. Here, water is stored in a closed unit, which lifts a piston while storing energy, whereas, the piston

descends when the energy is required for utilization. The descend of piston pressurizes the water, then the pressurized water flows through hydro turbine coupled with generator and generates electricity. Following this principle of P-PSH, Gravity Power, LLC designed Gravity Power Module in 2011 [77].

1.3.2.4. Flywheel Energy Storage

Flywheel stores energy in the angular momentum of a spinning body [71]. During charging, the flywheel is spun up by a motor, whereas, during discharge the same motor operates as a generator and produces electricity from the rotational energy of the flywheel. The total stored energy of the system depends upon the size and speed of the rotor of the flywheel; however, the power rating is dependent upon the motor-generator.

1.3.3. Electrical Energy storage

In this type of storage system, electrical energy is stored in the form of electric current or electric field and later, when required the stored energy is supplied in the form of electricity.

1.3.3.1. Superconducting Magnetic Energy Storage

Superconducting magnetic energy storage or SMES directly stores electric energy in the form of DC current in an inductor coil made up of superconducting material, niobium-titane (NbTi) operating at a temperature of -270°C [78]. The major advantages of this storage system are its high instantaneous efficiency of around 95%, capability of being almost complete discharge; unlike batteries and its fast response time below 100 ms [78]. The cryogenic refrigeration required to keep the temperature at -270°C is the major drawback of the system as it makes the system both costly and complicated (in terms of operation) [78].

1.3.3.2. Supercapacitor based Storage

Supercapacitors are electrochemical capacitors with increased capacitance and energy density than the conventional capacitors. The supercapacitor stores energy by means of an electrolytic solution between two solid conductors other than the common arrangement of a solid dielectric medium between the electrodes. The electrodes are generally made up of porous carbon or other high surface area material with an aqueous or non-aqueous electrolyte. Supercapacitors can have very

large amount of capacitance and stored energy due to the very high surface area (i.e. up to 2000 m^2/g) of activated carbon and the very small distance (< 1 nm) between the electrodes. Short duration along with high energy dissipation due to self-discharge loss are the major drawbacks of supercapacitor.

1.4. Objective of the Work

From the existing literature it is evident that hybrid microgrids provide comparatively higher stability than the single resource-based microgrids, but in majority of hybrid microgrids, diesel generators have been used, which implies that these microgrids are not fully green in terms of emission. There are also several problems like frequency & voltage instability, intermittency issues of renewable resources, harmonics problem in the ac side etc. as of technical aspect. In case of operation issues, energy management, forecasting and battery degradation issues are major challenges.

Therefore, the objectives of the work are -

i. To design a hybrid microgrid devoid of any diesel generator, which is similar in terms of voltage stabilization.
ii. To design an operation strategy using a single renewable resource to provide uninterrupted energy supply at stable voltage to an islanded microgrid.
iii. To design a hybrid microgrid with local resources to provide stabilized energy at cheaper rate than actual energy price in Indian context
iv. To apply a different optimization algorithm to optimize the microgrid to provide the most optimal solution

1.5. Novelties and Contribution of the Work

The novelties of the work are as follows -

i. Design of a wind turbine to alternatively charge one PSH and one GESS for continuous and stable renewable-based electricity supply.
ii. Design of a wind turbine to simultaneously charge and discharge of two GESSs for uninterrupted renewable-based electricity supply in stable voltage.
iii. System design to supply continuous electricity at stable voltage with renewable energy only at lower price than the actual government rate.

If these simulation-based works get practically implemented then it can partially replace the thermal electricity generating plants with the components of voltage stabilization and continuous flow of energy.

1.6. Flow of the Thesis

After the introduction part stated in chapter 1, chapter 2 states the State-of-Art of the thesis. Chapter 3 depicts the system descriptions and operation strategy followed by details of Algorithm in chapter 4. Chapter 5 describes the generated results of the proposed systems. Chapter 6 concludes the thesis concretizing the outcomes of the research works along with the illustration of future scope of work.

CHAPTER 2

2. State-of-Art Technicalities of Microgrid

The already defined objectives (section 1.4) of this thesis are derived from the literature review done in sections 1.1.2.3, 1.2 and 1.3. Several literatures [10-27, 36-48] discussed in section 1.1.2.3 have incorporated diesel generator sets along with renewable resource-based microgrids to generate stable electrical power. This is a drawback in terms of fossil fuel utilization and resulting in global warming. Therefore, there are motives to generate renewable-based stable power in self-sustainable microgrids with hybrid systems.

2.1. Hybrid Systems of Microgrid Developments

There are several articles available regarding different strategies to cater load in different conditions. Gupta *et al.* have described a solar PV, micro hydro, Biomass, Biogas generator-based system in Indian context [79]. A battery system along with a diesel generator is also kept in the system to handle uncertainties. Bahramara *et al.* have reviewed different strategies adopted to design hybrid RE system in context of different countries using HOMER [80]. Khan *et al.* have described a polygeneration process based on hybrid RE system. The study also includes desalination of water to provide pure drinking water to households [81]. Reddy has used multi-objective based stochastic technique to minimise the losses of a hybrid energy system and total operating cost of the renewable energy resources located at different parts of the grid [82]. Momoh and Reddy have discussed several stochastic optimization techniques for renewable energy based optimal power flow and voltage VAR problems [83]. Incorporation of renewable based energy system into grid is a challenging problem due to the intermittent nature of the renewable resources. However, Reddy has solved an optimal power flow problem considering the uncertainty issues of wind speed and solar irradiation [84]. Reddy and Momoh have discussed the realistic optimum day-ahead scheduling of a hybrid power system consisting of thermal generators, wind farm and solar PV, taking into account of the uncertain parameters of renewable resources [85]. To provide energy at low-cost Ahmad *et al*. have considered both energy management by efficient use of consumer's appliances and trading of renewable energy generated in decentralized manner to consumers and prosumers [86]. Peak power consumption has been handled by demand side management [87]. Installation of small-scale renewable resources-based energy generators like rooftop solar PV and wind turbine at home can also decrease the load on grid and cost of energy [88]. Also, necessity of energy management to minimize the carbon footprint, reduce the expenditures on energy consumption i.e. efficient energy consumption has been established [89]. But to completely eradicate the presence of fossil fuel in a renewable based hybrid system the amalgamation of energy storage is a must thing to do.

2.2. Energy Storages for Microgrid

There are several storage devices which are in use to enhance the reliability of energy supply from RE resources. Chen *et al.* have classified energy storage systems in broadly four categories namely; electrical, mechanical, chemical and thermal energy storage [71]. Several research articles also demonstrated applicability of energy storage devices in RE perspective such as SMES-battery energy storage in solar PV application [90], flywheel energy storage in PV and diesel hybrid microgrid [91] etc. However, chemical energy storage is the most convenient one in terms of microgrid application. Several applications related to RE system such as Lead-Acid battery [92], Lithium-ion battery [93], Flow battery [94] etc. are available in published literatures.

Another type of storage system, namely Gravity based energy storage is currently one of the most competitive in terms of usage simplicity and cost effectiveness. Pumped storage hydroelectric (PSH) generation system is the most matured one available in gravity-based storages [95]. However huge land and water requirement makes it a bit difficult to construct in some locations. To overcome these drawbacks of a conventional PSH, Gravitricity proposed a novel storage system called Gravity energy storage [96]. This storage system specifically utilizes a heavy weight to be lifted to charge and release energy during downward motion of the same weight due to gravity in a vertical tunnel underground. Morstyn *et al.* have further evaluated the estimated energy generation potential of this gravity energy storage system in terms of abandoned mine shaft under United Kingdom Government jurisdiction [97]. This type of system deserves special attention when there are too much hue and cry for a cost-effective storage system.

Energy storage devices play a crucial role in keeping the power quality of a microgrid in check. In terms of energy storage, there are several devices, but amongst them, apart from battery storage, most technologically matured one currently available is PSH [98, 99]. Conventionally, a PSH draws energy from grid during off-peak hours to charge and during peak-hours it generates energy through a reversible pump [100]. However, this scheme has its economic advantages, but from environmental aspect the scope is limited. Thus, a PSH [101, 102] or any other energy storage device, if charged through RE, is deemed to be worthwhile from environmental as well as an economic point of view. Likewise, PSH connected with a standalone PV-wind hybrid energy system [103] and double storage system, combination of battery and PSH is incorporated with a grid connected PV-wind hybrid energy system are presented in literatures [104].

As discussed in different literatures, energy generated from RE is directly supplied to the system load and energy storage devices are set aside for handling uncertainties. These systems are prone to complications, as uncertainty issues of RE may not be fully eradicated.

In this context, Pali *et al.* have represented a comparatively different kind of approach [105, 106, 107, 108]. Here, instead of direct load supply, solar energy [108, 109] and wind energy [105, 106]

are used to fill up the upper reservoir of PSH and the PSH supplies the load demand at a stable voltage. Instead of energy conversion (mechanical to electrical energy), Pali *et al.* utilized mechanical energy generated from wind turbine (WT) to operate a mechanically driven centrifugal pump (CP) to pump water in the upper reservoir (UR) of a PSH and released water through a separate turbine generator set to generate electricity in constant voltage for a constant load [105]. A relatively small-scale standalone system of 300 W is considered in Indian context.

Now, whenever there are a number of resources and storage systems are available to cater a fixed amount of load, it becomes necessary to optimize the system as such that the technical as well as economical aspect of the system remains rational. In this term, nature inspired algorithms are the best choice for their better optimal convergence as compared to conventional optimization algorithms.

2.3. Algorithms for Optimization for Microgrid Component Selection

There are a number of such algorithms available in literature. Amongst them Harmony Search Algorithm [110], Gray Wolf Optimization [111], Frog Leaping Algorithm [112], Gravitational Search Algorithm [113] to name a few. In this perspective, Singh *et al.* optimized a PV- biomass based hybrid RE system using artificial bee colony algorithm to find the optimal output of the system [114]. In this aspect authors of this article have considered The Whale Optimization Algorithm [115] for its better convergence capability, which is already tested on several benchmark functions such as Tension / Compression spring design, Welded beam design, Pressure vessel design etc.

2.4. Recent Trends in Research for Optimization for Microgrid

Researches are being going on in recent days over the application, optimal sizing and deployment of gravity energy storage system which is basically a closed loop PSH. Emrani *et al.* have optimally designed a gravity energy storage and incorporated it with a hybrid PV-wind plant to make it more competitive both technically and economically [116]. Ameur *et al.* have modeled a hybrid solar photovoltaic and gravity energy storage system to supply residential demand considering dynamic forecasting for a week [117]. Mondal *et al.* have provided an innovative application of gravity energy module, where the researchers have incorporated two solar PV powered gravity power modules around a multi-storied building along with a vanadium redox flow battery considering

the fact of lower space consumption by the system [118]. Tong *et al.* have proposed a hybrid solid gravity energy storage system, which comprises the advantage of a gravity energy storage and a supercapacitor, along with the structure and control strategies of the hybrid storage system [119]. Therefore, the recent research trends show that the researchers are now-a-days focused on the application of gravity energy storage systems in different hybrid renewable based systems to enhance the system reliability and properly utilize the system area. This trend helped to focus on the further development of renewable based schemes.

2.5. Proposed Schemes Concerning Gravity Storages

As per the previous reviews and present-day requirement, a renewable-based hybrid scheme has been proposed along with a lithium-ion battery to provide uninterrupted electricity to the worker's colony of tea estates of Assam and efficient enough to handle variations in wind speed, water flow rate and load demand. Another scheme has been proposed where Gravity energy storage system is planned to be amalgamated with solar PV and two biomass generators with an objective to achieve voltage stabilization along with uninterrupted electricity supply with an LCOE at per with the regional electricity tariff.

The approach of Pali *et al.* in [108] (already discussed in section 2.2) is commendable, but there remain certain drawbacks which are needed to be addressed. The output from PSH is uncontrolled as load fluctuation is not taken into consideration. However, a provision is proposed to divert excess energy to a purely resistive dump load if load is reduced, but if load is increased, the operation strategy seems missing. Other than that, the pumping scenario is unrestricted *i.e.* in case of fully filled upper reservoir (UR), water keeps on overflowing without restriction continuously, which seems to be a wastage of energy [105].

Taking into consideration of all these drawbacks, a dual mode wind turbine (DMWT) driven hybrid energy storage scheme has been proposed to regularize the uncertainty related issues of a conventional wind turbine (WT). The innovative novel scheme proposes an idea of operating two distinctive storage system with different operating procedure to provide energy generation predictability, enhanced reliability, operation simplicity and more efficient usage of wind energy. The proposed system is supposed to operate one mechanically driven PSH and one electrically driven VRFB simultaneously through a single Wind Turbine. Whereas, in existing literatures, operation of either mechanically driven storage system [105, 106] or electrically driven storage system [103, 104] using a single wind turbine is conceptualized. The concept of DMWT is visualized to be operating in two modes; namely Mechanical mode and Electrical mode. In Mechanical mode, DMWT is envisioned to provide mechanical energy (extracted from its shaft) to operate mechanically driven centrifugal pump (CP) to fill the upper reservoir (UR) of PSH. Whereas, in Electrical mode; the mechanical energy from DMWT is planned to be used to generate

electrical energy through a wind turbine alternator, to charge a Vanadium redox flow battery (VRFB) system. The energy stored in VRFB will basically be the excess energy that is not primarily required to serve the load as the PSH alone will be designed to be capable of handling it. In the proposed DMWT – PSH – VRFB system, PSH is considered for its predictable nature and VRFB for its economic advantage, operation simplicity and feasibility in different platforms [120,121,122].

This proposed system of one wind turbine, will alternatively be used to operate one mechanically powered pump storage system and one electrically powered battery storage system. Thus, the scheme will help in reducing the land requirement. However, the land requirement will still be considerably high due to the presence of PSH [123, 123]. These obstacles can be overpowered by the cutting-edge technology, Gravity Energy storage system (GESS) developed by Gravitricity [96]. This storage device fundamentally utilizes extremely low land area as compared to a conventional pump storage hydro, no water requirement, has long lifetime, highly efficient and generates energy at a comparatively cheaper rate [96]. Morstyn *et al.* have estimated that there is a huge potential for GESS in United Kingdom alone [97].

The GESS draws energy from the grid to operate a DC motor, which in turn pulls an underground suspended weight to charge the device. During discharge, the gravitational pull draws the suspended weight downwards, which in turn operates the DC motor in reverse breaking condition to generate energy [96]. A converter system is also present, to connect the GESS with the grid or microgrid. However, it is also evident that, any kind of energy storage device (ESD) requires energy to charge itself, thus it leaves carbon footprint and itself not a green energy, if charged through thermal generators. Therefore, it is quite a beneficial situation for the ESD in terms of environmental aspects, if it is charged using any RE system and this also may stabilize the energy generated from RE system itself.

In consideration of general aspects and above discussions, it is evident that charging an ESD with RE resources is genuinely a beneficial option. However, it requires multiple converter system and thus, the overall system efficiency is bound to fall due to converters internal power loss. Similar wastage of energy, due to multiple charging and discharging sequences of an electrical energy storage device may be observed in a recently published article [123]. Considering the technological gap, it seems quite beneficial, if multiple mechanically driver energy storage devices can be operated using a single wind turbine. In absence of an electrical energy storage device, the overall system efficiency will increase and a better method of maximum utilization of RE may be obtained.

In this context, a novel wind turbine driven dual gravity storage system scheme may be proposed. This scheme may aim at operating two GESS devices alternatively using mechanical energy, generated from a single Wind Turbine. The proposed system comprising of two GESS, one wind turbine (WT) and one DC motor-inverter assembly can further be conceived. Here, Mechanical power generated from wind turbine can be used to create a rotational motion to pull a suspended weight in upward direction for charging the GESS. During the charging of one GESS, the other

one may generate energy via the DC motor-inverter assembly and vice versa. Therefore, two GESS may utilize the wind turbine and the DC-motor assembly alternatively.

These above concepts/schemes based on GESS will be tried in the next chapters to find out their usability.

CHAPTER 3

3. Design and Problem Formulations of Proposed Hybrid Energy Systems inclusive of Load Data

Considering the objectives stated in section 1.4 and based on the reviews of section 2.4, four hybrid systems have been designed and mathematically formulated in this section. All the systems are devoid of diesel generator, which ensures the exclusion of fossil fuels in the systems making them completely renewable. In the first system, the focus is on creating hybrid system, that is capable of supplying incessant electricity.

In the second system, the emphasis has been given to generate electricity from a combination of two renewable resources along with a gravity-based energy storage for a particular region with an LCOE lower or equal to the existing tariff structure of the selected region.

The third system focuses on creating an operation strategy that relies solely on a single renewable resource to provide uninterrupted energy supply at a stable voltage to an islanded microgrid.

The fourth system also concentrates on using only a particular kind of renewable energy source to provide uninterrupted power supply with a single difference with the third system i.e. the choice of energy storage system. Two different types of storage systems have been incorporated in the third system whereas, only a single type of storage system has been integrated in the fourth system.

These approaches have been made to promote sustainability and contribute to cost savings for the energy for areas where normal supply is sparsely available. This was initially attempted for a standalone microgrid systems with an idea of extra available energy sale to the grid.

3.1. Standalone renewable-based Microgrid with Optional Grid Sales

3.1.1. Objective

Recent times has witnessed increasing importance of integration of renewable energy in main grid that can potentially replace conventional fossil fuel generators in future due to pollution caused by them. On the other hand, in this country it is a huge challenge to provide quality electricity to

everyone. This challenge may potentially be dealt with formation of micro-grid in rural and backward areas with quality 24 X 7 power supply. This literature deals with study of a potential micro-grid that can address both connectivity as well as pollution issues with great efficiency. A micro-hydro unit and several wind turbine units are included along with a Li-ion battery storage to provide uninterrupted clean energy at constant voltage. This structure was initially proposed efficiently for a tea estate in the state of Assam. The study is focused to supply electricity with constant voltage profile throughout the day with no interruption, along with sell out of excess energy that the system may produce throughout the day. The excess energy may be transacted to any commercial load or grid available nearby so that the tariff of energy for internal customers may be reduced. In absence of such a scenario the excess power can be utilized through a dummy load of that extent.

This study deals with backward areas or worker's colony of a tea estate in the state of Assam. There are quite abundancy of small rivers and waterfalls in the state, so a micro-hydro and wind turbine have been considered to provide energy to the micro-grid. Also, to discard the intermittency of wind turbine generators, a Li-ion battery is included in the system. The standalone micro-grid is tested with different wind speed, water flow rate and demand characteristics to establish its reliability. Its structure and operational strategies are given below.

3.1.2. Microgrid Structure and Mathematical Design

The proposed micro-grid, shown in Figure 3.1.1 consists of one micro-hydro with maximum generating capacity of 30 KW, and five wind turbines of 4.1 KW each. A 25 KWh Li-ion battery is included in the system. Details of the same is provided in Table 3.1.1.

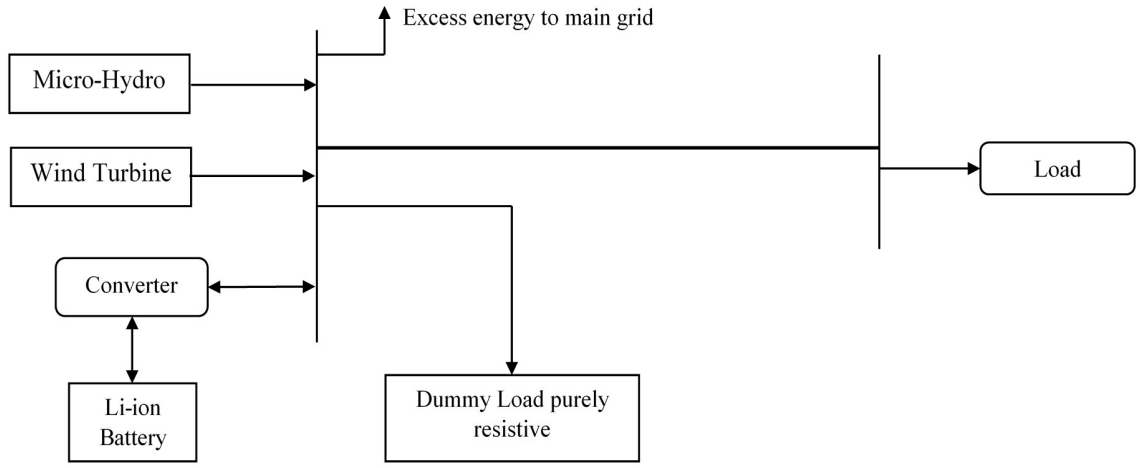

Figure 3.1.1. Structure of the Microgrid

TABLE 3.1.1. DETAILS OF DEVICES USED

Micro-hydro	
Flow rate (Cu.M/s)	0.61
Head (m)	9
Turbine efficiency	0.8
Generator efficiency	0.7
Water density (Kg/Cu.M)	1000
Gravity (Sq.M/s)	9.81
Wind Turbine	
Cut-in speed (m/s)	2
Cut-out speed (m/s)	10
Optimal speed (m/s)	3.75
Power Coefficient	40 %
Air density (Kg/m^3)	1.29
Rotor radius (m)	10
Alternator efficiency	0.96
Li-Ion Battery	
Energy rating (KWh)	25
Base Load (KW)	40

The Micro Hydro Turbine considered for the design of the microgrid is DLD POWER Medium Head Micro Tubular GD35-LZ of 30KW rating [124]. The wind turbine considered for the design of the microgrid is Ryse Energy E-5 HAWT [125].

A WT operates utilizing the wind velocity and converts the same into mechanical power. Generated power at the shaft of the wind turbine (P_{WT}^{Shaft}) can be mathematically expressed as:

$$P_{WT}^{Shaft} = 0.5\pi\mu_p\rho_{air}R_{WT}^2V_{air}^3\,, \qquad V_{air}^{cin} < V_{air} < V_{air}^{cout}$$
$$= 0\,, \qquad V_{air}^{cin} < V_{air} > V_{air}^{cout} \qquad (3.1.1)$$

Equation (3.1.1) is the conventional mathematical expression for wind power extraction. Here, (μ_p) is the power coefficient, dependent on blade pitch angle and tip speed ratio (TSR) of the WT. The value for modern WT may be around 50% as claimed in some literatures [105]. Air density is depicted as (ρ_{air}) whereas (V_{air}) is the wind speed. The rotor radius of wind turbine is (R_{WT}), cut in and cut out speed of WT is (V_{air}^{cin}) and (V_{air}^{cout}).

Generator output (P_{Gen}^{air})from wind turbine is directed by the efficiency of the same (η_{WT}) attached to the shaft of the turbine as shown in Equation (3.1.2).

$$P_{Gen}^{air} = \eta_{WT}P_{WT}^{Shaft} \qquad (3.1.2)$$

WTG output is governed by the mathematical equation as:

$$P_{Output}^{WTG} = \eta_{wt}\eta_{Gen}\rho_{water}gH_{MH}^{Rated}Q_{MH}^{release} \qquad (3.1.3)$$

At any given interval the micro-hydro unit generates electrical energy (P_{Output}^{WTG}) for water flow rate ($Q_{PSH}^{release}$) gets released from a height of (H_{MH}^{Rated}). However, the output depends on efficiency of water turbine (η_{wt}) and generator (η_{Gen}) both other than density of water (ρ_{water}) and gravity (g) of the geographical location.

Inclusive with these two generating units, a Li-ion battery is considered to maintain the stability of the system. At the starting of the day, we have considered a fully charged battery ready to be deployed according to requirement. It is to be noted that, the battery is only meant to supply power to the micro-grid and is in non-operating during any transaction outside of the micro-grid. The battery is charged by excess energy in each interval if there is any, from wind turbine is after supplying to the load.

The charging and discharging sequence may be expressed using the following equations.

$$SOC_{dch}^{i} = SOC^{(i-1)} - \frac{P_{Li-ion}^{i}T}{\eta_{Li-ion}^{dch}E_{Li-io}^{rated}} \qquad (3.1.4)$$

$$SOC_{ch}^{i} = SOC^{(i-1)} - \frac{P_{Li-ion}^{i}\eta_{Li-}^{ch} \quad T}{E_{Li-io}^{rated}} \qquad (3.1.5)$$

The SOC for discharging of a Li-ion is defined in equation (3.1.4) and the same for charging is shown in equation (3.1.5). The discharging and charging SOC are represented by (SOC_{dch}^{i}) and (SOC_{ch}^{i}) respectively for *'i^{th}'* interval. Whereas charging and discharging efficiency is defined by η_{Li-i}^{ch} and η_{Li-ion}^{dch} respectively. '*T*' is the duration of the time period and P_{Li-ion}^{i} is the dispatched power in *'i^{th}'* interval. Rated energy of the Li-ion is E_{Li-ion}^{rated}. In charging mode $P_{Li-i}^{i} < 0$ and in discharging mode $P_{Li-ion}^{i} > 0$.

3.1.3. Operation Strategy of the Hybrid System

The micro-grid, as discussed in section 3.1.2 is fully powered by renewable energy. Thus, to achieve standalone capability in spite of fully dependent on renewable energy, the Li-ion battery comes very handy. The steps of operation are as follows:

Step 1. Read: wind speed, water flow rate and battery storage data.
Step 2. Determine: wind turbine output, micro-hydro output.
Step 3. Prioritize generation from micro-hydro and allocate them first.
Step 4. Supply the residue power through wind turbine.
Step 5. If: wind turbine cannot fully deliver the residue power; supply from battery.
Step 6. If: wind turbine can fully deliver the residue power; check: if any excess generation is left from wind turbine.
Step 7. If: any excess power is left; charge battery if possible or transfer the excess power to any potential commercial customer or main grid otherwise deliver the power to dummy load.
Step 8. Repeat Step 1 to Step 7 till the end of the day.
Step 9. Show the results and exit.

Simulated results of this section (section 3.1) are presented in section 5.1.

This section only dealt with supplying continuous power supply using locally available renewable resources but have ignored the optimal techno-economic analysis of the system because of underprivileged community. However to overcome such situation in the next section (section 3.2) optimal techno-economic analysis of hybrid micro-grid has been established for a different region a bit far from our previous study site but capable of purchasing electricity at a price. Here attempts are made based on incorporation of GESS.

3.2. Techno-economic analysis of a Renewable based Hybrid Microgrid incorporating Gravity Energy Storage System

3.2.1. Objective

A grid connected renewable energy-based hybrid microgrid, incorporating solar PV, biomass generators and Gravity Energy storage system (GESS) has been proposed in this section to provide a viable alternative solution towards the thermal power generation in Indian perspective. A hybrid system has been designed to deliver uninterrupted energy to a hilly village of North-East India. Bi-directional energy transaction with the central grid is considered for handling uncertainties and to gain monetary benefit through energy sale. The GESS is only charged through solar PV and biomass generators, to reduce the carbon footprint. The outward energy transaction with the central grid helps in reducing the energy cost for consumers inside the microgrid. Whale optimization algorithm (WOA) has been used to find the optimal techno-economic solution of the proposed system.

The novelty of this study is to deliver uninterrupted energy supply to the consumers in a grid connected microgrid through renewable energy (RE) at competitive rate. Along with that this scheme emphasizes on the effectiveness of the Gravity Energy storage system in a microgrid environment. In several parts of the North-East region of India, providing uninterrupted energy to consumers is quite difficult due to hilly terrain and scattered population density. However, at present, electrification of those parts is achieved somehow, but transmission loss is comparatively high [126]. On the other hand, most of the places in the North-East region of India are blessed with ample solar irradiance and abundance of biomass resources. Therefore, a grid connected hybrid renewable-based system is quite a good option for these regions, as excess energy generated from the hybrid system may be sold to the nearby grid for both financial and environmental benefits. In this way the techno-economic analysis of PV, Biomass based Gravity Energy storage system delivers another scope of business.

3.2.2. Proposed Solar PV - Biomass – GESS Hybrid System

In this section, a hybrid RE based system is discussed based on Solar PV, Biomass and GESS.

Whenever there are a number of resources available to cater a fixed amount of load, it becomes necessary to optimize the system as such that the technical as well as economical aspect of the system remains rational. In this term, nature inspired algorithms are the best choice for their better optimal convergence as compared to conventional optimization algorithms.

In this aspect authors of this article have considered The Whale Optimization Algorithm [115] for its better convergence capability, which is already tested on several benchmark functions such as Tension / Compression spring design, Welded beam design, Pressure vessel design etc.

The proposed system in this section also deals with an optimal operating strategy of a grid connected microgrid system emphasizing on the RE system. The proposed strategy is a hybrid generating system incorporating solar PV and two Biomass generators with a Gravity energy storage system (GESS) to deliver the load demand in a stable manner. This combination is considered due to ample availability of solar and biomass resources in the studied area, whereas little to zero availability of hydro resource and low wind speed profile. GESS is considered for its high lifetime, lower space requirement and lower per unit energy cost as compared to other available energy storage devices [96].

Biomass generators are generally bound to limited time of operation, as their operating hours affect their lifetime. Thus, whenever these are in operation, they are directed to generate at maximum capacity. Any excess energy left after serving the load demand is used to charge the GESS and any leftover energy is sold to the grid for monetary as well as environmental benefit. There is also a provision to buy from the grid during requirement but this is the least preferred mode of operation irrespective of energy cost. The overall system cost includes all the related cost components as per Indian industry standards other than the GESS. Energy transaction cost through grid during different hours, are historic values presented by IEX in the year 2019. Human resource cost / Labour cost is also included as per government of India standards. For different combinations of loading pattern and GESS initial storage, the Levelized cost of energy (LCOE) is found to vary in between INR 2.71/kWh 1 to INR 3.41/kWh, which is lower than the current Nagaland state government approved tariff structure of INR 3.55/kWh. The proposed system is optimized in a multi objective scenario depending on minimization of Levelized cost of energy (LCOE) and energy brought from grid.

In this section, Khezhakeno village in the state of Nagaland, India is considered for the study. The village is situated in Phek district. According to the 2011 census total population of the studied area is 3281 with 606 households [127,128].

[1] $ 1 = INR 70 (Assumed)

3.2.3. Operation Strategy of the Hybrid System

The proposed system depicted in Figure 3.2.1, is to be operated considering the availability of resources and load demand. Solar PV panels are in operation during defined times only throughout the day due to geographical constraints. In absence of considerable amount of solar irradiance, Biomass generator 1 (BMG 1) is prioritized. If in any case BMG 1 is incapable to deliver the entire load, Biomass generator 2 (BMG 2) comes into play. GESS is utilized as the last resort when all the generators are fully utilized or unavailable due to system constraints. In all the cases, any excess energy generated from solar PV, BMG 1 or BMG 2, if available, is utilized to charge GESS in the first place. Secondly, if any excess energy is left, it is sold to the grid in accordance to the current grid price. The theme of the proposed system is to utilize only RE to meet the demand so that the carbon footprint may be reduced. But it is also essential to ensure uninterrupted supply of load demand. Thus, a bi-directional flow of energy is also considered in term of the nearby grid system. However, it is a priority to only sell energy to the grid but in extreme condition energy may be bought from the grid too. It is also worth mentioning that as buying energy from grid is the last resort, thus the GESS is operated as such no energy is to be drawn or delivered to the grid from it. The bi-directional energy flow is considered to handle uncertainties related to technical or natural phenomenon only. The flowchart of operational strategy of the proposed system is shown in Figure 3.2.2 with a continuation in Figure 3.2.3. Mathematical model of different equipment is discussed in section 3.2.3 for their respective output determination.

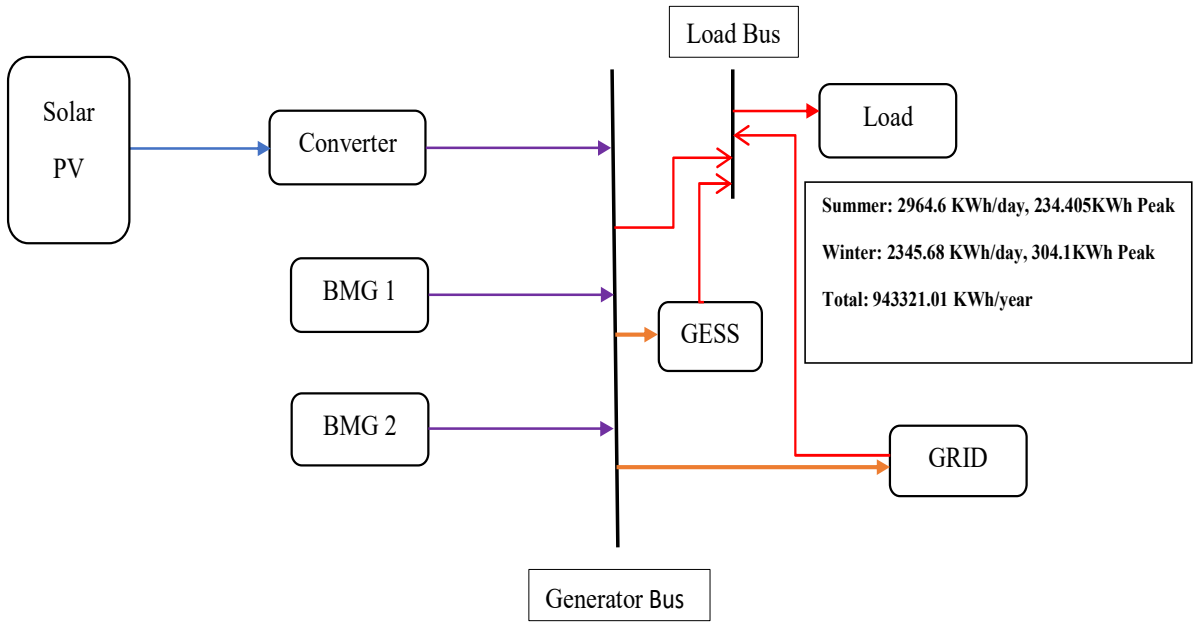

Figure 3.2.1. Proposed Grid-connected solar PV-BMG-GESS-based Microgrid

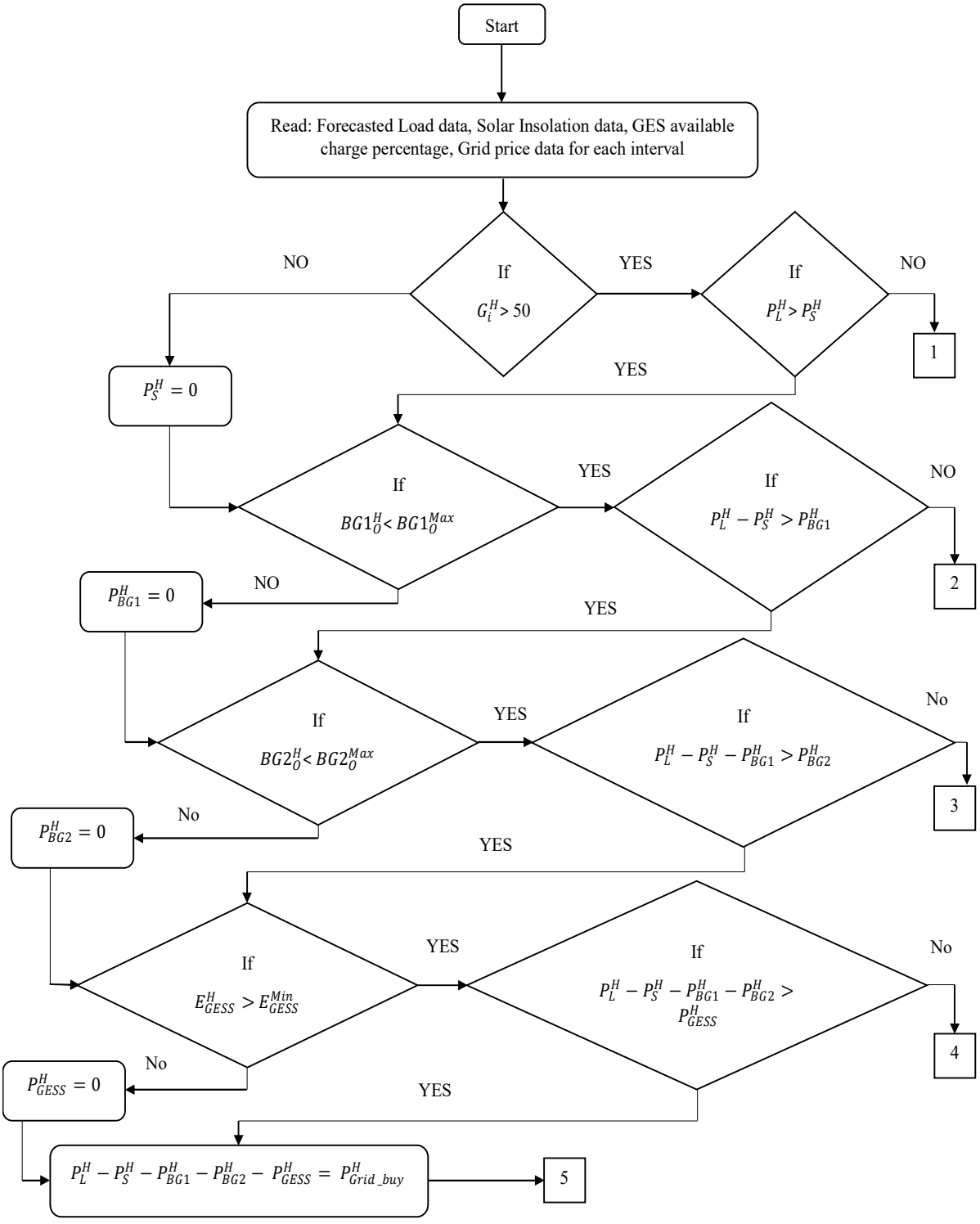

Figure 3.2.2. Operation Strategy of the Proposed System (PART-I)

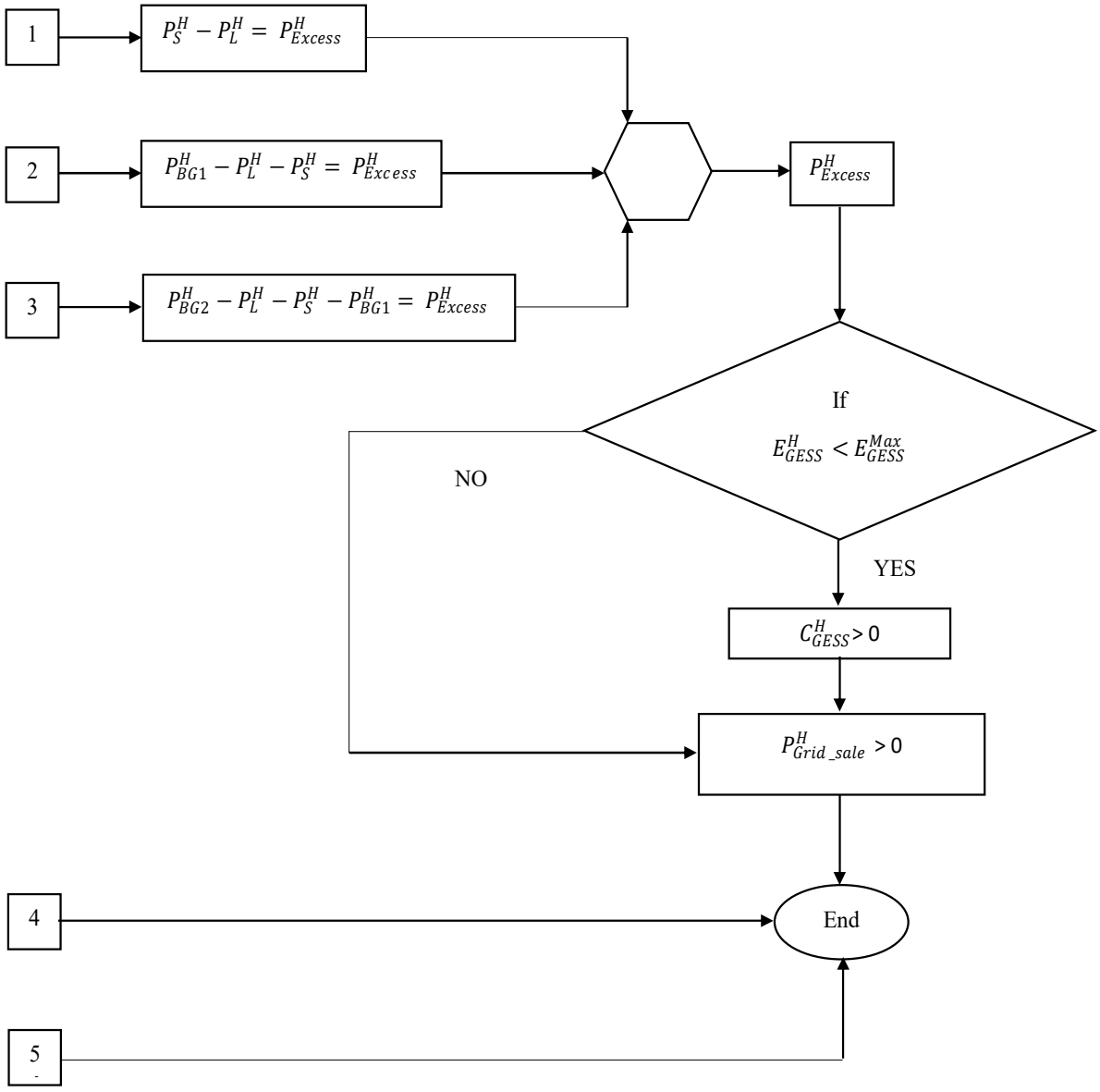

Figure 3.2.3. Operation Strategy of the Proposed System (PART-II)

3.2.4. Mathematical Modelling of Solar PV Biomass and GESS System

The system thus proposed is based on a grid connected microgrid concept. In this section detailed mathematical analysis of different resources and storage system will be discussed.

3.2.4.1. Solar PV

The Solar PV system has been modelled in accordance to its ambient temperature and hourly solar irradiance level of the desired location [129]. The power output at maximum power point is calculated as in Eq. 3.2.1. [129]

$$P_S^H = N_{PV}^S . N_{PV}^P . \left[P_S^{STC} . \frac{G_i^H}{G^{STC}} \{1 - \alpha (T_c - T_c^{STC})\} \right] \quad (3.2.1)$$

Where, $' P_S^H '$ is the hourly load served through solar PV modules (kW). $' N_{PV}^S '$ and $' N_{PV}^P '$ are the number of solar panels in series and parallel respectively. $' P_S^{STC} '$ is power generated from single solar panel at Standard Test Conditions (STC). $' G_i^H '$ and $' G^{STC} '$ is the hourly solar irradiance at 'i^{th}' hour and solar irradiance at STC. Temperature coefficient of solar modules is presented by $' \alpha '$. Cell temperature of solar module is $' T_c '$ and nominal cell temperature at STC is $' T_c^{STC} '$. The hourly power output from solar PV generator is dependent on the cell temperature of panels available as shown in Eq. 3.2.1. The cell temperature at any given time is dependent on the nominal operating cell temperature (NOCT) and air temperature of the panel. In Eq. 3.2.2 the cell temperature calculation is shown [129]. Wind speed of the surrounding is considered to be 1m/s.

$$T_c = T_a^{NOCT} + \frac{G_i^H}{G^{NOCT}} (NOCT - 20) \quad (3.2.2)$$

Where, $' T_a^{NOCT} '$ and $' G^{NOCT} '$ are ambient air temperature and solar irradiance at NOCT respectively.

3.2.4.2. Biomass Generator

Biomass generator is considered to be at second priority in dispatching the load demand in absence or non-adequate availability of solar resource. A biomass generator converts combustible biomass resources into producer gas in controlled air using partial combustion. Producer gas is utilized to generate electricity through combustion engine. The maximum installation capacity of a biomass generator in a particular area mainly depends on the availability of raw material in the installation zone. The mathematical equation of maximum installation capacity is shown in Eq. 3.2.3 [114].

$$P_{BG}^{max} = P_{BG}^{H} = \frac{\eta_{BG} * M_{BM} * 1000 * C_{BM}}{365 * 860 * H_{BG}} \quad (3.2.3)$$

Where, the maximum installation capacity of biomass generator is $' P_{BG}^{max} '$ in kW. Hourly generation from biomass generator is $' P_{BG}^{H} '$. Efficiency of biomass generator $' \eta_{BG} '$ is 21%. Tons of biomass available per year in the study area is $' M_{BM} '$. Calorific value of biomass is $' C_{BM} '$ in kcal/kg and maximum operation time of a biomass generator in a day $' H_{BG} '$ is 12 hrs. Biomass generators can be operated for a fixed time interval in a day. Excess operation may lead to lifetime reduction of the generator itself. Thus, total generation from biomass generator limited to certain amount related to operating hour and maximum installed capacity. However, in this work, Biomass generator is utilized in its full capacity whenever the generator is in operation. Excess energy generated is either stored in the GESS or sold to the grid. This enables maximum utilization of biomass resource and monetary benefit in terms of overall energy cost of the system.

In this study two different biomass generators are considered. According to the MNRE (Ministry of New and Renewable Energy), Govt. of India, Phek district has surplus agro-residues of 14.2 kT/Year. Also, the district has surplus biomass potential of 73.5 kT/Year from forest and wasteland. The cumulative energy generation capability through biomass of Phek is at 12 MWe [130]. The location is selected due to its availability of biomass and solar resources. Also, authentic data on population is readily available.

3.2.4.3. Gravity Energy Storage System

There are several matured gravity-based energy storages like PSH is available currently, but huge amount of land and water requirement make PSH difficult to install in any terrain. Overcoming this drawbacks Gravitricity proposed a new modern gravity energy storage [96]. Unlike a PSH it requires lower land area and easy to install in any terrain. Also, in comparison to several other energy storage devices (Chemical, gravity-based, mechanical etc.) the GESS is comparatively cheaper and easy to operate. GESS utilizes a suspended weight to be drawn against the gravity and released with gravitational pull to generate energy using a DC motor and converter system. The system is divided in three major parts; the suspended weight, motor system and wire to suspend the weight.

3.2.4.4. The Suspended weight of the GESS

There may be different shapes of the suspended weight. Due to calculation simplicity, a cylindrical weight is assumed. Let us assume the weight is suspended underground in a vertical tunnel of depth $'D^T'$. If the cylindrical object is having a height $'H^{SW}'$, diameter $'d^{SW}'$,then the volume of the object $' V^{SW} '$ is:

$$V^{SW} = \frac{\pi {d^{SW}}^2 H^{SW}}{4} \tag{3.2.4}$$

As we know for any object with density $'\rho^{SW}'$, the mass of the object $'M^{SW} = \rho^{SW} V^{SW}'$. Therefore, the usable depth of the GESS $' D^{GESS} '$ is:

$$D^{GESS} = D^T - H^{SW} = D^T - \frac{4M^{SW}}{\pi {d^{SW}}^2 \rho^{SW}} \tag{3.2.5}$$

The maximum energy storage capacity $'E_{GESS}^{max}'$ with a roundtrip efficiency $'\eta^{GESS} = 0.8'$ [97] is:

$$E_{GESS}^{max} = \eta^{GESS} M^{SW} g D^{GESS} = \eta^{GESS} M^{SW} g \left(D^T - \frac{4M^{SW}}{\pi {d^{SW}}^2 \rho^{SW}} \right) \tag{3.2.6}$$

In comparison within Eq. 3.2.4, 3.2.5 & 3.2.6, it is quite clear that the mass of the suspended weight is directly proportional to the height of the same. Whereas, the increasing height of the suspended weight inversely impacts the usable depth of GESS. Thus, energy storage capacity of GESS per unit mass of the suspended weight may be formulated as:

$$\frac{dE^{GESS}}{dM^{SW}} = \eta^{GESS} g \left(D^T - \frac{8M^{SW}}{\pi d^{SW} \rho^{SW}} \right) \tag{3.2.7}$$

3.2.4.5. Motor and Associated System of the GESS

The suspended weight is to be drawn by the motor connected to it. Let us assume the force $'F^M'$ is required to pull the suspended weight against gravity at an acceleration $'a = \frac{dv}{dt}'$. Thus, the amount of force required is:

$$F^M = M^{SW}(g + a) \tag{3.2.8}$$

For a motor of torque $'T^m'$ with radius of the traction sheave $'R_s'$ and rotational inertia $' J'$ The differential equation for the motion is:

$$T^m = F^M R_s + J\frac{d\omega}{dt} = M^{SW} R_s (g + a) + a\frac{J}{R_s} \tag{3.2.9}$$

Where the angular velocity $'\omega = \frac{v}{R_s}'$ and thus, the motor power output is:

$$P_m = \omega T^m = M^{SW} v(g + a) + va\frac{J}{R_s{}^2} = M^{SW} vg + va\left(M^{SW} + \frac{J}{R_s{}^2}\right) \quad (3.2.10)$$

Thus, to maintain the motor speed at constant, the steady state power $'P_m{}^{SS}'$ required may be calculated from Eq. 3.2.10 by replacing the value of $'a = 0'$. Therefore, the steady state power is as given elsewhere is [97]:

$$P_m{}^{SS} = M^{SW} vg \quad (3.2.11)$$

3.2.4.6. Connecting Wires and Ropes of the GESS

Wire rope is used to connect the suspender weight with the motor drive system. The weight of the wire is comparatively lower in comparison to the suspended weight itself. But is practical scenario the weight of the rope is bound to impact the overall system performance. Thus, it is important to design the rope accordingly.

To draw a suspended weight with a maximum acceleration of $'\bar{a}'$, the cross-sectional area of the rope is calculated as [97]:

$$A_{Wire} = \frac{M^{SW}(g+\bar{a})}{\bar{\sigma}_{wire} - L_{wire}\rho_{wire}(g+\bar{a})} \quad (3.2.12)$$

Where, $'\bar{\sigma}_{wire}'$ is the tensile strength and $'\rho_{wire}'$ is the density of the material. For a rope of length $'L_{wire}'$, the mass of the rope maybe calculated as:

$$M_{wire} = \rho_{wire} A_{Wire} L_{wire} \quad (3.2.13)$$

The wire may be made of different materials such as steel ($\bar{\sigma}_{wire} = 896\ MPa$, $\rho_{wire} = 4706\ Kg/m^3$), iron ($\bar{\sigma}_{wire} = 230 - 345\ MPa$, $\rho_{wire} = 7874\ Kg/m^3$) etc. In Section 4 load, resource availability and cost data of equipment is discussed.

3.2.5. Real Data Accusation for System Evaluation

One of the most important parts of the proposed work is the data support. There are several series of data required such as load, solar irradiance, biomass production capability etc. Along with that, cost related data for solar PV and allied system, Biomass generator, GESS, labour wage, grid price etc. is very much important. In case of the load variation a probabilistic approach is adhered considering the number of household and basic public amenities such as primary and secondary school, primary health care, community lighting etc. Also, to determine a probable realistic impact, several load and GESS initial storage variation study is performed in this literature.

3.2.5.1. Design of Load Data

The proposed system is studied in Khezhakeno village in Phek District of Nagaland state of India. According to the Census of India for the state of Nagaland 2011, the studied area is having a total of 606 households and 483 child population within an age of 0-6 years. Number of electrical equipment present in the system in domestic, community and commercial entities is presented in Table 3.2.1 along with their respective wattage. In Table 3.2.2 basic load distribution of the system in an hourly basis is shown for domestic consumers. Basic load distribution for commercial and community consumers in an hourly basis is shown in Table 3.2.3. Graphical representation of total load demand variation is shown in Figure 3.2.4.

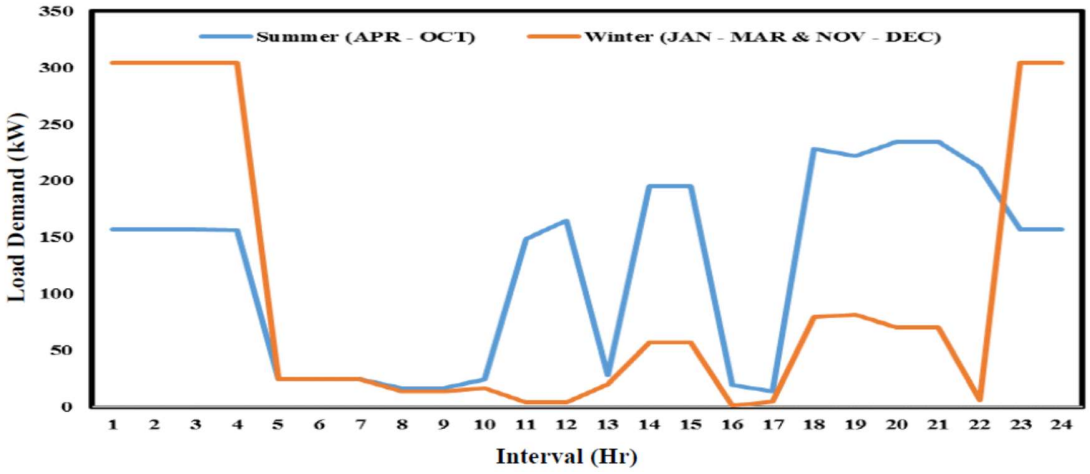

Figure 3.2.4. Hourly Load Variation (KW) during Summer and Winter Season for Studied Area

TABLE 3.2.1. EQUIPMENT DISTRIBUTION IN DIFFERENT CONSUMERS

Load Type	**Domestic**						**Community**			
Entity Type	**Household (606 Nos.)**						**Primary School (3 Nos.)**		**Secondary School (1 No.)**	
Item	LED Tube	Fan	TV	Radio	Refrigerator	Heater	LED Tube	Fan	LED Tube	Fan
Wattage	20	75	90	25	160	1500	20	75	20	75
Nos. per Entity	4	3	-	-	-	-	15	10	30	20
Total Number of equipment	2424	1818	300	500	100	200	45	30	30	20

Load Type	**Community**					**Commercial**	
Entity Type	**Primary Health Care 1 (2 Nos.)**		**Primary Health Care 2 (1 Nos.)**		**Street Light**	**Shop (50 Nos.)**	
Item	LED Tube	Fan	LED Tube	Fan	LED Bulb	LED Tube	Fan
Wattage	20	75	20	75	20	20	75
Nos. per Entity	10	6	5	3	-	2	1
Total Number of equipment	20	12	5	3	200	100	50

TABLE 3.2.2. BASIC LOAD DISTRIBUTION IN HOURLY BASIS FOR DOMESTIC CONSUMERS

	Domestic (Summer / Winter) kW						
Interval	**LED Tube**	**Fan**	**TV**	**Radio**	**Refrigerator**	**Heater**	**Total**
1	0 / 0	136.35 / 0	0 / 0	0 / 0	16 / 0	0 / 300	152.35 / 300
2	0 / 0	136.35 / 0	0 / 0	0 / 0	16 / 0	0 / 300	152.35 / 300
3	0 / 0	136.35 / 0	0 / 0	0 / 0	16 / 0	0 / 300	152.35 / 300
4	0 / 0	136.35 / 0	0 / 0	0 / 0	16 / 0	0 / 300	152.35 / 300
5	24.24 / 24.24	0 / 0	0 / 0	0 / 0	0 / 0	0 / 0	24.24 / 24.24
6	24.24 / 24.24	0 / 0	0 / 0	0 / 0	0 / 0	0 / 0	24.24 / 24.24
7	24.24 / 24.24	0 / 0	0 / 0	0 / 0	0 / 0	0 / 0	24.24 / 24.24
8	0 / 0	0 / 0	0 / 0	12.5 / 12.5	0 / 0	0 / 0	12.50 / 12.50
9	0 / 0	0 / 0	0 / 0	12.5 / 12.5	0 / 0	0 / 0	12.50 / 12.50
10	0 / 0	0 / 0	0 / 0	12.5 / 12.5	0 / 0	0 / 0	12.50 / 12.50
11	0 / 0	136.35 / 0	0 / 0	0 / 0	0 / 0	0 / 0	136.35 / 0
12	0 / 0	136.35 / 0	0 / 0	0 / 0	16 / 0	0 / 0	152.35 / 0
13	0 / 0	0 / 0	0 / 0	0 / 0	16 / 16	0 / 0	16 / 16
14	0 / 0	136.35 / 0	27 / 27	12.5 / 12.5	16 / 16	0 / 0	191.85 / 55.50
15	0 / 0	136.35 / 0	27 /27	12.5 / 12.5	16 / 16	0 / 0	191.85 / 55.50
16	0 / 0	0 / 0	0 / 0	0 / 0	16 / 0	0 / 0	0 / 0

17	0 / 0	0 / 0	0 / 0	12.5 / 0	0 / 0	0 / 0	12.50 / 0
18	48.48 / 48.48	136.35 / 0	27 / 27	12.5 / 0	0 / 0	0 / 0	224.33 / 75.48
19	48.48 / 48.48	136.35 / 0	27 / 27	0 / 0	0 / 0	0 / 0	211.83 / 75.48
20	48.48 / 24.24	136.35 / 0	27 / 27	12.5 / 12.5	0 / 0	0 / 0	224.33 / 63.74
21	48.48 / 24.24	136.35 / 0	27 / 27	12.5 / 12.5	0 / 0	0 / 0	224.33 / 63.74
22	48.48 / 0	136.35 / 0	0 / 0	0 / 0	16 / 0	0 / 0	200.83 / 0
23	0 / 0	136.35 / 0	0 / 0	0 / 0	16 / 0	0 / 300	152.35 / 300
24	0 / 0	136.35 / 0	0 / 0	0 / 0	16 / 0	0 / 300	152.35 300

TABLE 3.2.3. BASIC LOAD DISTRIBUTION IN HOURLY BASIS FOR COMMUNITY AND COMMERCIAL CONSUMERS

	Community (Summer / Winter) kW					**Commercial (Summer / Winter) kW**	
Interval	**Primary School**	**Secondary School**	**Primary Health Care 1**	**Primary Health Care 2**	**Street Light**	**Shop**	**Total**
1	0 / 0	0 / 0	0 / 0	0.325 / 0.1	4 / 4	0 / 0	4.325 / 4.1
2	0 / 0	0 / 0	0 / 0	0.325 / 0.1	4 / 4	0 / 0	4.325 / 4.1
3	0 / 0	0 / 0	0 / 0	0.325 / 0.1	4 / 4	0 / 0	4.325 / 4.1
4	0 / 0	0 / 0	0 / 0	0 / 0	4 / 4	0 / 0	4 / 4
5	0 / 0	0 / 0	0 / 0	0 / 0	0 / 0	0 / 0	0 / 0
6	0 / 0	0 / 0	0 / 0	0 / 0	0 / 0	0 / 0	0 / 0
7	0 / 0	0 / 0	0 / 0	0 / 0	0 / 0	0 / 0	0 / 0
8	2.85 / 0.9	0 / 0	1.3 / 0.4	0 / 0	0 / 0	0 / 0	4.15 / 1.3

9	2.85 / 0.9	0 / 0	1.3 / 0.4	0 / 0	0 / 0	0 / 0	4.15 / 1.3
10	2.85 / 0.9	2.1 / 0.6	1.3 / 0.4	0 / 0	0 / 0	5.75 / 2.0	12.0 / 3.9
11	2.85 / 0.9	2.1 / 0.6	1.3 / 0.4	0 / 0	0 / 0	5.75 / 2.0	12.0 / 3.9
12	2.85 / 0.9	2.1 / 0.6	1.3 / 0.4	0 / 0	0 / 0	5.75 / 2.0	12.0 / 3.9
13	2.85 / 0.9	2.1 / 0.6	1.3 / 0.4	0 / 0	0 / 0	5.75 / 2.0	12.0 / 3.9
14	0 / 0	2.1 / 0.6	1.3 / 0.4	0 / 0	0 / 0	0 / 0	3.4 / 1.0
15	0 / 0	2.1 / 0.6	1.3 / 0.4	0 / 0	0 / 0	0 / 0	3.4 / 1.0
16	0 / 0	2.1 / 0.6	1.3 / 0.4	0 / 0	0 / 0	0 / 0	3.4 / 1.0
17	0 / 0	0 / 0	1.3 / 0.4	0 / 0	0 / 4	0 / 0	1.3 / 4.4
18	0 / 0	0 / 0	0 / 0	0 / 0	4 / 4	0 / 0	4 / 4
19	0 / 0	0 / 0	0 / 0	0.325 / 0.1	4 / 4	5.75 / 2.0	10.075 / 6.1
20	0 / 0	0 / 0	0 / 0	0.325 / 0.1	4 / 4	5.75 / 2.0	10.075 / 6.1
21	0 / 0	0 / 0	0 / 0	0.325 / 0.1	4 / 4	5.75 / 2.0	10.075 / 6.1
22	0 / 0	0 / 0	0 / 0	0.325 / 0.1	4 / 4	5.75 / 2.0	10.075 / 6.1
23	0 / 0	0 / 0	0 / 0	0.325 / 0.1	4 / 4	0 / 0	4.325 / 4.1
24	0 / 0	0 / 0	0 / 0	0.325 / 0.1	4 / 4	0 / 0	4.325 / 4.1

3.2.5.2. Solar Insolation and PV Panel Cost

Daily solar insolation data for the studied area is considered to find the PV panels output. The studied area is at longitude $94.2167° E$ and latitude $25.5186° N$. Solar irradiation data and temperature data are collected from Photovoltaic Geographical Information System [131]. The daily average solar irradiance data and average temperature profile is shown in Figure 3.2.5 and Figure 3.2.6 respectively.

The solar PV panels hence considered are of maximum generation capacity of 335 Watt (Wp). The system also includes on-grid solar inverter and all allied infrastructural requirements including installation cost [132]. Cost of Solar PV system is 549 $ / kW[2] without government subsidy and 384.30 $ / kW [132] with subsidy for the same. The operation and maintenance cost of solar panels is 4$/kW and inverter 1.34$/kW [114].

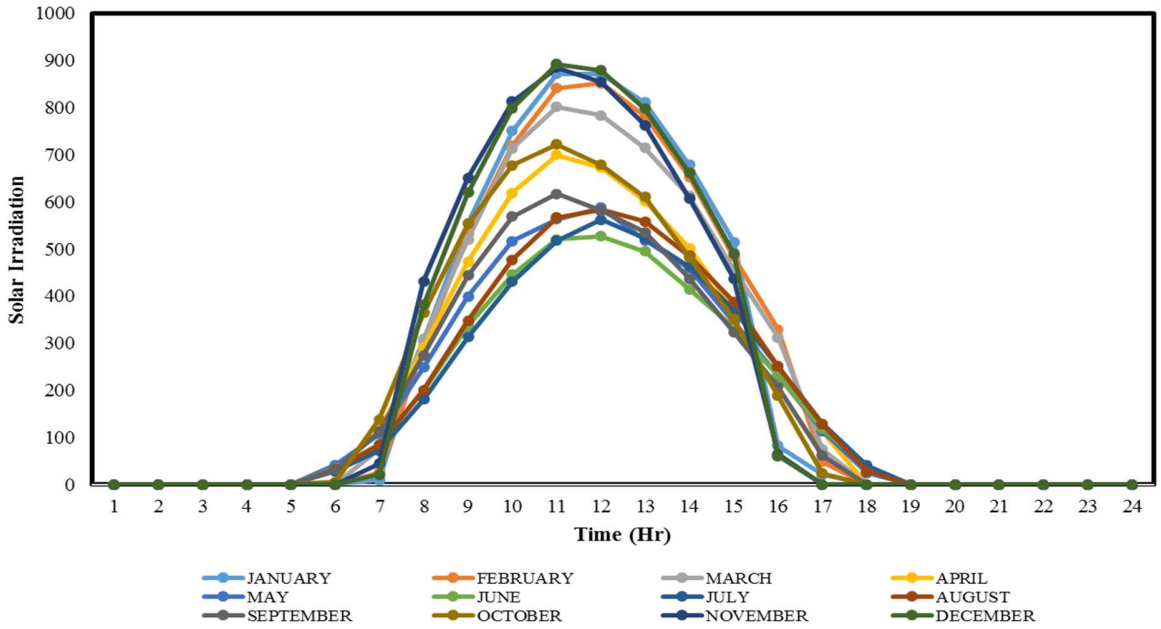

Figure 3.2.5. Daily Average Solar Irradiation Data (W/m^2)

[2] 1$ = Rs. 70 (Assumed)

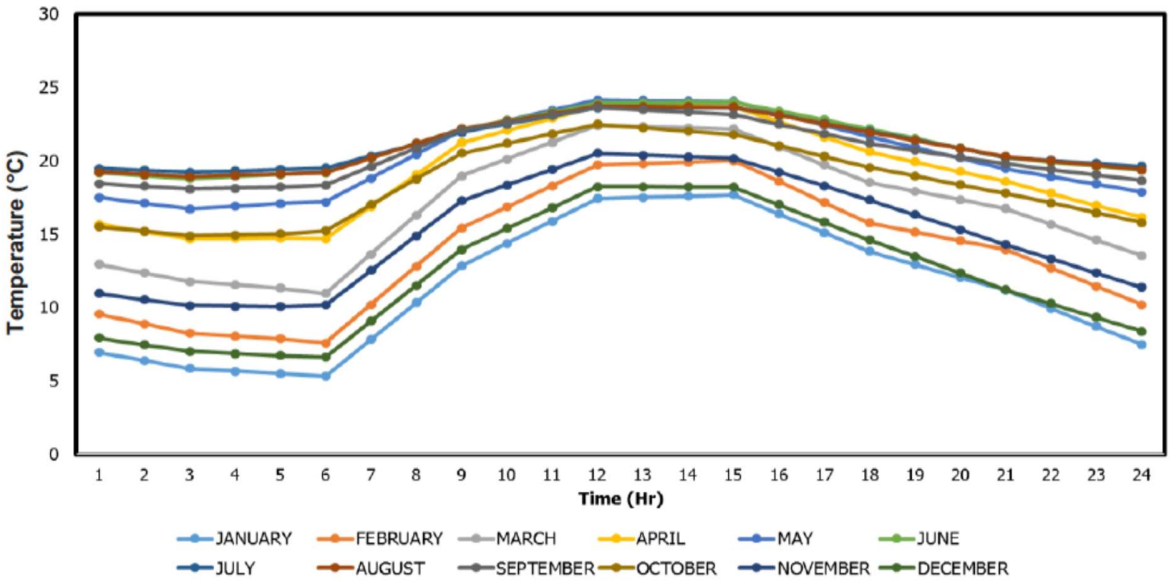

Figure 3.2.6. Daily Average Temperature Profile (^{0}C)

3.2.5.3. Biomass Generator Cost

Biomass generator installation cost is considered to be 1111.24 $ /kW, inflation adjusted and yearly maintenance cost is 4.5% of the installation cost [133]. Locally available biomass is used as fuel to the generator and charged as 0.04 $ / kg [133]. The amount of biomass required to generate energy is 1.2 kg / kWh [133]. In this study two biomass generators are considered.

3.2.5.4. GESS Cost

The GESS does consist of cost of the suspended weight, Motor and allied system, Ropes etc. However, most of the investment cost consists of excavation charges for an underground vertical tunnel and corresponding concrete structure. According to Gravitricty, the levelized cost of storage is 141 $/ kW-year [96], which includes investment, charging, O&M & replacement cost.

3.2.5.5. Labor Cost

According to the Govt. of India norms, the studied area resides in category ‘C’. Thus, the minimum wage for industrial worker stands at Rs. 569 / day or 8.13$ / day [134]. Therefore, the wage for

labour is considered at 3000 $ / Year. In this study, 3 numbers of industrial worker are taken into consideration for maintenance and allied works.

3.2.5.6. Energy transaction cost of Grid

The cost of energy transacted with the grid is considered from the data available from the website of Indian energy Exchange (IEX). Hourly energy rate is taken from the historically available data for 15th of each month for the entire period of the year 2019 [135]. If the 15th day is weekend or holiday, next weekday is considered. The hourly grid price for each month of the year 2019 is represented in Figure 3.2.7 [135]. The system operation is needed to be optimized to ensure best operation scenario. Thus, in Section 3.2.5 two objective functions are considered to be optimized using the Whale Optimization algorithm.

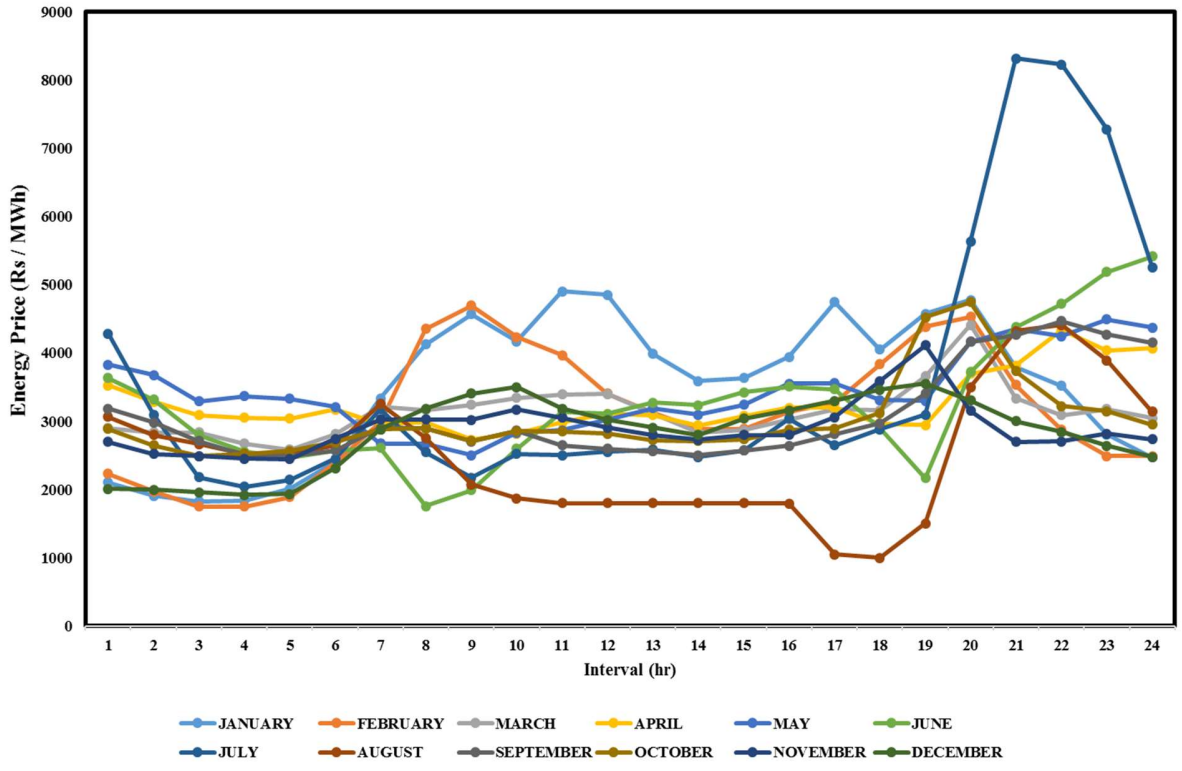

Figure 3.2.7. Hourly Grid Price for Each Month of the Year 2019

3.2.6. Objective Function for System Optimization

This study is based on a multi-objective scenario. Two objectives with equal weightage are considered here. The first objective is the Levelized cost of energy (LCOE) and the second objective is the amount of energy drawn from the grid. As the aim of this study is to propose a GESS based self-sustainable renewable energy based microgrid, it is important to minimise the energy drawn from the grid as much as possible. Also, the LCOE of the system needs to be lower or at par with current energy price of the location. To keep the LCOE, lower excess energy is transacted to the grid for monetary benefit. The LCOE is calculated as:

$$LCOE = \frac{C_{Capital}^{Annual} + C_{O\&M}^{Annual} + C_{Biomass\_fuel}^{Annual} + C_{GESS}^{Annual} + C_{Grid\_P}^{Annual} + C_{Labour}^{Annual} - C_{Grid\_S}^{Annual}}{P_{Load\_served}^{Annual}} \quad (3.2.14)$$

The annualized capital cost ($C_{Capital}^{Annual}$) consists of solar PV ($C_{Capital}^{Solar}$)and Biomass generator ($C_{Captital}^{Biomass}$)installation cost. The capital cost of solar PV ($C_{Capital}^{Solar}$) is dependent on the solar panel, inverter and allied services in ready to use format [132] and is shown in Eq. 3.2.15.

$$C_{Capital}^{Solar} = \frac{C_{Per\_KW}^{Solar} * P_{STC}^{Solar} * N_{Panel}^{Solar}}{1000} \quad (3.2.15)$$

Where, $C_{Per\_KW}^{Solar}$ is the cost of solar panel, inverter and allied services per kW in dollar. Solar panel output at STC (P_{STC}^{Solar}) in Watt. Total number of installed solar panel is represented by N_{Panel}^{Solar}. Capital cost of biomass generator ($C_{Capital}^{Biomass}$) is calculated in Eq. 4.16.

$$C_{Capital}^{Biomass} = C_{Per\_KW}^{Biomass} * P^{Biomass} \quad (3.2.16)$$

Where, per kW installation cost of biomass generator is represented by $C_{Per\_KW}^{Biomass}$ and installed capacity of biomass generator is $P^{Biomass}$.

Hence, annualized cost of installation is represented as [114]:

$$C_{Capital}^{Annual} = \left(C_{Capital}^{Solar} + C_{Captital}^{Biomass}\right) * CRF \quad (3.2.17)$$

Where, CRF is the capacity utilization factor and is represented as:

$$CRF = \frac{R(1+R)^N}{(1+R)^{N-1}} \quad (3.2.18)$$

Where, 'R' is the rate of interest and 'N' is the lifetime.

The annual operation and maintenance cost of equipment ($C_{O\&M}^{Annual}$) is calculated as:

$$C_{O\&M}^{Annual} = \left(C_{O\&M}^{Solar} * P_{Installed}^{Solar}\right) + \left(C_{O\&M}^{inv} * P_{Installed}^{inv}\right) + \left(C_{O\&M}^{Biomass} * P_{Installed}^{Biomass}\right) \quad (3.2.19)$$

Where, annual O&M cost per kW of solar PV, inverter and Biomass generator installed is represented as $C_{O\&M}^{Solar}$, $C_{O\&M}^{inv}$ and $C_{O\&M}^{Biomass}$ respectively. The installed capacity is represented as $P_{Installed}^{Solar}$, $P_{Installed}^{inv}$ and $P_{Installed}^{Biomass}$ respectively.

Annual fuel cost of Biomass generator may be calculated as:

$$C_{Biomass\_fuel}^{Annual} = C_{Fuel}^{Biomass} * W_{Fuel}^{Biomass} * E_{Biomass}^{Annual} \quad (3.2.20)$$

Where, Cost of per kg of biomass is '$C_{Fuel}^{Biomass}$' , Weight of biomass required to generate each kW of energy is $W_{Fuel}^{Biomass}$ and annual energy production per kW from Biomass generator is presented as $E_{Biomass}^{Annual}$.

Levelized cost of Energy (LCOE) is considered as the objective function. The final objective function may be defined as:

$$Minimize\ (A) = LCOE \quad (3.2.21)$$

In this study, the number of solar panels in series and parallel, sizes of two biomass gasifier and GESS storage capacity is taken as variables. The minimum and maximum ranges of each equipment are tabulated in Table 3.2.4. The Whale Optimization Algorithm (WOA) is then applied to determine the minimum LCOE during operation of the system while satisfying every technical aspect. The next section discusses the mathematical modelling of Whale optimization algorithm. The WOA is discussed in Chapter 4.

TABLE 3.2.4. MINIMUM AND MAXIMUM LIMIT OF VARIABLES

Sl. No.	Parameters / Variables	Minimum	Maximum
1	Solar PV Modules in Series (Nos.)	0	30
2	Solar PV Modules in Parallel (Nos.)	0	30
3	Biomass Generator 1 (kW)	0	100
4	Biomass Generator 2 (kW)	0	100
5	GESS Storage Capacity (kW)	0	1000

The simulated results of this section (section 3.2) are discussed in section 5.2.
This section techno-economically optimized a hybrid micro-grid with a meta-heuristic algorithm. Both researches depicted in section 3.1 and 3.2 have used multi renewable resources to provide continuous flow of energy. But generating continuous electrical energy from a single renewable resource is challenging. That challenge has been innovatively handled in section 3.3 and 3.4.

3.3. A dual mode Wind Turbine operation with Hybrid Energy Storage System incorporating Vanadium Redox Flow Battery and Pump Storage Hydro

A novel dual mode wind turbine driven hybrid energy storage scheme with electromagnet-based mode changing operation is proposed in this section. The hybrid storage system includes a pump storage hydro and a vanadium redox flow battery. The proposed system provides uninterrupted energy at stable voltage to consumers in an isolated microgrid. The system is capable in handling different effects of wind speed related uncertainties at the load end, up to a certain limit. Advantages of the system lies in its reliability, operation simplicity, robustness and energy output at stable voltage irrespective of normal wind speed variation. The proposed system also provides an idea of efficient usage of renewable energy. This section deals with the proposed system structure, operation strategy, mathematical modelling; also simulates result using real wind speed data and shows that the system is viable, upon simulation with a variable loading pattern.

3.3.1. The Proposed Dual Mode Wind Turbine – Pump Storage Hydro – Vanadium Redox Flow Battery Hybrid System Description

The proposed DMWT – PSH – VRFB system has two operating modes, namely

(i) Mechanical Mode
(ii) Electrical Mode.

Mechanical mode of the system is shown in Figure 3.3.1 and Electrical mode in Figure 3.3.2. As observed from Figure 3.3.1 and Figure 3.3.2 the DMWT is solely utilized to charge those storage devices. In the Mechanical mode (Figure 3.3.1), the energy *i.e.* mechanical energy extracted from DMWT shaft is used to operate a mechanically driven CP. The CP pumps water to UR of the PSH from lower reservoir (LR). The LR may be a pond, well or any other similar water body. In absence of such water body, a LR needs to get constructed with the volume of water storage at least be equal to the volume of UR. In the Electrical mode; mechanical energy extracted from DMWT shaft is utilized to operate a wind turbine alternator and the electrical energy generated is stored in the VRFB. The inward and outward energy flow from VRFB is controlled through a converter.

The mode changing operation takes place at the starting of any interval. During the Electrical mode, water stored in UR of the PSH is utilized to generate electrical energy at stable voltage and the VRFB gets charged through the DMWT. During this mode of operation, when the water level in UR goes below certain limit where the PSH cannot support the demand, the operation changes to Mechanical mode. The CP operates only during the Mechanical mode, and the mode continues till water level in the UR is above a certain limit where the PSH is able to supply the system load for the next interval. During this interval, predominantly the VRFB supports the demand. However, if during an interval, the water level in UR reaches above the certain limit or even the UR is completely filled up, the operation continues in mechanical mode till the interval is finished. In the next interval, the DMWT operation switches to Electrical mode.

In Mechanical mode, PSH and VRFB (if charge available) both may supply the load, while in Electrical mode, PSH only can supply the load. This is due to the fact that VRFB cannot charge and discharge at the same time. The proposed DMWT – PSH – VRFB system operates in Electrical mode, only when the water level in UR is above the certain limit, where it can supply the load demand for the next interval and VRFB has state – of – charge (SOC) lesser than maximum. However, if the SOC of the VRFB is at maximum and water level in UR is above the certain limit, where it can support the demand of the next interval, the system operates in Mechanical mode. Details of the proposed system operation is shown in Section 3.3.3.

Several parts of the proposed system are as follows -

i. The Dual mode wind turbine (without alternator and converter) and mechanical transmission system (efficiency = 0.8)
ii. Rotating mechanical part, connecting mechanical transmission system with CP, namely: **"MR"**
iii. The PSH, including CP, LR, UR, water turbine generator and pipes
iv. Rotating mechanical part, connecting mechanical transmission system with alternator, namely: **"ER"**
v. The alternator (to be operated in Electrical mode), converter and VRFB
vi. Control Unit
vii. Fixed connecting rod, connected between **MR** and **ER**, namely**: "FR"**

viii. Mode changer spring with hook, namely: **"MCS"**

ix. Mode changer electromagnet and magnetic material strip, namely: **"MCE"**

In the Electrical mode, the electromagnet "MCE" remains non-operational as shown in **Figure 3.3.2** using dotted lines. Due to absence of any attractive force, the mode changer spring "MCS" retains its normal position. The upward force exerted by "MCS" gets transmitted from "MR" to the rotating mechanical part, connecting mechanical transmission system with alternator "ER" via the fixed connecting rod "FR". As a result, the assembly "MR – FR – ER" gets pulled up and "ER" gets connected with the mechanical transmission system. This establishes the connection between the DMWT and the alternator. This enables the alternator to start generation and the energy gets stored in the VRFB after AC to DC conversion in converter. In this mode VRFB does not generate any energy and the entire system load is served by the PSH. Again, at the starting of any interval, if the water level in UR is below the certain limit, where it can support the demand of the next interval, the proposed system operates in Mechanical mode as shown in **Figure 3.3.1**. In this mode, a part of the energy generated from VRFB is utilized to activate the electromagnet. As soon as the **"MCE"** becomes operational, it attracts the **"ER"** and the attraction force gets transmitted to **"MR"** via **"FR".** As a result, the assembly **"ER – FR – MR"** gets lowered. This results in disconnection of **"ER"** from the DMWT and **"MR"** gets connected. This established connection of **"MR"** with the DMWT enables the CP to operate and water gets pumped. In this mode, VRFB serves the system load. If in any case, the VRFB alone cannot serve the load, PSH serves a part of it.

It is to be noted that, the attraction force of the electromagnet **"MCE"** should be equal or higher than the force required to expand the mode changer spring **"MCS"** or in other words, the attraction force of the electromagnet should compensate the force of the mode changer spring so that the MR – FR – ER assembly comes down due to its own weight. Also, the force exerted by the mode changer spring **"MCS"** should be higher than that of the force required to move the cumulative weight / mass of the assembly **"MR – FR – ER"** as the MCE becomes non-operational.

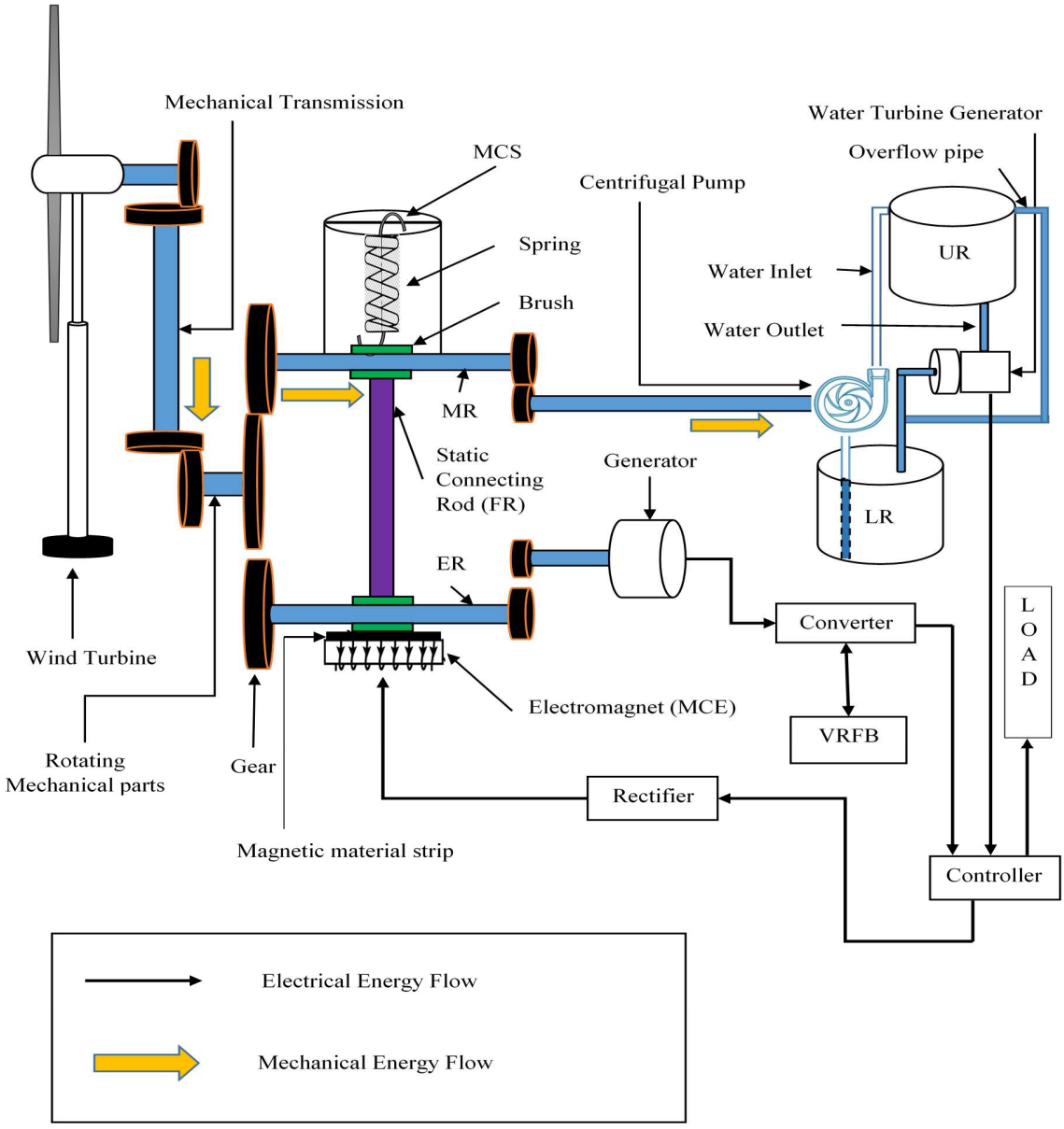

Figure 3.3.1. Mechanical Mode of the Proposed Dual Mode Wind Turbine - Pump Storage Hydro - Vanadium Redox Flow Battery System

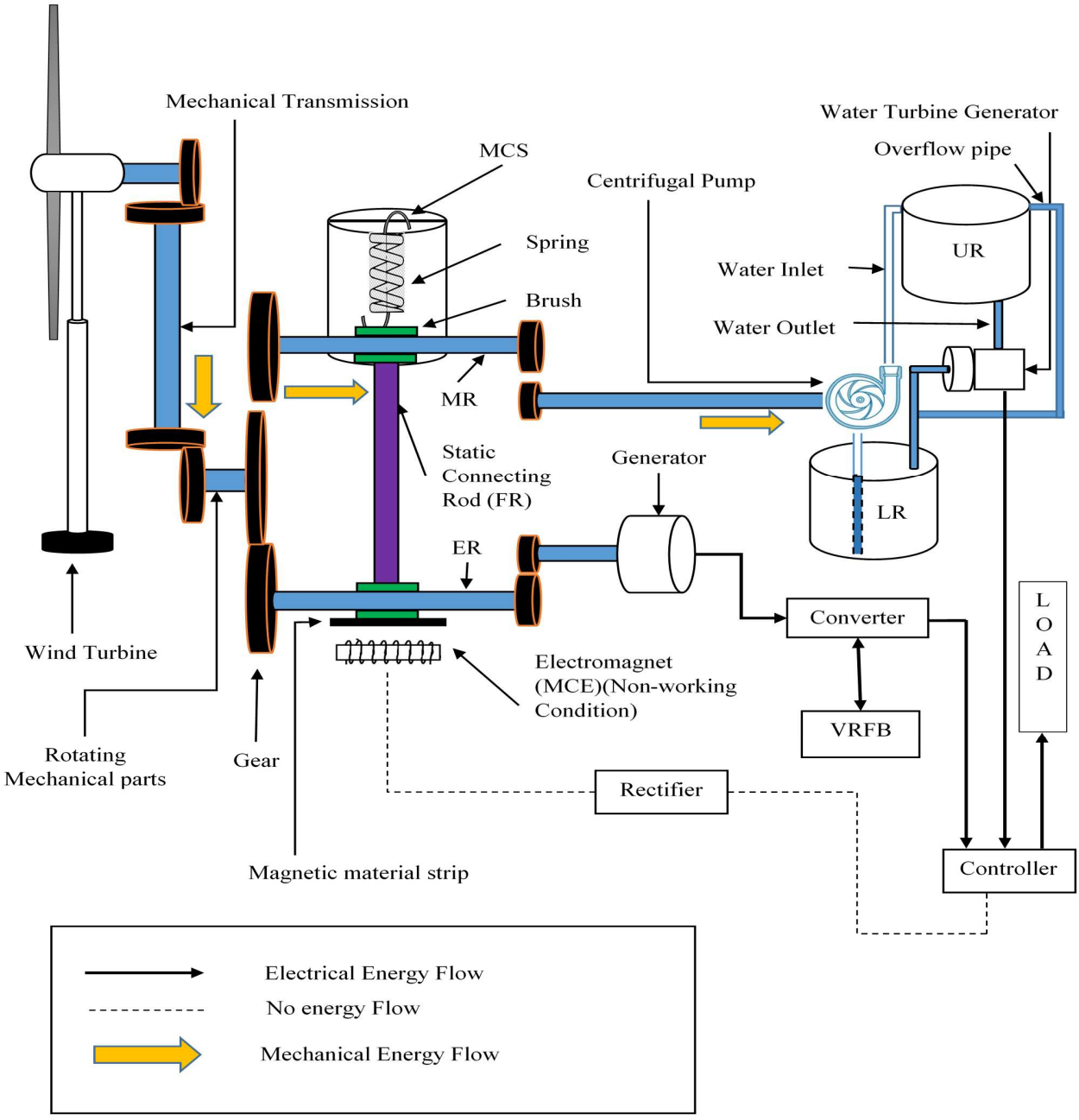

Figure 3.3.2. Electrical Mode of the Proposed Dual Mode Wind Turbine - Pump Storage Hydro - Vanadium Redox Flow Battery System

3.3.2. Operation Strategy of Different Scenarios

The proposed system operation depends on certain parameters like load demand, water level in UR and stored charge in VRFB to operate. Figure 3.3.3 depicts the flowchart of operation strategy of the proposed scheme.
The operation procedures in different conditions are as follows:

TABLE 3.3.1. DESCRIPTION OF SYSTEM OPERATION

Sl No.	Condition	Mode of Operation	Remarks
1	**i.** Water level in UR above certain limit, where it can support the demand of the next interval **ii.** VRFB is not fully charged	Electrical	**i.** PSH supports the load demand **ii.** VRFB gets charged **iii.** If charging of VRFB is completed before end of interval, excess energy is delivered to dummy load **iv.** Voltage remains stable
2	**i.** Water level in UR below a certain limit, where it can support the demand of the next interval **ii.** VRFB can supply the demand alone	Mechanical	**i.** VRFB supports the load demand **ii.** Water gets pumped to UR **iii.** If UR is completely filled during the interval, water gets spilled and collected in LR **iv.** Voltage remains stable
3	**i.** Water level in UR below a certain limit, where it can	Mechanical	**i.** PSH and VRFB together support the load demand

	support the demand of the next interval **ii.** VRFB is neither fully charged nor fully discharged **iii.** Neither PSH nor VRFB alone can support the load demand **iv.** PSH and VRFB together can support the load demand		**ii.** Water gets pumped to UR **iii.** Voltage remains stable
4	**i.** Water level in UR is above a certain limit, where it can support the demand of the next interval / water level in UR is maximum **ii.** VRFB is fully charged	Mechanical	**i.** PSH supports the load demand **ii.** Water gets pumped to UR **iii.** Voltage remains stable
5	**i.** PSH and VRFB cannot support the load demand together	Mechanical	**i.** PSH and VRFB delivers together to their maximum extent **ii.** Water gets pumped to UR **iii.** Voltage drops

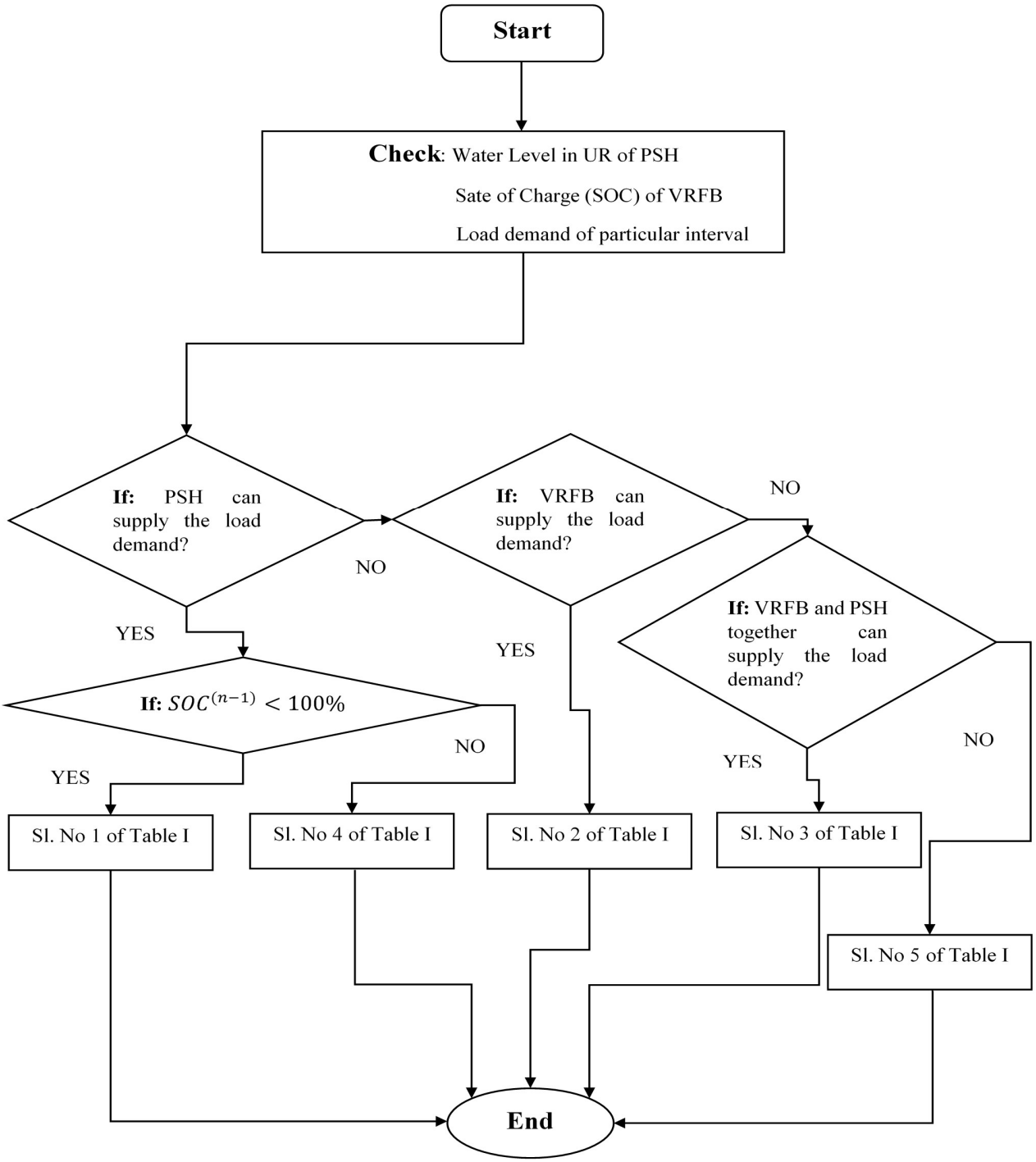

Figure 3.3.3. Operation Flowchart of the Proposed System

3.3.3. Mathematical Modelling of the Proposed DMWT – PSH – VRFB system

An elaborated concept of the proposed DMWT – PSH – VRFB system structure along with its operation strategy is discussed in Section 3.3.2 and 3.3.3 respectively. In this section the mathematical modelling of the proposed system is provided.

The DMWT is a modified arrangement of a wind turbine which enables an opportunity to maximize the uninterrupted harvesting of energy from wind source. As discussed above, depending upon the requirement, DMWT can be operated in two exclusive modes; I. Mechanical mode and II. Electrical mode. Mathematical modelling of these two modes is discussed in section 3.3.4.1 and 3.3.4.2.

Specification of DMWT considered in this study; resembles with commercially available Aeolos 10 kW Wind turbine [136]. The length of each blade is 8 m with rated wind speed as 10 m/s, cut-in speed as 2.5 m/s and survival wind speed as 45.5 m/s.

3.3.3.1. Mechanical Mode of Operation

As discussed in Section 3.3.2, the DMWT in mechanical mode converts wind energy into usable mechanical energy to operate the CP. Generated mechanical power in any instant at the shaft of the DMWT (P_{DMWT}^{Shaft}) can be mathematically expressed as:

$$P_{DMWT}^{Sha} = 0.5\pi\mu_p\rho_{air}R_{DMWT}^2V_{air}^3, \quad V_{air}^{cin} < V_{air} < V_{air}^{cout}$$
$$= 0, \quad V_{air}^{cin} > V_{air} > V_{air}^{cout} \qquad (3.3.1)$$

Equation (3.3.1) is the conventional mathematical expression for wind power extraction. Here, (μ_p) is the power coefficient, dependent on blade pitch angle and tip speed ratio (TSR) of the DMWT. The value of μ_p for modern wind turbine maybe around 50% as claimed in some literature [105]. The air density and wind speed are denoted as $'\rho_{air}'$ and $'V_{air}'$ respectively. The rotor radius of the DMWT is $'R_{DMWT}'$. Cut – in and Cut – out speed of the DMWT are $'V_{air}^{cin}'$ and $'V_{air}^{cout}'$ respectively. The produced mechanical power is transferred through a mechanical transmission system to the CP for pumping operation. The output $'P_T^O'$ produced from the transmission system is limited by its efficiency $'\eta_T'$. This can be mathematically expressed as:

$$P_T^O = \eta_T P_{DMWT}^{Shaft} \qquad (3.3.2)$$

The transmission shaft directly powers the CP; the output of the transmission system is the input $' P_{CP}^{in} '$ of the CP. Hence,

$$P_{CP}^{in} = P_T^O \qquad (3.3.3)$$

Mechanical mode of operation commences at the starting of any interval in which water level in UR is below a certain limit. Using which it can deliver the load of the next interval and terminates when the water level in UR is at certain height, at which the PSH can serve the load of the next interval. However, the operation continues until the end of the interval as no mode changeover is allowed within a particular interval. The CP pumps water to UR of the PSH.

The Pump storage hydro (PSH) system consists of an Upper reservoir (UR) of internal height 5 m stationed at a height of 30 m from ground. The rated head of the PSH is chosen as such to satisfy the rated head of commercially available 3 kW hydro turbine [137]. The PSH system is broadly divided into three subsystems, i.e. centrifugal pump, reservoirs and water turbine generator. Details of these subsystems are discussed below.

3.3.3.1.1. Centrifugal Pump of the PSH

The centrifugal pump used, should be compatible with wind turbines *i.e.* their speed should be synchronous with the cut-in and cut-out speed of DMWT. However, optimal speed of DMWT which is reflected in electrical mode of operation, has minimal significance in performance during mechanical mode.

The rotational motion of DMWT converts into the upward motion of water by virtue of the CP thus employed. Utilizing the energy from DMWT, CP sucks water from lower reservoir (LR) and stores into UR, which in turn enables the PSH to operate. The amount of water being sucked $' Q_{PSH}^{dis} '$ in m^3/s, depends on the efficiency $'\eta_{CP}'$ of CP, rated height of UR $'H_{UR}^{Rated}'$ from the ground, maximum height of UR $'H_{UR}^{Max}'$, the density of water $'\rho_{water} \approx 1000\ \mathrm{kg/m3}'$ and gravitational acceleration (g) of the place of installation (in this literature the value of gravitational acceleration is considered to be standard). The volume of water discharged into UR is as follows:

$$Q_{PSH}^{dis} = \frac{\eta_{CP} P_{CP}^{in}}{g \rho_{water} (H_{UR}^{Rated} + H_{UR}^{Max})} \qquad (3.3.4)$$

3.3.3.1.2. Reservoir Design of the PSH

The basic structure of PSH requires two reservoirs to store water. The LR may either be a natural lake or a similar water body. In the absence of such, an artificial storage tank needs to be constructed. Similarly, an UR is required to set up. The UR should be at a decent height from the LR so that the stored water gets enough potential energy which could be converted into electrical energy when released. It is to be noted that volume of LR should be equal or higher to that of the UR. Reservoirs, while constructed, requires extensive planning and survey of the geographical location. Characteristics of soil are one of the main concerns, depending on which the foundation of reservoirs needs to be designed. Also, characterization of seismic zone of the location should be taken into consideration as the system involves dealing with huge amount of low-density liquid.

In this study the internal height of UR is assumed as 5 m and it is at a height of 30 m from ground. The mathematical representation of the water level at the starting of any interval is shown in equation (3.3.6).

$$H_{UR}^{n} = H_{UR}^{n-1} + \frac{(Q_{PSH}^{dis^{n-1}} - Q_{PSH}^{release^{n-1}})}{A_{UR}} \qquad (3.3.5)$$

Water level at UR $'H_{UR}^{n}'$ at the starting of any interval $'n'$ is calculated by means of water level at the starting of the preceding interval $'H_{UR}^{n-1}'$, Water discharge into UR $'Q_{PSH}^{dis^{n-1}}'$ and water released from the UR for power generation through turbine-generator $'Q_{PSH}^{release^{n-1}}'$ during the preceding interval. The area of UR $'A_{UR}'$ is assumed as 20 m^2. Assumptions are considered purely for simulation purposes.

It should also be noted that in the last interval of the mechanical mode of DMWT if UR gets overloaded, amount of water released through the overflow vent is calculated as:

$$Q_{PSH}^{overflow} = \left[(H_{UR}^{n} \times A_{UR}) + Q_{PSH}^{dis^{n}} - Q_{PSH}^{release^{n}}\right] - (H_{UR}^{Max} \times A_{UR}) \quad (3.3.6)$$

However, from Eq. 3.3.6 it may be observed that the numerical value of water overflown from UR $'Q_{PSH}^{overflow}'$ may have a negative value, which indicates that there is no overflow from UR during that interval and a positive magnitude indicates overflow from the UR. Maximum height of UR is represented as $'H_{UR}^{Max} = 5m'$.

3.3.3.1.3. Water Turbine Generator Design of the PSH

Water from UR passes through a controlling valve to the water turbine and then gets discharged into LR. The WTG converts potential energy of water into electrical energy. The output is controlled via the rate of water flow to the turbine.
In this literature the WTG is having a maximum capacity of 3 kW [137].

WTG/PSH output is governed by the mathematical equation as:

$$P_{PSH}^{Gen} = \eta_{WTG}\rho_{water}gH_{UR}^{Rated}Q_{PSH}^{release} \qquad (3.3.7)$$

At any given interval the PSH output $'P_{PSH}^{Gen}{}'$ depends on volume of water released from UR $'Q_{PSH}^{release}{}'$ and rated height of UR from ground $'H_{UR}^{Rated}{}'$. The output of PSH also depends on the efficiency of the water turbine generator $'\eta_{WTG}'$, density of water $'\rho_{water}'$ and gravity $'g'$ of the geographical location.

Assuming the load being fully resistive; the output voltage $'V_o'$ may be expressed as [105]:

$$V_o = \sqrt{R_{Load}P_O} \qquad (3.3.8)$$

At the end of Mechanical mode of operation, the proposed system changes its mode to Electrical mode and VRFB starts to get charged. PSH alone gets responsible to supply load in Electrical mode.

3.3.3.2. Electrical Mode of Operation

From the next interval in which the Mechanical mode ends, the DMWT – PSH – VRFB system starts operating in Electrical mode till the next mode changing operation takes place. In this mode the DMWT operates the alternator and the generated electrical energy gets stored in VRFB. Considering the efficiency $'\eta_{Alt} = 0.9'$, electrical power output $'P_{DMWT}^{Elec}{}'$ may be expressed as:

$$P_{DMWT}^{Elec} = \eta_{Alt}P_{DMWT}^{Shaft} \qquad (3.3.9)$$

This mode continues till the water level of UR is above a certain limit through which it can serve the load of the next interval. During this mode the PSH alone serves the load and VRFB gets charged.

3.3.3.2.1. Vanadium Redox Flow Battery

The Vanadium redox flow battery (VRFB) is a rechargeable battery having vanadium ion as electrolyte. In comparison to Li-ion or Ni-Cd battery, VRFB has lower efficiency, which is around 60% - 70%, lower energy density of around 25 Wh/Kg but higher current density of around 10-130 mA/cm^2 [138]. Comparatively lower operation and maintenance costs make it a viable option for consideration. Choi *et al.* have reported the installation cost as low as 180-250 $/kWh and for grid-connected system the cost is around 750-830 $/kWh [138] which is significantly lesser than that of popular Li-ion or Ni-Cd battery. Due to this reason some notable researches on effectiveness of VRFB in renewable energy application are reported in literature [139, 140, 141]. In the prposed scheme, a VRFB is considered with a storage capacity of 7.5kW and generation capacity of 5.25kW at an output efficiency of 70%.

A VRFB consists of two cells connected by the intermediate proton exchanger membrane. In one half cell, it contains V^{5}+ and V^{4}+ ions as the electrolyte and in another half-cell V^{3}+ and V^{2}+ ions are used [138]. The discharge of the battery takes place due to chemical change occurred inside the positive half-cell, which receives an electron from the negative half-cell. During this process, one VO_2+ ion receives one electron and converts into VO^{2}+ ion. At the same time in the negative half-cell, one V^{2}+ ion loses one electron and converts into V^{3}+ ion. Two pumps are used to pump the electrolyte in the corresponding half-cells from the electrolyte tank and an open circuit voltage of 1.0 V - 1.6 V is received at room temperature [138]. For a VRFB one of the most important parameters is state of charge (SOC) and it can be calculated at any given interval *'i'* as [139]:

$$SOC_{dch}^{n} = SOC^{(n-1)} - \frac{P_{VRFB}^{n} T}{\eta_{VRFB}^{dc} E_{VRFB}^{rated}} \tag{3.3.10}$$

$$SOC_{ch}^{n} = SOC^{(n-1)} - \frac{P_{VRFB}^{n} \eta_{VRFB}^{ch} T}{E_{VRFB}^{rated}} \tag{3.3.11}$$

The SOC for discharging of a VRFB is defined in Eq. 3.3.10 and the same for charging is shown in Eq. 3.3.11. The discharging and charging SOC are represented by $'SOC_{dch}^{n}'$ and $'SOC_{ch}^{n}'$ respectively for $'n^{th}'$ interval. Whereas, charging and discharging efficiency is defined by $'\eta_{VRFB}^{ch}'$ and $'\eta_{VRFB}^{dc}'$ respectively. $'T'$ is the duration of the time period and $'P_{VRFB}^{n}'$ is the dispatched power in $'n^{th}'$ interval. Rated energy storage of the VRFB is $'E_{VRFB}^{rated}'$. In charging mode $'P_{VRFB}^{n} < 0'$ and in discharging mode $'P_{VRFB}^{n} > 0'$. The operation strategy of the proposed DMWT – PSH – VRFB method is discussed in Section 3.3.2 and 3.3.3.

3.3.3.3. The Mode Changer Assembly Design

In this section the mode changing operation will be discussed. As shown in Figure 3.3.1 and Figure 3.3.2, the Mode Changer Assembly **(MCA)** consists of the mode changer spring **(MCS)** and mode changer electromagnet **(MCE)**.

When the mode changer electromagnet is powered (in Mechanical mode) the electromagnet attracts the ER – FR – MR assembly. The spring expands and the assembly lowered. This results in operating the system in Mechanical mode. As soon as the **'MCE'** is terminated from being energized (in Electrical mode), the **'MCS'** returns to its normal position and the ER – FR – MR assembly is drawn upward by the **'MCS'**. This results in mode change to Electrical mode from Mechanical mode. Mathematical representation of this mode changing operation is discussed in this section.

It is evident that from previous discussions that, the mode changer spring will retain its actual shape without having any expansion only if the force required to expand the spring is higher than the weight of the MR – FR – ER assembly.

Therefore, applying Hooke's Law, if the force required to expand the spring of length $'L_{MCS}'$ by a level $'\Delta L_{MCS}'$, is $'F_{MCS}'$, then the force is:

$$F_{MCS} = -k\Delta L_{MCS} \tag{3.3.12}$$

$$F_{MCS} > g\, M_{RA} \tag{3.3.13}$$

Where, $'k'$ is the spring constant, $'M_{RA}'$ is the mass of MR – FR – ER assembly and $'g'$ is the gravitational acceleration. Therefore, it may be stated from Eq. 3.3.12, that the weight of the MR – FR – ER assembly is not capable to expand the **'MCS'** (Electrical mode).

In Mechanical mode, the spring is needed to be expanded and the force is applied by the mode changer electromagnet (MCE). Therefore, the force of attraction should be equal to the force $'F_{MCS}'$. When the attraction force of **'MCE'** *i.e* $'F_{MCE}'$ becomes equal to $'F_{MCS}'$, it compensates for the opposing force exerted by the **'MCS'** and the MR – FR – ER assembly moves downward due to its weight. DMWT gets disconnected from CP and connection with the generator is established. This is mathematically represented as:

$$F_{MCE} = F_{MCS} = -k\Delta L_{MCS} \tag{3.3.14}$$

In this scheme, 100 Wh energy is assumed to be supplied to the **'MCE'.** The assumption is made for simulation purpose only. In practical scenario the energy requirement may change, but it will follow the same principle. In the next section, simulation results of the proposed DMWT – PSH – VRFB system operation are discussed in details.

The results of this section are accessible in section 5.3.

In this section a single wind turbine was operated in both electrical mode and mechanical mode to charge two different types of storages for continuous power supply. But more restricted operation of WT can also take place, where only mechanical power of WT can be utilized for uninterrupted power supply. This sort of problem formulation is provided in section 3.4.

3.4. Operation of two mechanically driven Gravity Energy Storage Systems using one Wind Turbine

3.4.1. Objective

The main objective of this system is to charge the energy storage devices (ESD) and energy gets discharged as required to cater the load demand in stable voltage. There are a number of ESDs presently available with different working principles such as Mechanical type energy storage devices - Compressed air energy storage [32], Flywheel energy storage [142], Pump storage hydroelectricity 143, 144] etc., Electrical type energy storage devices - Superconducting magnetic energy storage [145], Supercapacitor [146] etc. , Electrochemical type energy storage devices - Vanadium redox flow battery [147], Lead-acid battery [148], Li-ion battery [149], Li-Po battery [150] , chemical energy storage devices - hydrogen storage with fuel cells [151] and thermal energy storage devices - sensible heat storage [152, 153] and latent heat storage [154, 155] etc. Other than those above mentioned ESDs, there are also several other types available at present. However, there are several limitations associated with different ESDs such as high installation and maintenance cost, huge land requirement etc. Depending on several factors like energy density, response time, capital cost etc., different storage devices are used for different purposes.

In this section two mechanically driver GESS is operated using the mechanical of one wind turbine.

The scheme intends to provide a idea of maximum utilization of wind energy, also eradicating its intermittency related issues which negatively affects the voltage of the load in a standalone microgrid.

3.4.2. The Proposed Wind Turbine Driven Dual GESS System

Gravitricity proposed the utilization of same DC motor and converter for both the operation of charging and discharging of GESS. Therefore, for two GESS systems; two DC motor-converter assembly is required. The proposed system works differently from the GESS designed by Gravitricity [96]. It utilizes wind turbine (WT) generated mechanical energy to charge GESS and during discharge, it uses reverse braking of a DC motor to generate electricity. The generated electrical energy is converted through an inverter for distribution. The proposed system operation is divided broadly into two sections:

(i) The charging Section

(ii) The generating section

3.4.2.1. Description of the Charging Section

The charging section of the proposed Wind Turbine driven dual Gravity energy storage system is divided into several parts as shown in Figure 3.4.1 and Figure 3.4.2:

(i) The Wind Turbine (without wind turbine generator and converter) and mechanical transmission ($\eta = 0.8$) [123]

(ii) Charging side rotating mechanical connection between WT mechanical transmission and GESS 1 namely **"M 1"**

(iii) Charging side rotating mechanical connection between WT mechanical transmission and GESS 2 namely **"M 2"**

(iv) Fixed mechanical connection with brush between 'M 1' and 'M 2' namely **"F 1"**

(v) Mode changer spring with brush connected to 'M 1' namely **"SP 1"**

(vi) Mode changer weight (suspended) above 'M 2' namely **"MCW 1"**

(vii) Required gears

As shown in Figure 3.4.1 and Figure 3.4.2, the wind turbine transmits generated mechanical energy through the mechanical transmission system to 'M 1' through a gear assembly of the transmission system. There are two GESS systems that is driven (charged)

by one WT and they are intended to charge one at a time. Therefore, there is a switchover mechanism in place to operate these GESS alternatively. This switchover mechanism is achieved by using the mode changer spring 'SP 1' and mode changer weight 'MCW 1'. The 'SP 1' and 'MCW 1' are used to switch connection between 'M 1' and 'M 2' with WT – GESS 1 and WT – GESS 2 correspondingly. When the weight 'MCW 1' rests on 'M 2', it applies a downward force which in turn transfers to 'M 1 / M 2' and the mode changer spring 'SP 1' through the fixed mechanical connection 'F 1'. One end of 'SP 1' is connected with 'M 1' through a brush and one end is connected to a fixed plate. Thus, the downward vertical force exerted by 'MCW 1' directly transmits to the spring 'SP 1'.

As one end of 'SP 1' is connected to a fixed plate, the downward force on 'SP 1' results into contraction of the spring. Thus, due to the applied force of 'MCW 1' the whole assembly *i.e.* 'M 2 – F 1 – M 1' gets lowered. This lowering of the assembly results in connection of 'M 2' with the wind turbine and disconnection of 'M 1' from the wind turbine as observed from Figure. 3.4.2. Now when the weight 'MCW 1' gets gradually pulled above 'M 2', the downward force gets released and the spring 'SP 1' comes into its original state, results in an upward thrust to the whole assembly *i.e.* 'M 1 – F 1 – M 2'. Due to the upward force provided by 'SP 1', 'M 2' gets disconnected from the wind turbine and 'M 1' gets connected with the same as shown in Figure. 1. Therefore, it is evident from the above discussion that while 'MCW 1' hangs above 'M 2', the spring 'SP 1' retains its normal state, 'M 1' gets connected with the wind turbine and 'GESS 1' which is driven by 'M 1' gets charged. In this condition as 'M 2' is out of function and 'GESS 2' cannot be charged; thus, it is free to generate if required as shown in Figure. 1. The exactly opposite scenario occurs when the weight 'MCW 1' rests on 'M 2'. Then 'GESS 2' gets charged and 'GESS 1' is free to generate if required (Figure 3.4.2). Thus, it is clear from the above discussion that either 'GESS 1' or 'GESS 2' can be charged at any particular interval.

3.4.2.2. Description of the Generating Section

GESS being a mechanical device cannot charge and discharge at the same time. From the discussion in Section 3.4.2.1, it is to be observed that at any point of time either 'GESS 1' or 'GESS 2' is free to generate electricity *i.e.* whichever GESS is getting charged, the other one is free to generate electricity. The generating section of the proposed system comprises of several parts as shown in Figure 3.4.1 and Figure 3.4.2:

(i) Generating side rotating mechanical connection between GESS 1 and DC motor namely **"M 3".**
(ii) Generating side rotating mechanical connection between GESS 2 and DC motor namely **"M 4".**
(iii) Fixed mechanical connection with brush between 'M 3' and 'M 4' namely **"F 2".**
(iv) Mode changer spring with brush connected to 'M 3' namely **"SP 2".**
(v) Mode changer weight (suspended) above 'M 4' namely **"MCW 2"**
(vi) DC Motor Assembly with Inverter

(vii) Required gears

In the generating section as shown in Figure 3.4.1 and Figure 3.4.2, GESS 2 and GESS 1 is generating alternatively. From Figure. 3.4.1 it is observable that GESS 1 is charging, thus GESS 2 is free to generate. The mode changer weight **'MCW 2'** rests on **'M 4'**, which applies a downwards force on it (Figure. 3.4.1). The applied force gets transmitted to **'M 3'** through **'F 2'**, which forces the mode changer spring **'SP 2'** to contract. This results in lowering of the assembly **'M 4 – F 2 – M 3'** and **'M 4'** gets connected with the DC motor assembly, thus GESS 2 generates energy. Similarly, when the mode changer weight **'MCW 2'** is pulled up, the downwards force gets released and the spring returns to its original position, making the assembly **'M 4 – F 2 – M 3'** to move upwards. In this condition GESS 2 gets disconnected from DC motor and GESS 1 gets connected with the same as shown in Figure. 3.4.2. Hereby it is also to be noted that mode changer weights **'MCW 1'** and **'MCW 2'** are lowered alternatively. When **'MCW 1'** gets lowered on **'M 2'**, at the same time **'MCW 2'** is pulled up from **'M 4'** and vice versa. This enables continuous operation of the system *i.e.* at any given interval either GESS 1 or GESS 2 is generating, making energy available to load continuously. When one GESS is generating the other one is getting charged. Operation strategy of the proposed system in an isolated microgrid is discussed in Section 3.4.3.

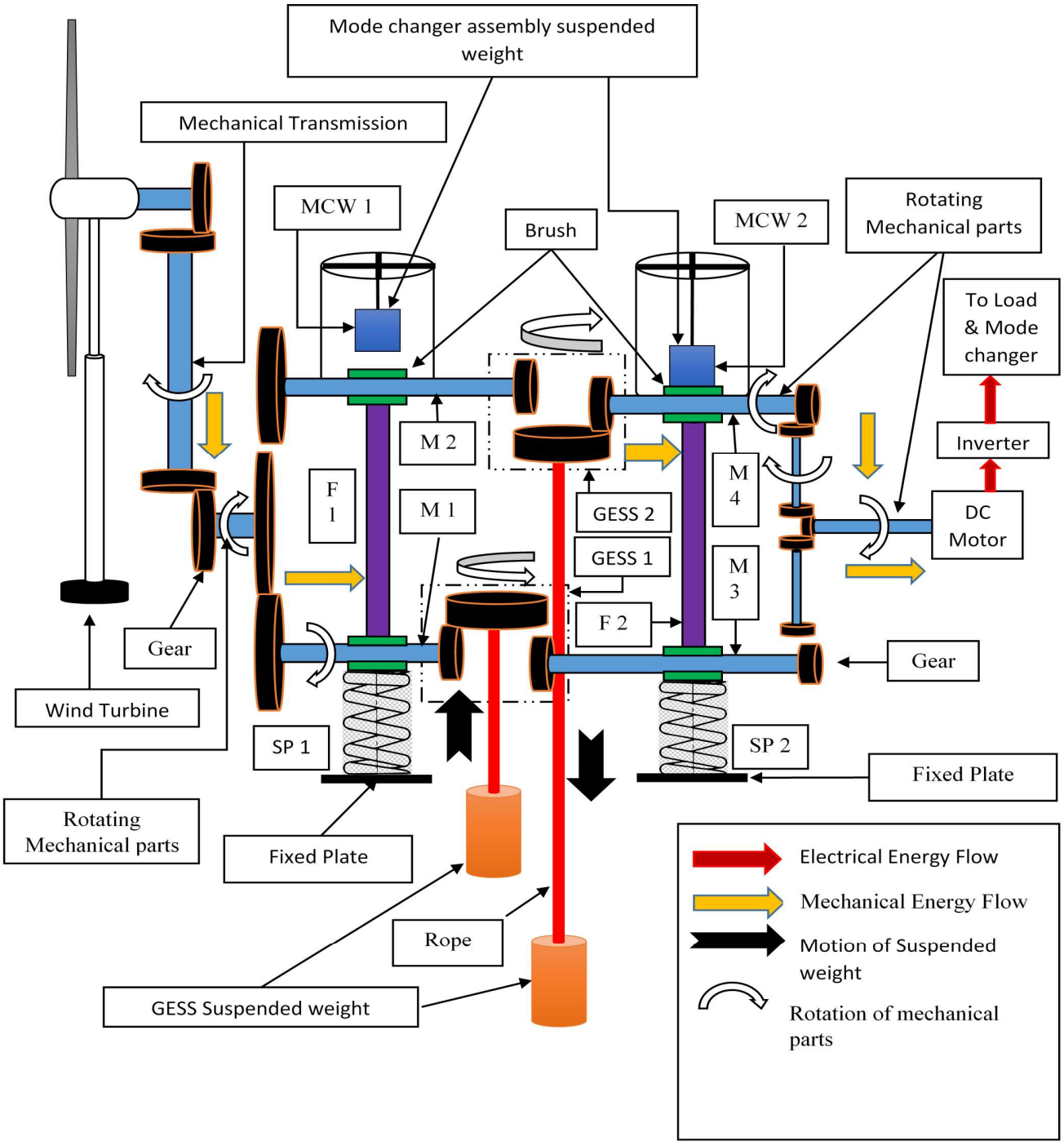

Figure 3.4.1. The Wind Turbine Driven Dual Gravity Energy Storage System (Mode 1: GESS 1 Charging GESS 2 Generating)

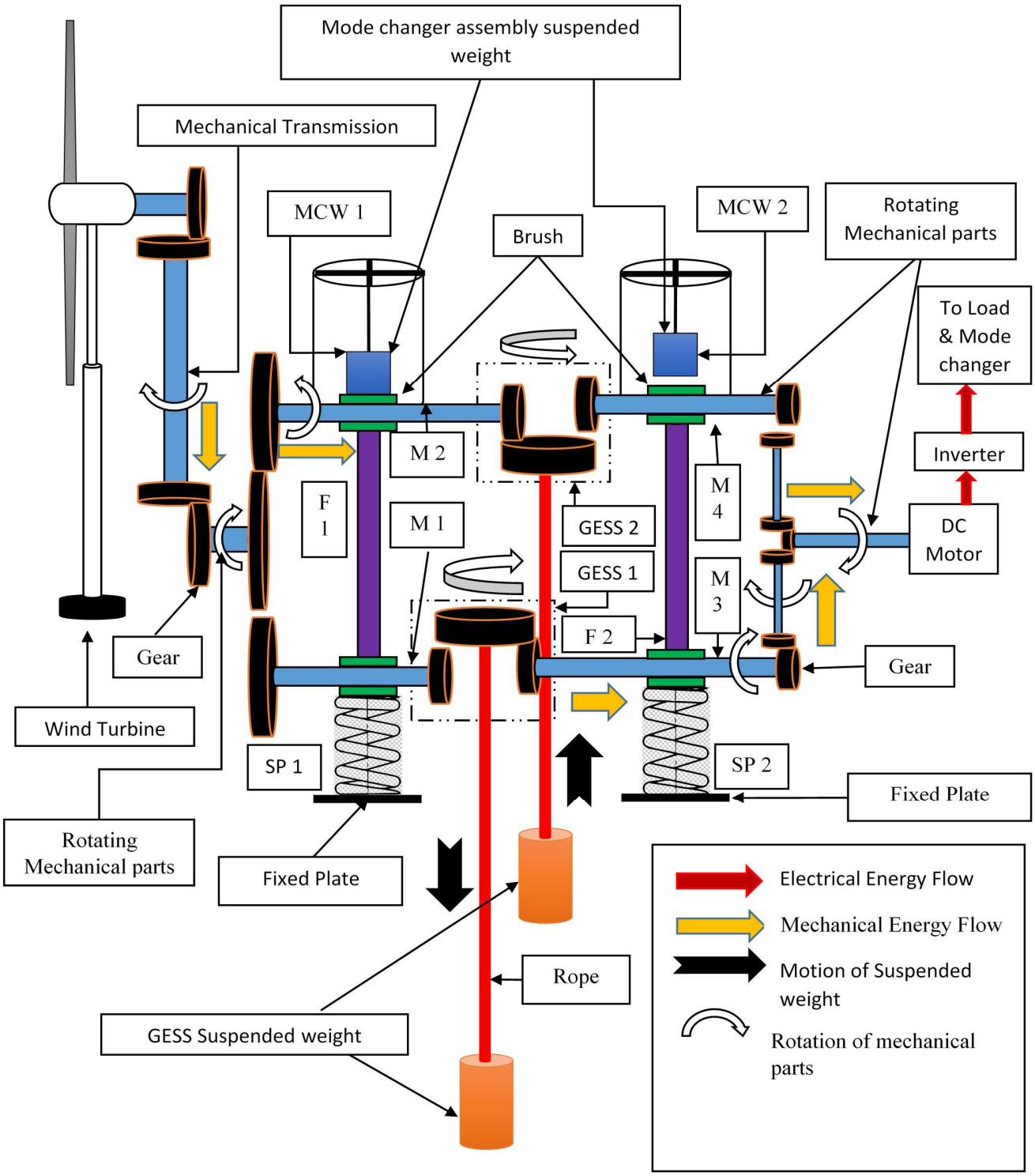

Figure 3.4.2. The Wind Turbine Driven Dual Gravity Energy Storage System (Mode 2: GESS 1 Generating GESS 2 Charging)

3.4.3. Operation Strategy

The wind turbine driven dual GESS system generates at stable voltage and in a cost-effective manner. Two GESS are operated from a single wind turbine and one DC motor-inverter assembly. GESS being a mechanical storage device; can either charge or discharge at any particular interval. Thus, to ensure continuous energy generation at fixed voltage; two GESSs are required. The combined operation of GESS 1 and GESS 2 is divided into two modes:

1. **Mode 1:** GESS 1 Charges and GESS 2 Generates
2. **Mode 2:** GESS 1 Generates and GESS 2 Charges

The system operation is designed as such that, it can deliver required energy demand at any given interval in an isolated microgrid. An entire day of operation is divided into 24 intervals of 1 hour each. The system operates as follows:

(iii) At starting of any interval, the system checks the system load and determines which one of the two GESS can deliver the entire load. If GESS 1 is capable to supply the load, it is assigned as such and for that interval GESS 2 is charged via the wind turbine. In another interval if it is determined that GESS 2 can supply the entire load, it is assigned as such and GESS 1 is charged via wind turbine.

(iv) If in any case it is found that any of the two GESS is capable to supply the full load, GESS 1 is assigned to supply the load and other one is charged via the wind turbine i.e. GESS 1 continues to generate till it holds enough charge to supply the entire load of any particular interval.

(v) If in any case, it is estimated that none of the two GESS is capable to supply the full load; then it is evaluated that which one of these two GESS is having higher energy storage currently; that one is assigned to supply a part of the load till it is fully discharged, rest of the load is delivered by the Diesel generator connected with the microgrid. The other GESS is connected to WT for charging.

These conditions are followed throughout the day to ensure continuous power supply to the microgrid. Diesel generator only comes into operation if there is no other way left to supply the load. Mathematical design of the proposed system is discussed in Section 3.4.4.

3.4.4. Mathematical Design

The proposed system is divided into two distinct sections; charging and generating. Wind turbine is the source of mechanical energy required to charge the dual GESS. Mechanical energy extracted from wind turbine is mathematically represented in Eq. 3.4.1. Generated mechanical energy at the shaft of the WT (P_{WT}^{Shaft}) can be mathematically expressed as [123]:

$$P_{WT}^{Shaft} = 0.5\pi\mu_p\rho^{Air}R_{WT}^2V_{Air}^3, \quad V_{Air}^{c-in} < V_{Air} < V_{Air}^{c-out}$$
$$= 0, \quad V_{Air}^{c-in} > V_{Air} > V_{Air}^{c-out} \quad (3.4.1)$$

Equation (3.4.1) is the numerical expression for energy extraction from WT. Here, $'\mu_p'$ is the power coefficient. It is dependent on tip speed ratio (TSR) and blade pitch angle of the WT, valued around 50% [105]. Air density and wind speed is shown as $'\rho^{Air}'$ and $'V_{Air}'$ respectively. The wind turbine rotor radius, cut-in and cut-out speed is represented as $'R_{WT}'$, $'V_{Air}^{c-in}'$ and $'V_{Air}^{c-out}'$ respectively. Produced mechanical power is transferred through a mechanical transmission system to GESS for charging operation. The output $'P_{Trans}^{O}'$ produced from the mechanical transmission system is limited by its efficiency $'\eta_{Trans} = 0.8'$. This is mathematically expressed as [123]:

$$P_{Trans}^{O} = \eta_{Trans}\, P_{WT}^{Shaft} \quad (3.4.2)$$

The transmission shaft powers the GESS through a gear arrangement. Considering gear efficiency $'\eta_{Gear}^{Ch} = 0.9'$; the input mechanical power to GESS $'P_{GESS}^{in}'$ is:

$$P_{GESS}^{in} = \eta_{Gear}^{Ch} P_{Trans}^{O} \quad (3.4.3)$$

For a cylindrical suspended weight of a GESS with radius $'R_{CSW}'$, perpendicular length $'H_{CSW}'$ and density of the material $'\rho_{material}'$; the volume $'V_{CSW}'$ and mass $'M_{CSW}'$ is:

$$V_{CSW} = \pi R_{CSW}^2 H_{CSW} \quad (3.4.4)$$

$$M_{CSW} = \rho_{material} V_{CSW} \quad (3.4.5)$$

Now, if the vertical tunnel depth of the GESS is $'D_{VT}'$; then the maximum usable depth of the GESS $'D_{GESS}^{Max}'$ is:

$$D_{GESS}^{Max} = D_{VT} - H_{CSW} \quad (3.4.6)$$

Therefore, during any interval, if the WT provides a mechanical energy of P_{Trans}^{O} (as in Eq. 3.4.2) and final available energy to the GESS for charging P_{GESS}^{in} (as in Eq. 3.4.3); then the cylindrical suspended weight is pulled up against gravity $'g'$ at a height of $'D_{GESS}'$ from the end point of the tunnel. This height of the suspended weight depicts the amount of stored energy of the GESS and is shown in Eq. 6.7.

$$D^{GESS} = \frac{P_{GESS}^{in}}{gM_{CSW}} \quad (3.4.7)$$

The maximum storage capacity of a GESS $'E_{GESS}^{max}'$ is:

$$E_{GESS}^{max} = gM_{CSW}D_{GESS}^{Max} = gM_{CSW}\left(D_{VT} - \frac{M_{CSW}}{\pi\rho_{material}R_{CSW}^2}\right) \quad (3.4.8)$$

While discharging, the cylindrical suspended weight is lowered with gravity assistance. The GESS enables the DC motor to run at a speed more than its no-load speed. This reverses the polarity of

the current and energy generates using regenerative braking principle. This downward motion of the suspended weight translates into rotation of the DC motor thorough gear assembly.

If the terminal Voltage of the motor is $'V_t'$ and $'K_m'$ is the motor torque constant, then motor speed during regenerative braking $'\omega_R'$ is [156]:

$$\omega_R = \omega_R^0 + \frac{T_B R_a}{K_m^2} \tag{3.4.9}$$

Where, $'\omega_R^0'$ is the no-load speed, $'T_B'$ is the braking torque and $'R_a'$ is the rotor armature resistance.

The braking torque of the motor for armature current $'I_A'$ is:

$$T_B = -K_m I_A \tag{3.4.10}$$

The no-load speed of the motor is:

$$\omega_R^0 = \frac{V_t}{K_m} \tag{3.4.11}$$

During regenerative braking condition the emf of the motor $'E_R'$ and current $'I_R'$ is represented as:

$$E_R = K_m \omega_R \tag{3.4.12}$$

$$I_R = \frac{K_m}{R_a}(\omega_R^0 - \omega_R) \tag{3.4.13}$$

The corresponding power generated from the DC motor during regenerative braking $'P_R'$ is:

$$P_R = E_R I_R \tag{3.4.14}$$

Considering efficiency of gear assembly $'\eta_{Gear}^{dch} = 0.8'$ and DC motor – inverter assembly $'\eta_{DC-inv} = 0.9'$; if the generated energy in any interval is $'E_{GESS}^{Gen}'$ and the suspended weight is released for a height of $'D_{Released}^{GESS}'$, then the height released of the weight is:

$$D_{Released}^{GESS} = \frac{\eta_{Gear}^{dc}\, \eta_{DC-in}\ \ g\, M_{CSW}}{E_{GESS}^{Gen}} \tag{3.4.15}$$

Possible maximum energy generation from a GESS $'E_{GESS}^{Gen\ Max}'$ is:

$$E_{GESS}^{Gen\ Max} = \eta_{Gear}^{dch}\, \eta_{DC-inv}\, g\, M_{CSW}\, (D_{VT} - H_{CSW}) \tag{3.4.16}$$

In practical scenario, the energy generation from a GESS is also dependent on the mass of the wire / rope, which connects the suspended weight to the main pulley. However, the mass of the wire / rope is negligible as compared to the mass of the suspended weight itself, although considering it is important in practical case. If $'\bar{\sigma}_W, \rho_W, L_W'$ are the tensile strength, density of the material and length of the rope respectively, then the minimum cross-sectional area of the rope, $'A_W'$ required

to draw the suspended weight with a maximum acceleration $'\bar{A}'$ and corresponding mass of the rope $'M_W'$ are:

$$A_W = \frac{M_{CSW}(g + \bar{A})}{\bar{\sigma}_W - L_W \rho_W (g + \bar{A})} \tag{3.4.17}$$

$$M_W = \rho_W A_W L_W \tag{3.4.18}$$

The proposed system of this article operates two GESSs using single WT and One DC motor inverter. For this operation, a mode changer assembly is conceptualized, as shown in Figure 3.4.1 and Figure 3.4.2. The mode changer assembly consists of a suspended weight (MCW 1) and one spring (SP 1) for charging section and similar arrangement, MCW 2 and SP 2 for generating section. The operation of this assembly is also discussed in Section 3.4.2. Now to contract the spring of Length $'L_S'$ by a desired level $'\Delta L_S'$, the force required is supplied by the mode changer suspended weight of mass $'M_{MCW}'$. Applying Hooke's Law, the force required $'F_{MC}'$ is:

$$F_{MC} = -k\Delta L_S \tag{3.4.19}$$

$$F_{MC} = g(M_{MCW} + M_C)\,, For\ charging\ Side \tag{3.4.20}$$

$$F_{MC} = g(M_{MCW} + M_G)\,, For\ generating\ Side \tag{3.4.21}$$

Where, $'k'$ is the spring constant and is dependent on the Young's modulus of the material used, $'M_C\ and\ M_G'$ are mass of the charging and generating side assembly including mass of gears etc. respectively.

This section depicts a design of a mechanism where a WT can single handedly operate two GESSs to supply electricity incessantly. The simulated results of this section are represented in section 5.4.

Various forms of designs are given in the previous sections along with required data. To analyze the optimality of technical and economical aspect of one of the design, Whale Optimization Algorithm is used, details of which is discussed in Chapter 4. Details discussion regarding the algorithm operation is described in the next chapter. Results thus, obtained are given in Chapter 5.

CHAPTER 4

4. Algorithm used for System Optimization

As discussed in section 2.3 there are several meta-heuristic algorithms available for system optimization. Whale optimization algorithm (WOA) is one of the promising algorithms available. According to [157, 158] a good number of publications have taken place from the development of WOA. Researches have used this algorithm in different field of electrical engineering like - Voltage Source Inverters [159], Economic Load Dispatch [160], Optimal Power Flow [161], Economic Load Dispatch [162], Hydrothermal Scheduling [163], Radial Distribution Systems [164, 165], Distribution Networks [166, 167], Power System Stability [168], Economic Dispatch Problem [169], Optimal Reactive Power Dispatch [170], Optimal capacitor allocation in distribution system [166] etc. In this work WOA is utilized for the optimization processes.

4.1. Whale Optimization Algorithm (WOA)

In this section detail of WOA is discussed. The objective function discussed in section 3.2.5 is implemented in Matlab to determine the optimal solution. This optimization algorithm is used to determine the effects of sizing and size variation of different resources on the objective function. WOA is based on hunting behaviour of humpback whales [115]. These mammals tend to hunt school of fish near sea surface. According to Goldbogen *et al.* humpback whales create a distinctive '9' shaped bubble path underwater to encircle their prey, called 'upward spiral' [171]. Mirjalili and Lewis mathematically formulated this hunting behaviour of humpback whales, named Whale Optimization Algorithm.

4.1.1. Mathematical Formulation of WOA

Mathematical modelling of WOA is characterized using the search and encircling of prey, bubble-net feeding method [115]. Humpback whales can recognize the location of prey and encircle them. The random search criteria are characterized as [115] follows:

$$D = \gamma . Y_{rand}(t) - Y_C(t) \quad (4.1)$$

$$Y_C(t+1) = Y_{rand}(t) - \beta . D \quad (4.2)$$

Where, Y_{rand} is a randomly selected position vector and Y_C is the current position vector. The coefficient vectors β and γ may be represented as:

$$\beta = 2c . w - c \quad (4.3)$$

$$\gamma = 2w \quad (4.4)$$

Where 'c' decreases linearly from 2 to 0. 'w' is a random number in [0,1]. While declining the value of 'c', the net value of 'β' does steadily decreases. This reduction in value of 'β' achieves 'The shrinking encircling mechanism' for bubble-net attack. WOA assumes the present best solution as the target and best agent is defined accordingly. Other solutions update their positions towards the best one. This is represented as [171] follows:

$$D = \gamma . Y_B(t) - Y_C(t) \quad (4.5)$$

$$Y_C(t+1) = Y_B(t) - \beta . D \quad (4.6)$$

In case the value of $\beta \geq 1$, the searching of target is performed according to Eq. 4.1 & Eq. 4.2, else the encircling of prey is achieved using Eq. 4.5 & Eq. 4.6. The location vector of the best result obtained so far is 'Y_B'.

It is also to be taken into consideration that a humpback whale encircles its prey simultaneously in a shrinking circle and a spiral-shaped path to update its existing location. Thus, both methods hold equal probability ('p') of 0.5. The spiral-shaped path is mathematically represented elsewhere [171]:

$$Y_C(t+1) = |Y_B(t) - Y_C(t)| . e^{bl} . \cos 2\pi l + Y_B(t) \quad if\ p \geq 0.5 \quad (4.7)$$

$$Y_C(t+1) = |Y_B(t)| - \beta . D \quad if\ p < 0.5 \quad (4.8)$$

Where 'b' is a constant to provide the spiral shape and 'l' is a random number in [-1,1].

The microgrid system is optimized using following steps:

Step 1. Initialize the parameters of the microgrid (Series and Parallel Solar PV module, Generation capacity of Biomass generator 1 & 2, GESS maximum storage capacity) & WOA parameters.

Step 2. Calculate the LCOE and total energy purchase from central grid (fitness) for each set of microgrid parameters (search agent).

Step 3. Determine the best search agent

Step 4. Iteration i =1

Step 5. Update $'c , \gamma , \beta , l , p'$ for each search agent

Step 6. If, $(p < 0.5)$& $(|\beta| < 1)$, update the position of the current search agent according to Eq. 22

Step 7. If, $(p < 0.5)$& $(|\beta| \geq 1)$, Select a random search agent and update the position of the current search agent according to Eq. 4.6

Step 8. If, $(p \geq 0.5)$, update the position of current search agent according to Eq. 4.7

Step 9. Calculate for any maximum and minimum limit violation by the search agents and update them accordingly

Step 10. Calculate LCOE and total energy purchase from central grid for each search agents

Step 11. Update the best search agent, if there is a better solution

Step 12. Iteration i = i+1

Step 13. Repeat Step 5 to Step 12, till the maximum number of iterations is completed

Step 14. Display the best search agent and corresponding LCOE and total energy purchase from grid

In this chapter, details optimization procedure using WOA is discussed. This leads to the results of the system operation, which is discussed in chapter 5. Taken into consideration different loading patterns and different operation conditions results have been derived, to provide a clear picture of effectiveness of proposed systems.

CHAPTER 5

5. Results and Discussion

The results with proper discussion of the four design approaches as developed in sections 3.1, 3.2, 3.3 and 3.4 are represented in sections 5.1, 5.2, 5.3 and 5.4 respectively.

5.1. Results of Standalone Renewable-based Microgrid with Optional Grid Sales

The objective of the work presented in section 3.1.1, is to design a micro-grid fully renewable energy based at constant voltage, while prioritizing the energy resources and having grid supply potential to reduce the tariff for backward areas of Assam. Due to abundant water availability in the state of Assam we have kept the water flow rate fixed in this literature. The system thus designed is tested in several platforms to validate its viability. The test platforms are:

(i) Three different characteristics of variable wind speeds.

(ii) Three different load patterns.

Variable wind speed platform is checked while keeping the water flow rate and load platform fixed.

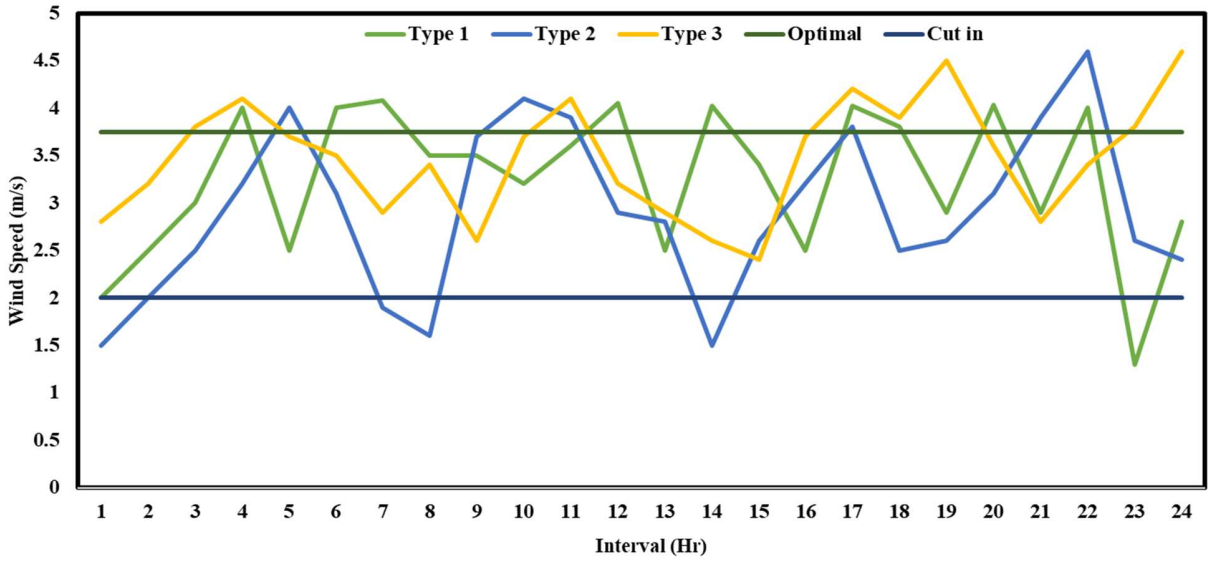

Figure 5.1. Different Types of Wind Speed

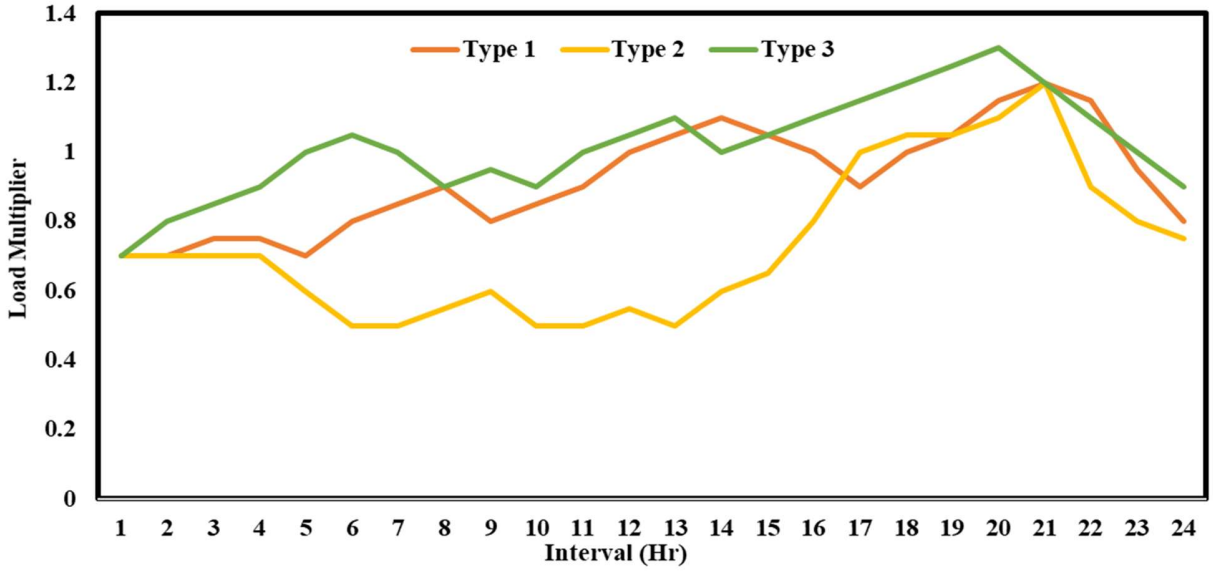

Figure 5.2. Different Types of Load Pattern

Three types of wind speed are considered with different profile. Type 1 amongst them as shown in Figure 5.1 is the base wind speed. Type 2 is of comparatively lower wind speed whereas Type 3 shows the wind speed on higher side. Optimal and cut-in wind speed is also shown and accordingly output from wind turbine is calculated and used. From Figure 5.2 we can observer three different load patterns. While Type 1 is the base pattern, Type 2 idealizes a load pattern in accordance with worker's colony of a tea estate. Type 3 may be considered as an area with a comparatively better development; thus, the load demand is on the higher side than the rest. The results of the proposed method can be observed below.

The data of Wind speed shown in Figure 5.1 has been taken from Indian Metrological Department website. Figure 5.2 described a load pattern which is designed keeping in mind a small cluster of load for basic amenities for Tea Garden workers colony in Assam.

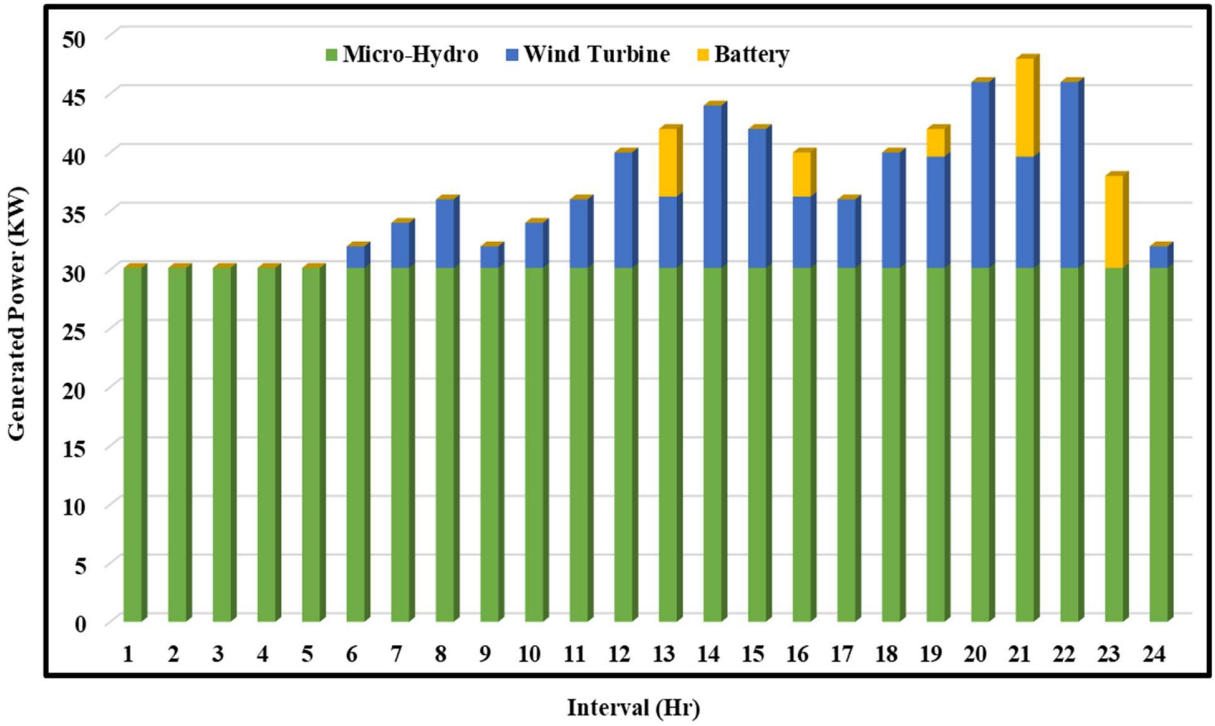

Figure 5.3. Generated Power at Base Load

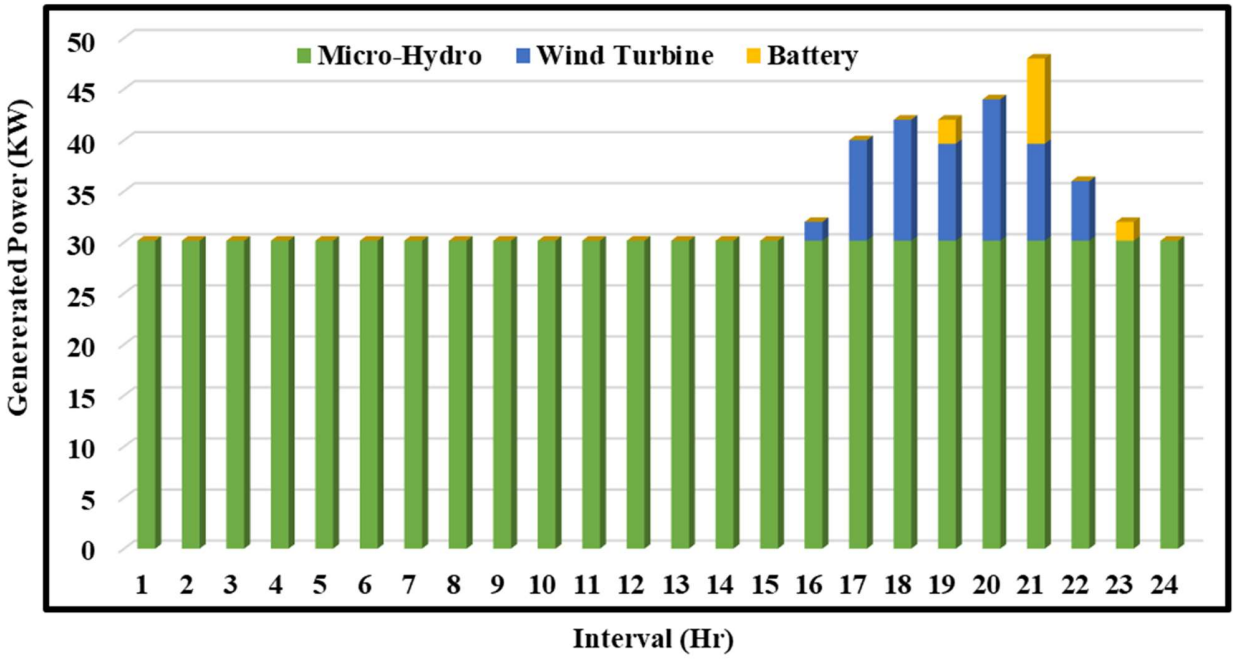

Figure 5.4. Generated Power at Type 2 Load

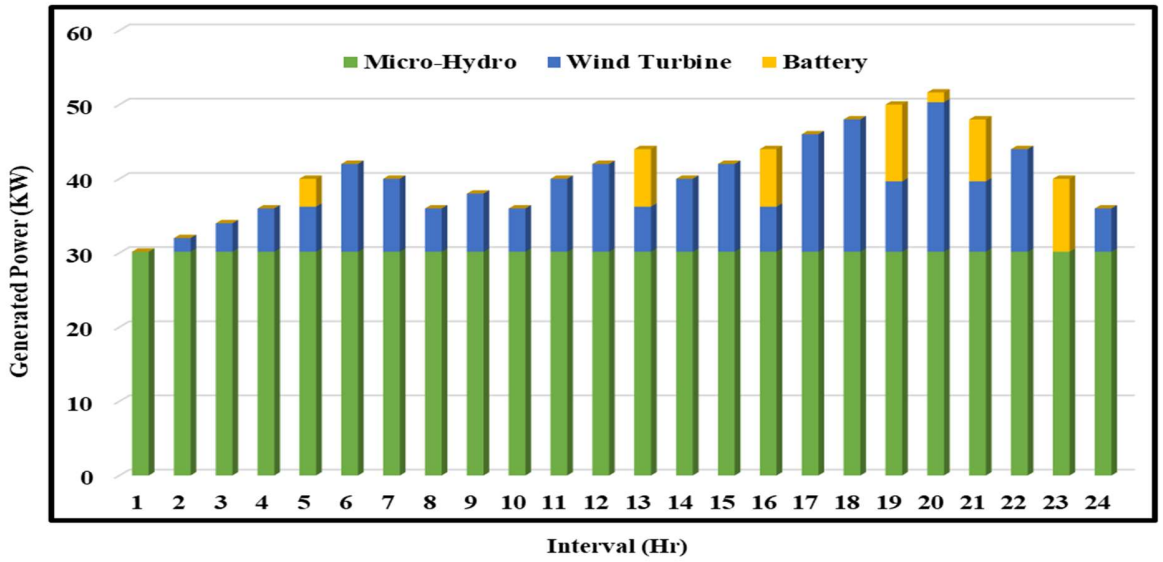

Figure 5.5. Generated Power at Type 3 Load

As discussed at the beginning of this section distribution of generated power may be observed from Figure 5.3 to Figure 5.5 for different load pattern. It is well observed that usage of wind turbine power as well as battery stored energy is used as the power demand increased. With the prioritization of micro-hydro based generation, we have actually made sure that minimal disturbance related to frequency of the system can be maintained. This is the reason that micro-hydro generation is fully utilized first, then focus is diverted to wind turbine and finally to battery, if required. Also prioritizing micro-hydro generation, wind turbine gets ample scope to charge the battery as required. From Figure 5.6 and Figure 5.7, we will observe the generation pattern in two different wind speed profile for base load, while for the wind profile of Type 1 is already shown in Figure 5.3.

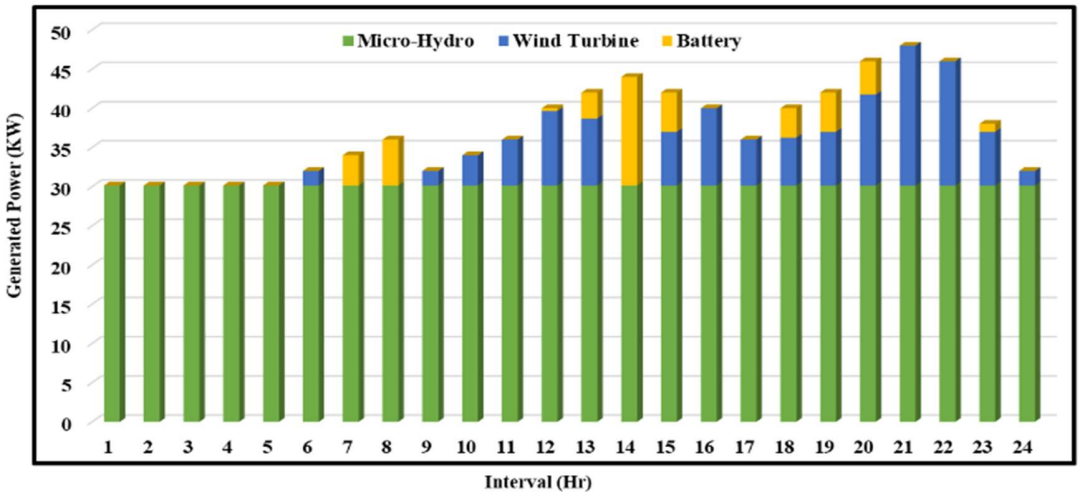

FIGURE 5.6. Generation Pattern for Wind Speed Profile Type 2

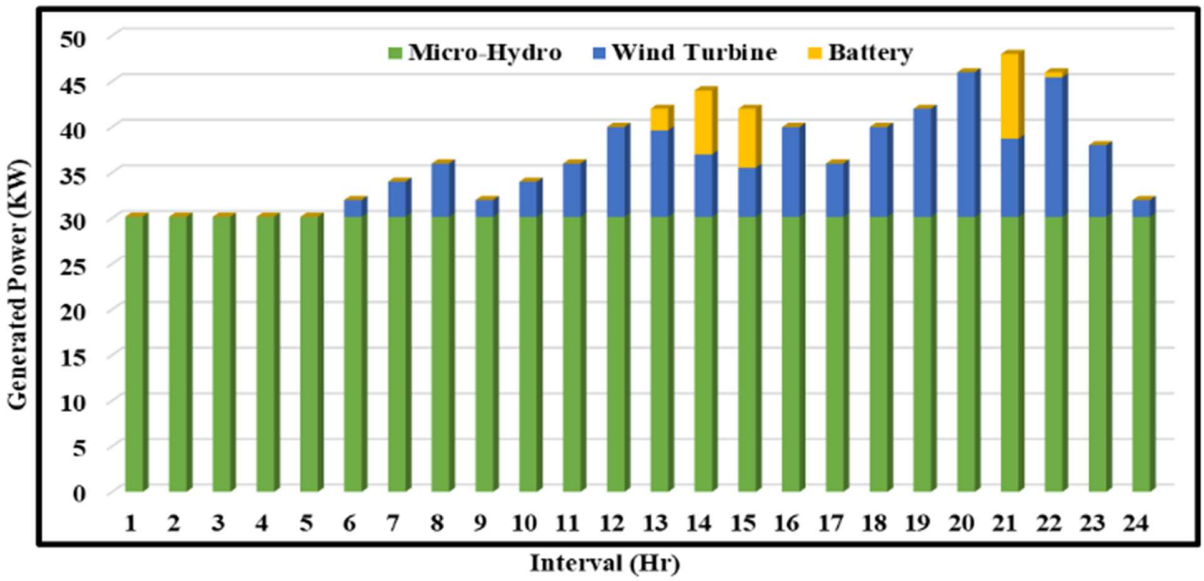

Figure 5.7. Generation Pattern for Wind Speed Profile Type 3

It is well observed that for Type 2 of wind profile battery stored energy is used most of the times due to low wind speed whereas in case of Type 3, battery is used much lesser intervals comparatively due to relatively high wind speed as in Figure 5.6 & Figure 5.7 respectively. At 7th, 8th & 14th interval during wind profile of Type 2 battery has fully supplied the residue load as seen in Figure 5.6 due to wind speed below cut-in speed as seen in Figure 5.1, whereas no such phenomenon is observable at 1st interval due to lower load demand which is entirely supplied by micro-hydro unit. The amount of excess energy available for sale is shown in Table 5.1.

TABLE 5.1. AMOUNT OF EXCESS ENERGY GENERATED

Varying load profile	
Base Load	228.8657
Type 2	110.0657
Type 3	281.3562
Varying wind speed profile	
Type 1	228.8657
Type 2	377.0101
Type 3	170.7892

Table 5.1 provides a comparatively clear idea about the energy sale capability outside of the micro-grid. As observable, during higher wind speed or lower load considerable amount energy is left unused, which upon properly utilized may bring down the energy tariff for the internal customers of the micro-grid itself. Also due to the load is entirely served, it may be stated that within the micro-grid constant voltage gets maintained throughout the operating.

5.2. Results of Techno-economic Analysis of a Renewable-based Hybrid Microgrid incorporating Gravity Energy Storage System

The proposed system in section 3.2 is a hybrid RE based microgrid to supply electricity at equal or lower than current rate (Rs. / kWh) in the Nagaland state of India. The proposed microgrid is powered with locally available renewable resources. Considering all the essential amenities required for the livelihood of the people of the region, the system is tested on a load demand with basic annual per capita energy consumption of 1151.27 kWh. Whereas, the actual annual energy consumption of 345 kWh per capita, for the state of Nagaland has been reported in 2016-2017 [172]. Therefore, the proposed system is future ready. The hybrid system incorporating a GESS, enables minimal / nil inward transaction from the grid towards the microgrid. In India, major share of energy supplied through central grid is generated from thermal resources. Thus, due to energy selling capacity of the microgrid to the central grid, the proposed renewable based system is beneficial in terms of emission reduction. As it is discussed in the introduction, that as per the government of India, there is an establishment of 100% electrification in India, so it is evident that there should be a nearby grid.

The system is optimized to determine optimal sizing of different resources and compared with respect to LCOE and energy drawn from the central grid. The system is optimized for the Base case scenario with load as shown in Figure 3.2.4. The final settings of parameters / variables obtained through optimization are shown in Table 5.2. Comparing the values obtained during the optimization process (Table 5.2) with the range of variables shown in Table 3.2.4, it is observed that the output settings of variables lie within the maximum and minimum range of the same.

TABLE 5.2. PARAMETER SETTINGS FOR THE BASE CASE

Sl. No.	Parameters / Variables	Final Settings
1	Number of Solar Panels in Series	30
2	Number of Solar Panels in Parallel	30
3	Capacity of Biomass Generator 1(kW)	100
4	Capacity of Biomass Generator 2 (kW)	14.07
5	GESS Storage Capacity (kW)	1000

The system operation during winter and summer season is shown in Table 5.3 and Table 5.4 respectively. The system is optimized in a year ahead model to determine the LCOE of the system and the related optimization curve is shown in Figure 5.8.

There are several aspects in which the system ~~is~~ has also been tested other than the base case scenario. The system has been tested on different combinations of load demand and GESS initial storage availability and results are reported in Table 5.5.

Table 5.3 presents the daily energy served by different resources along with GESS charging, Grid sale and purchase during winter season (January to March and November to December). Whereas, the same for summer season has been presented in Table 5.4. From Table 5.3, it may be observed during 1^{st} to 6^{th} interval, there is no solar insolation available. During 1^{st} to 4^{th} interval, the load is supplied by Biomass Generator 1, Biomass Generator 2 and GESS. During 5^{th} and 6^{th} interval the load alone is supplied by Biomass Generator 1 as the load due to heater in households are switched off. However, as the Biomass generator is always operated in its maximum capacity, the excess energy is utilised to charge the GESS. During the 7^{th} interval load remains same as the previous interval and the solar insolation becomes available, but only 2.72 kWh energy is generated from it, which is not enough to supply the load demand. Therefore, the Biomass Generator 1 continues to operate and the excess energy is used to charge the GESS. During the 8^{th} interval, load goes down and energy available from solar panels increases. Thus, the Biomass Generator 1 has to be switched off. From 8^{th} to 11^{th} intervals the energy availability from Solar panels gradually increases with the increment in solar insolation and excess energy continues to charge the GESS. During the 12^{th} interval, GESS gets completely charged and the rest of the excess energy is sold to the grid. From 13^{th} to 17^{th} intervals energy is continuously sold to grid, as the load is comparatively lower due to weather conditions.

TABLE 5.3. SYSTEM OPERATION DURING WINTER (JANUARY TO MARCH & NOVEMBER TO DECEMBER)

Load: 1 p.u. & GESS charge availability at the starting of the day: 1 p.u. (Base Case)

Interval	Load Served through Solar PV (kWh)	Load Served through Biomass Generator 1 (kWh)	Load Served through Biomass Generator 2 (kWh)	Load Served through GESS (kWh)	Energy intake for GESS Charging (kWh)	Grid Sale (kWh)	Grid Purchase (kWh)
1	0	100	14.07	190.03	0	0	0
2	0	100	14.07	190.03	0	0	0
3	0	100	14.07	190.03	0	0	0
4	0	100	14.07	189.93	0	0	0
5	0	24.24	0	0	68.184	0	0
6	0	24.24	0	0	68.184	0	0
7	2.72	21.52	0	0	70.63	0	0
8	13.8	0	0	0	61.91	0	0
9	13.8	0	0	0	122.38	0	0
10	16.4	0	0	0	167.15	0	0
11	3.9	0	0	0	207.36	0	0
12	3.9	0	0	0	87.38	142.75	0
13	19.9	0	0	0	0	198.19	0
14	56.5	0	0	0	0	126.43	0
15	56.5	0	0	0	0	82.56	0
16	1.0	0	0	0	0	21.54	0
17	4.4	0	0	0	0	1.31	0
18	0	79.4	0	0	0	20.6	0
19	0	81.5	0	0	0	18.5	0
20	0	69.84	0	0	0	30.16	0
21	0	69.84	0	0	0	30.16	0
22	0	6.1	0	0	0	93.9	0
23	0	0	14.07	290.03	0	0	0
24	0	0	14.07	290.03	0	0	0

The night phase begins from the 18th interval, which means solar insolation becomes zero. During 18th to 22nd interval the load is served by Biomass Generator 1 alone and GESS being fully charged, the excess energy is sold to the grid. This may be observed from Table 5.3, that at the 22nd interval, Biomass Generator 1 completes its operation of 12 hours per day, so it has been switched off. During 23rd and 24th interval, Biomass generator 2 operates. As the load demand during night

hours, are comparatively high and solar or Biomass Generator 1 is not available GESS serves the load along with Biomass Generator 2. It has to be observed that during those two hours, no energy is sold to the grid, as entire energy generated from Biomass Generator 2 is utilised and there is a restriction in place for energy sell from GESS to grid. During the 24 hours of operation, energy from solar panels is available for 11 hours, Biomass generator 1 operates for 12 hours, Biomass Generator 2 and GESS operates for 6 hours each. There is no energy required to be brought from the grid. The microgrid has been operated completely using local RE resources.

Table 5.4 represents the system operation during the month of April to October (Summer Season). Solar PV panels remain non-operational from 1st to 5th interval, which is 1 hour lesser than the winter season (Table 5.3). During 1st to 4th interval BG1, BG2 and GESS together serves the load demand. As compared to the winter season (Table 5.3) the output of GESS is lower, as the use of domestic heater is obsolete during summer time. The operation of 5th interval is similar to that of the winter season, only BG1 serves the load and excess energy is used to charge the GESS. During the 6th interval, energy from solar PV becomes available but not sufficient to supply the complete load demand of the load demand. Therefore, BG1 also operates in the 6th interval and the generated excess energy is used to charge GESS. During 7th interval BG1 is switched off, as energy from solar PV becomes adequate to deliver the load as well as charge the GESS. During the 8th interval GESS becomes completely charged and the excess energy is sold to the grid. From 9th to 11th interval solar PV alone delivers the load with excess energy being sold to the grid. During the 12th interval, solar PV alone is unable to deliver the entire load, which invites BG2 to deliver the remaining load, and after load supply, the extra generation is sold to the grid. With the decrement in load demand at 13th interval, energy generated from solar PV only, becomes excess after supplying the demand. This excess energy is again sold to the grid to earn monetary benefit. During 14th and 15th interval, BG2 operates at its maximum but solar PV and BG2 could not deliver the full load together. So, the GESS delivers the excess load. It may be observed that during these two intervals, energy sold to grid is zero. During 16th and 17th interval, solar PV delivers the load alone and excess energy is used to charge the GESS, grid sale is zero. During the 18th interval, solar insolation becomes very low. So, it only supplies a little amount of load. BG1 and BG2 operate at their maximum but remain unable to supply the full load demand. Therefore, the balance load is delivered through the GESS. From 19th to 22nd interval, BG1, BG2 and GESS together delivers the load. During 23rd interval BG2 is shutdown, as its operation duration of 12 hours in a day gets completed. Due to same reason, in the next interval i.e. 24th, BG1 is turned off and the GESS alone serves the load. From 18th interval onwards, there has been no energy sold to the grid.

TABLE 5.4. SYSTEM OPERATION DURING SUMMER (APRIL TO OCTOBER)

Load: 1 p.u. & GESS charge availability at the starting of the day: 1 p.u. (Base Case)

Interval	Load Served through Solar PV (kWh)	Load Served through Biomass Generator 1 (kWh)	Load Served through Biomass Generator 2 (kWh)	Load Served through GESS (kWh)	Energy intake for GESS Charging (kWh)	Grid Sale (kWh)	Grid Purchase (kWh)
1	0	100	14.07	42.6	0	0	0
2	0	100	14.07	42.6	0	0	0
3	0	100	14.07	42.6	0	0	0
4	0	100	14.07	42.28	0	0	0
5	0	24.24	0	0	68.184	0	0
6	11.41	12.82	0	0	78.46	0	0
7	24.24	0	0	0	4.33	0	0
8	16.65	0	0	0	42.22	8.61	0
9	16.65	0	0	0	0	91.53	0
10	24.5	0	0	0	0	115.1	0
11	148.35	0	0	0	0	3.57	0
12	158.61	0	5.74	0	0	8.34	0
13	28	0	0	0	0	112.13	0
14	124.03	0	14.07	57.14	0	0	0
15	93.37	0	14.07	87.8	0	0	0
16	19.4	0	0	0	38.89	0	0
17	13.8	0	0	0	14.44	0	0
18	6.8	100	14.07	107.46	0	0	0
19	0	100	14.07	107.83	0	0	0
20	0	100	14.07	120.33	0	0	0
21	0	100	14.07	120.33	0	0	0
22	0	100	14.07	96.83	0	0	0
23	0	100	0	56.675	0	0	0
24	0	0	0	156.675	0	0	0

During 12^{th}, 14^{th} and 15^{th} interval, BG2 operates instead of BG1 even when BG1 has operated for only 6 intervals before that. This is due to the fact that, after the supply from solar PV the remaining load demand is lower than 100 kWh in the 12^{th} and 14^{th} interval and only 1.87 kWh more than the capacity of BG1 in the 15^{th} interval and there is also a provision of GESS recharging from solar PV in 16^{th} and 17^{th} interval. So, if BG1 is operated in 12^{th} and 14^{th} interval, there would have been

excess energy which ultimately would be sold to the grid at lower price (Figure 3.2.7) and if operated in the 15th interval then only 1.87 kWh would have been used from GESS, which could have been easily recovered from the 16th interval, creating more grid sale at lower price in the two consecutive intervals (16th and 17th). Again, after operating for those 3 intervals, there would be only 3 operating hours left to BG1 and 8 hours to BG2. In this situation BG1 would have operated during 18th, 19th and 20th interval. During 21st, 22nd and 23rd intervals GESS would have supported those 100 kWh load in each interval. After 21st interval there would have been 382.26 kWh stored energy left in GESS. After 22nd interval it would have been 163.57 kWh. During 23rd interval, GESS could deliver 147.213 kWh and 9.462 kWh energy would have to be bought from the grid. During 24th interval 156.675 kWh energy had to be bought from the grid at much higher price than the selling price to the grid at 12th, 14th, 16th or 17th interval. Moreover, during the 1st interval of the next day the served energy from GESS would have to be bought from the grid, as a result the overall energy cost (LCOE) for the consumers would have increased.

Therefore, it may be stated that the system operation is optimized as such, that, the consumer gets electricity at lowest possible rate. Whale optimization algorithm has been used to find the optimal size and operation strategy (minimization of LCOE) of Solar PV, BG1, BG2 and GESS.

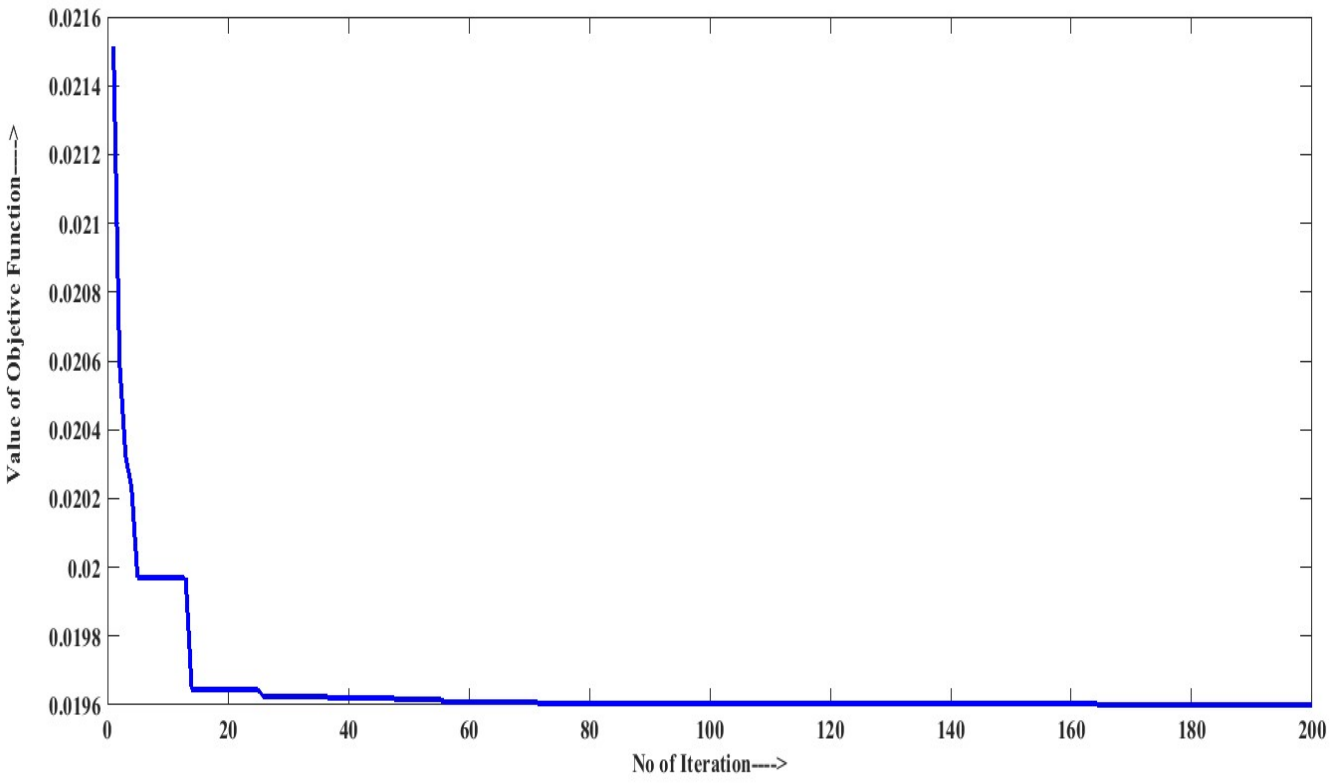

Figure 5.8. Optimization Curve for Minimization of the Objective Function

5.2.1. Comparative Techno-economic Study on Load and GESS Initial Storage Variation

The system is verified with different combinations of load and GESS initial charge availability settings. Optimal sizing of solar PV, BG1, BG2 and GESS is obtained upon optimizing the system Grid sale, Grid purchase and LCOE is also included in the verification process. Along with that, a comparative study on LCOE with current local energy price is also performed. Load demand of the system is considered in four different patterns and they are denoted as:

1. L1: Load demand at 0.9 pu
2. L2: Load demand at 1.0 pu
3. L3: Load demand at 1.1 pu
4. L4: Load demand at 1.2 pu

Available charge of GESS at the starting of the day may be different under different circumstances. Three initial energy availability value of GESS is taken under consideration. They are denoted as:

1. G1: GESS initial storage at 0.5 pu
2. G2: GESS initial storage at 0.75 pu
3. G3: GESS initial storage at 1.0 pu

As may be observed from **Table 5.5**, the LCOEs for same load patterns decrease with increasing initial storage of GESS at the starting of the day. As compared to L1/G1 and L1/G2 the LCOE of L1/G3 is much lower as Biomass Generator 2 is entirely non-operational and GESS compensates the load, obviously at cheaper rate. Only in two cases L3/G1 and L4/G1, energy is bought from the grid and in both the cases initial storage of GESS is at 0.5pu and the load is comparatively higher. In all the cases, LCOE is lower if the GESS is initially at maximum capacity, which enables the system to minimize energy drawn from the grid as well as lowering the energy drawn from Biomass generators.

TABLE 5.5. COMPARISON OF LCOE ON DIFFERENT COMBINATIONS OF LOAD AND GESS INITIAL ENERGY

Parameter	L1/G1	L1/G2	L1/G3	L2/G1	L2/G2	L2/G3	L3/G1	L3/G2	L3/G3	L4/G1	L4/G2	L4/G3
No. of Solar Panel	900	900	900	900	900	900	900	900	900	900	900	900
Max capacity of BG 1 (kW)	100	100	100	100	69.84	100	100	76.82	76.82	100	97.80	95.28
Max capacity of BG 2 (kW)	100	100	0	100	100	14.07	100	100	100	100	100	94.27
Max Storage capacity of GESS (kW)	654.82	436.55	1000	925.11	795.47	1000	1000	934.27	948.99	1000	990.16	1000
Total Load Served (kWh)	896326	896326	896326	995917	995917	995917	1095509	1095509	1095509	1195101	1195101	1195101
Total load Served through Solar (kWh)	164687	164687	164687	175102	175102	175102	183352	183352	183352	190077	190077	190077
Total load Served through BG 1 (kWh)	332125	332125	332125	338849	252885	338849	345573	278453	278453	352296	346260	338964
Total load Served through BG 2 (kWh)	266523	266523	0	274166	304092	47229	290992	315050	315050	301263	303146	293533
Total load Served through GESS (kWh)	132991	132991	399514	207800	263838	434737	262315	318654	318654	319821	355618	372527
Total Grid Purchase (kWh)	0	0	0	0	0	0	13277	0	0	31644	0	0

Total Grid Sale (kWh)	309208	397106	222061	209346	279018	194805	153141	229996	323556	124743	195880	286628
LCOE ($)	0.0473	0.0429	0.0388	0.0487	0.0430	0.0392	0.0478	0.0431	0.0393	0.0463	0.0435	0.040
LCOE (INR)	3.31	3.00	2.71	3.41	3.01	2.74	3.35	3.02	2.75	3.24	3.05	2.76
Decrease in Energy price (%)	6.76 %	15.49 %	36.90 %	3.94 %	15.21 %	22.82 %	5.63 %	14.93 %	22.54 %	8.73 %	14.09 %	22.25 %

Whenever GESS energy storage is at maximum during the starting of the day, energy drawn from biomass generators is tending to be lower for load demand at 0.9 pu and 1.0 pu. However, much difference may not be observed if the load demand is higher. In this proposed microgrid, the overall LCOE does depend on the energy sale to the grid. As in L1/G2, in spite of initial GESS storage capacity is lower, the LCOE is reduced eventually, due to lower load demand and higher grid sale. Therefore, if there is no nearby grid connectivity available, there may be a shortage of energy in some cases and also LCOE is bound to increase. However, in all the cases in spite of inward energy transaction from the grid (in some cases), the overall reported LCOE is comparable and somewhat lesser than the existing energy price of the Nagaland State, which is minimum @ Rs.3.55/kWh for up to 30 kWh for domestic and @Rs.6.50/kWh for up to 60 kWh for commercial loads [173].

5.3. Results of a Dual Mode Wind Turbine Operation with Hybrid Energy Storage System

The proposed DMWT – PSH – VRFB system structure and operation strategy is discussed in section 3.3.3. The system operation is simulated in an isolated microgrid scenario to determine its effectiveness. A 48 hours continuous operation of 48 equal intervals with variable system loads are considered for the simulation (Figure 5.9). The PSH is considered to be at its maximum storage capacity and VRFB is considered to be empty at the starting of the 1st interval in this simulation. The wind speed considered (Figure 5.10) is the real wind speed data of October 15, 2017 of Barmer, Rajasthan, India [105]. It is assumed that the wind speed remains similar on the next 24 hours to that of the previous day.

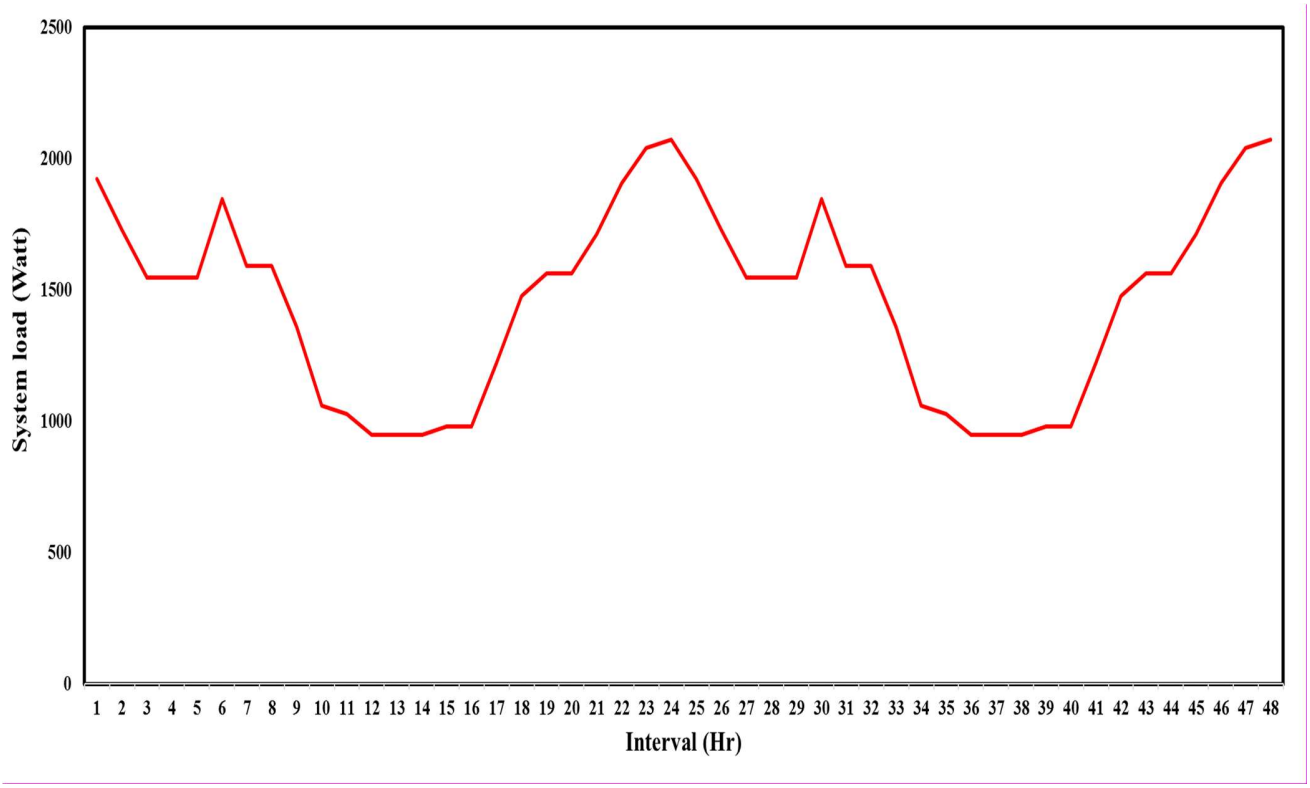

Figure 5.9. System Load in Each Interval in a Day Ahead Scenario

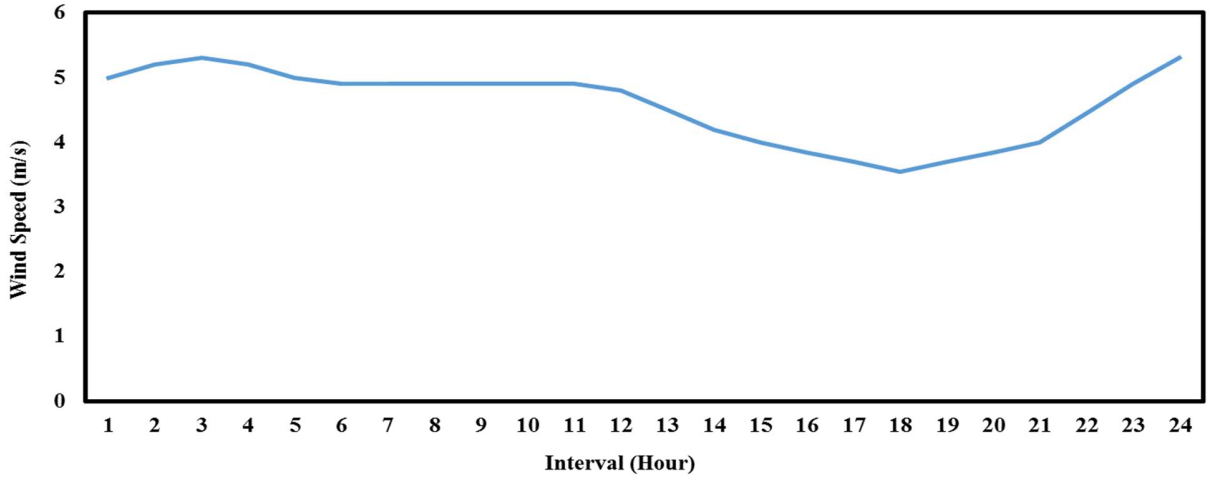

Figure 5.10. Wind Speed of Barmer, Rajasthan on October 15, 2017 [105]

As discussed throughout the section 3.3.3, the system load is supplied by either the PSH or the VRFB or both together if required, as the main purpose of this system is to serve the load as much as possible. Being an isolated microgrid system, there is limitation of non-connectivity of the main grid. Output of the PSH and VRFB for first 24 hours is shown in Figure 5.11 whereas that for the next 24 hours is shown in Figure 5.12. The corresponding water level and VRFB stored charge at

the end of each interval for 1st to 24th interval and for 25th to 48th interval are shown in Figure 5.13 and Figure 5.14 respectively. In Figure 5.11 and Figure 5.12, $\boxed{E}$ and $\boxed{M}$ denotes the Electrical and Mechanical mode of operation respectively.

In this scheme it is assumed that at the starting of the 1st interval, water level in the UR is at maximum *i.e.* 5 m and the VRFB is completely discharged. Therefore, in the 1st interval the proposed system operates in Electrical mode, PSH delivers the load and VRFB gets charged (Figure 5.11). At the end of 1st interval stored water level in UR reduces to 3.32 m and stored charge in VRFB stands at 3735 Wh which is shown in Figure 5.13.

At the starting of the 2nd interval, it is observed that with the stored water in UR, the PSH can serve the load demand. Therefore, the system continues to operate in Electrical mode, PSH delivers the load and VRFB gets charged. At the end of 2nd interval the water level in UR has reduced to 1.81 m and VRFB gets fully charged (Figure 5.13).

At the starting of the 3rd interval, it is observed that with the stored water in UR, the PSH cannot support the demand, thus, the mode changeover takes place and the system starts to operate in Mechanical mode. During this interval the VRFB delivers the load and water gets pumped to the UR (Figure 5.11). At the end of this interval, water level in UR reaches 3.75 m and stored charge in VRFB reduces to 5440 Wh as depicted in Figure 5.13.

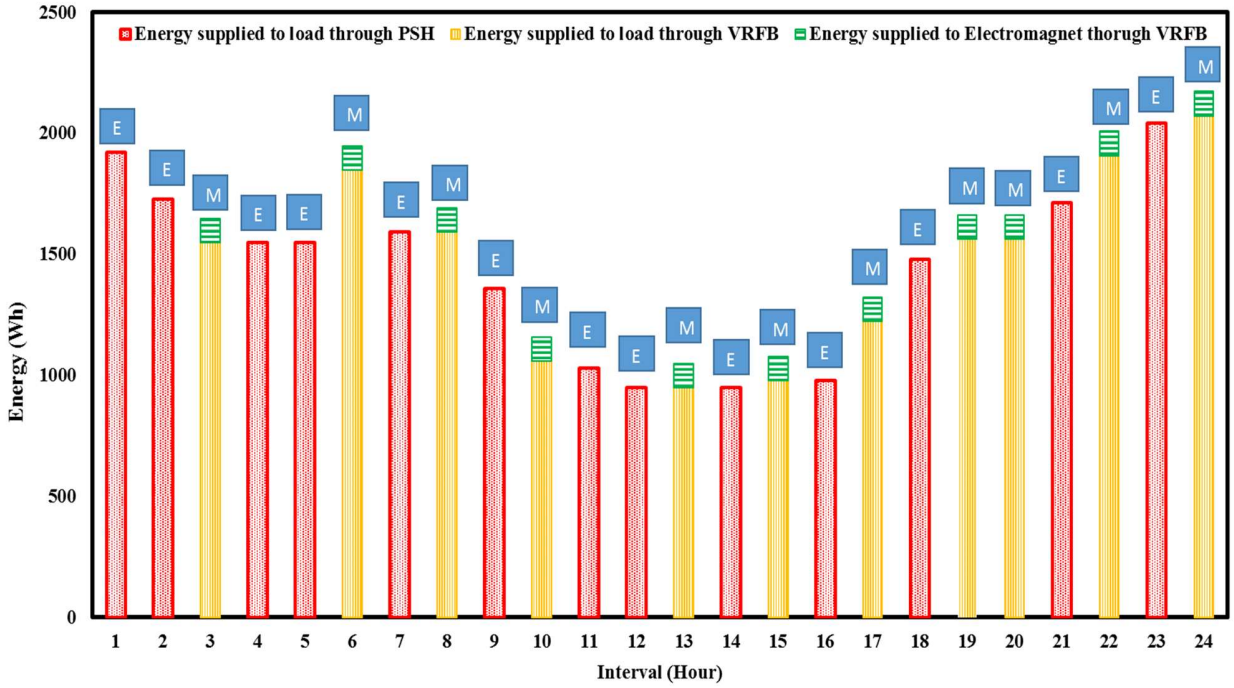

Figure 5.11. Energy Supplied to Load from PSH and VRFB along with Energy Supplied to Electromagnet for Mode Changing Operation (Interval 1 – 24)

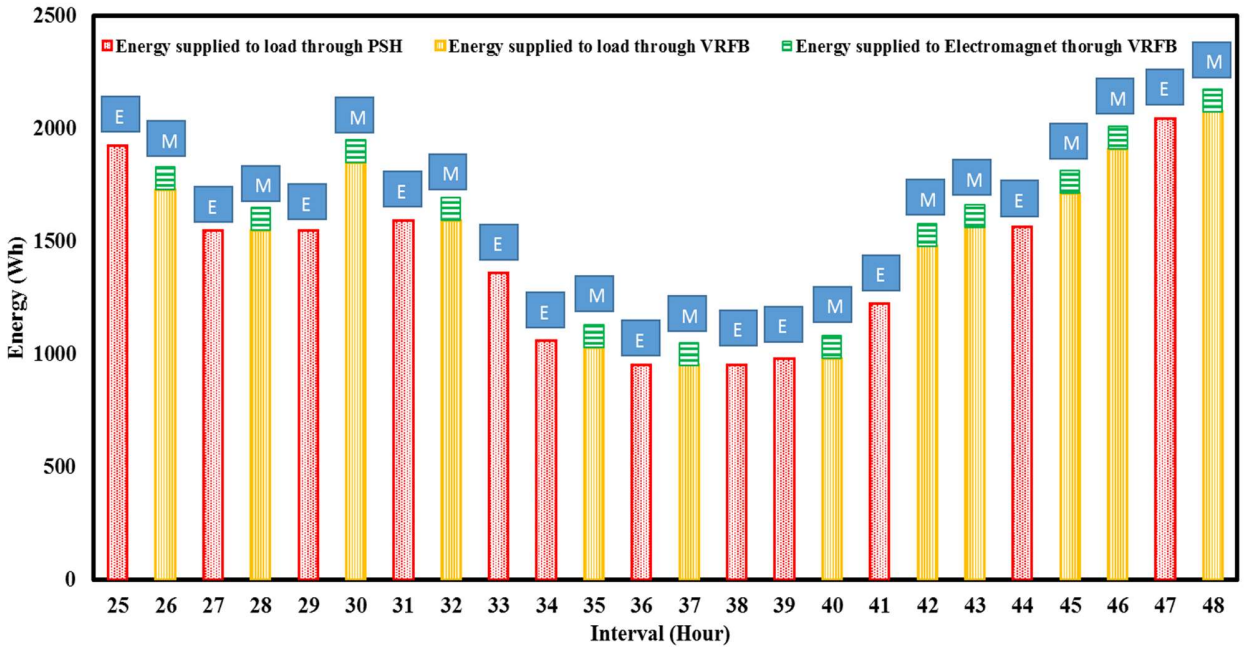

Figure 5.12. Energy Supplied to Load from PSH and VRFB along with Energy Supplied to Electromagnet for Mode Changing Operation (Interval 25 – 48)

At the starting of 4th interval, it is detected that with the stored water in the UR, PSH can deliver the load, therefore the system operation changes to Electrical mode. At the end of this interval VRFB reaches its maximum storage limit and water level in UR reduces to 2.4 m (Figure 5.13).
As observed from Figure 5.9, the system load is lower than previous intervals, water utilization is also lower as compared to 1st and 2nd interval. Due to lower demand in 4th interval, the stored water in UR is enough to supply the demand of the next interval (Figure 5.13). Thus, the system continuous to operate in Electrical mode as the stored water can supply the lower demand in 5th interval. At the end of 4th interval, VRFB has reached its maximum storage whereas the system is still operating in Electrical mode (Figure 5.13). Thus, the generated energy from DMWT is delivered to dump load during the 5th interval, as the water level of UR is on the higher side, PSH keeps on generating with no requirement of mode changeover. Similar situation is observed during 12th interval, which is evident from Figure 5.13.
A sort of opposite scenario is observed during the 19th and 20th interval. At the end of 18th interval due to higher load demand the water level in UR reduces to 1.06 m. Further, due to lower wind speed [105], the water level reaches only up to 1.72 m by the end of 19th interval, which is not sufficient to deliver the load of the next interval. It took one more interval i.e. 20th interval for the water level to reach above the limit, in which the stored water of UR is sufficient to deliver the load of the next interval. Therefore, mode changeover took place at the beginning of the 21st interval.

At the starting of 24th interval, the water level was 0.33 m which finally reached to 2.73 m at the end of 24th interval. This is an increase of 2.4m, due to comparatively higher wind speed as compared to 19th interval. In the 19th interval, the water level in UR increased by only 0.66 m due to lower wind speed. Due to this lower wind speed during 19th and 20th interval, the water pumped in UR is of small volume. Thus, during these intervals, VRFB supplies the load and the system was operated in Mechanical Mode. This was possible as the stored energy in VRFB, at the end of 18th interval reached to 7182 Wh and the cumulative output during 19th and 20th interval was 3126 Wh. At the end of 20th interval the stored energy in the VRFB reduced to 3024 Wh.

It may be observed that at the end of the 24th interval, water level in UR was at 2.73 m and SOC of the VRFB was around 43 % (3226 Wh).

The next interval *i.e.* 1st interval of the next day or the 25th interval of the 48 hour operation, started with PSH delivering the load demand. Mode changeover took place at the starting of the 25th interval as stored water in UR was enough to deliver the load of this interval (Figure 5.12). However, at the strating of the next interval *i.e.* 26th interval again mode changeover took place. During the 25th interval VRFB has got charged as the system was operated in Electrical mode. At the end of this interval, stored charge in VRFB stood at 6961 Wh and water level in the UR at 0.59 m (Figure 5.14). Therefore, in the 26th interval, VRFB delivered the load and water was pumped in the UR, as the system was operated in Mechanical mode. From 25th to 33rd interval, mode changeover took place in every interval (Figure 5.12) as compared to 1st to 10th interval. This is due to the fact that, initially in the 1st interval, UR was completely filled (5 m) and VRFB was completely discharged (0 Wh) but during the 25th interval UR stood at 2.73 m and VRFB stored charge at 3326 Wh. It is also to be noted that during first day of operation (1st to 24th interval) PSH was found to be operated in 13 intervals whereas VRFB was observed to be operated in 11 intervals. As compared to the next day of operation (25th to 48th interval) where each PSH and VRFB was operated in 12 intervals each. Also, mode changeover took place 19 times on the first day as compared to 20 times (including the mode changeover at the starting of 25th interval) during the second day. Therefore, it is established that, the initial stored volume of water and SOC of VRFB at the starting of the 1st interval of any given day (24 hr) affected the system operation scenarios.

At the end of 48th interval stored water in UR was at 3.04 m and VRFB stored energy was 1175 Wh (Figure 5.14). This established that the system was ready to be deployed in the next interval or the 1st interval of the next day. Therefore, it may be stated that the system provided uninterrupted energy to the consumer end and normal fluctuations in wind speed did not affect the voltage at the consumer end. However, extreme fluctuation in wind speed (storm, extremely low speed etc.) may affect the voltage of the consumer end, but even then, the proposed system as designed can maintain the stable voltage at the consumer end for some intervals depending on the microgrid load demand.

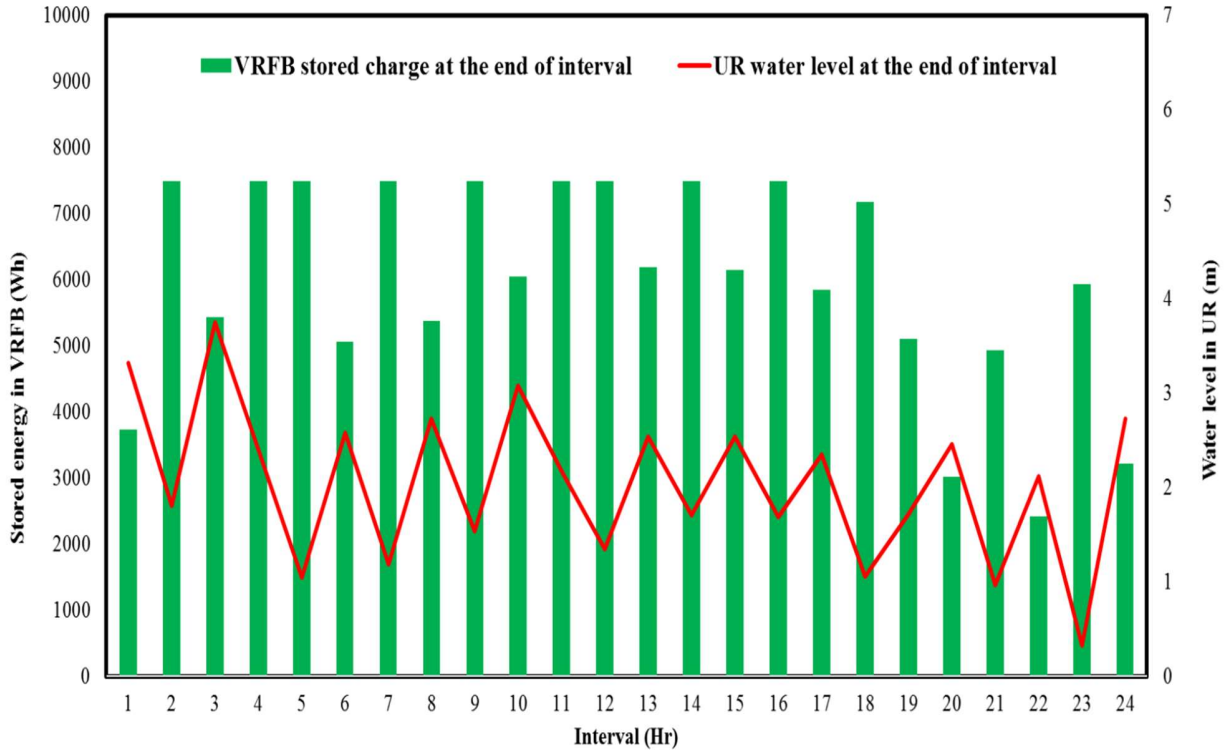

Figure 5.13. VRFB Stored Charge and UR Water Level at the end of Each Interval (Interval 1-24)

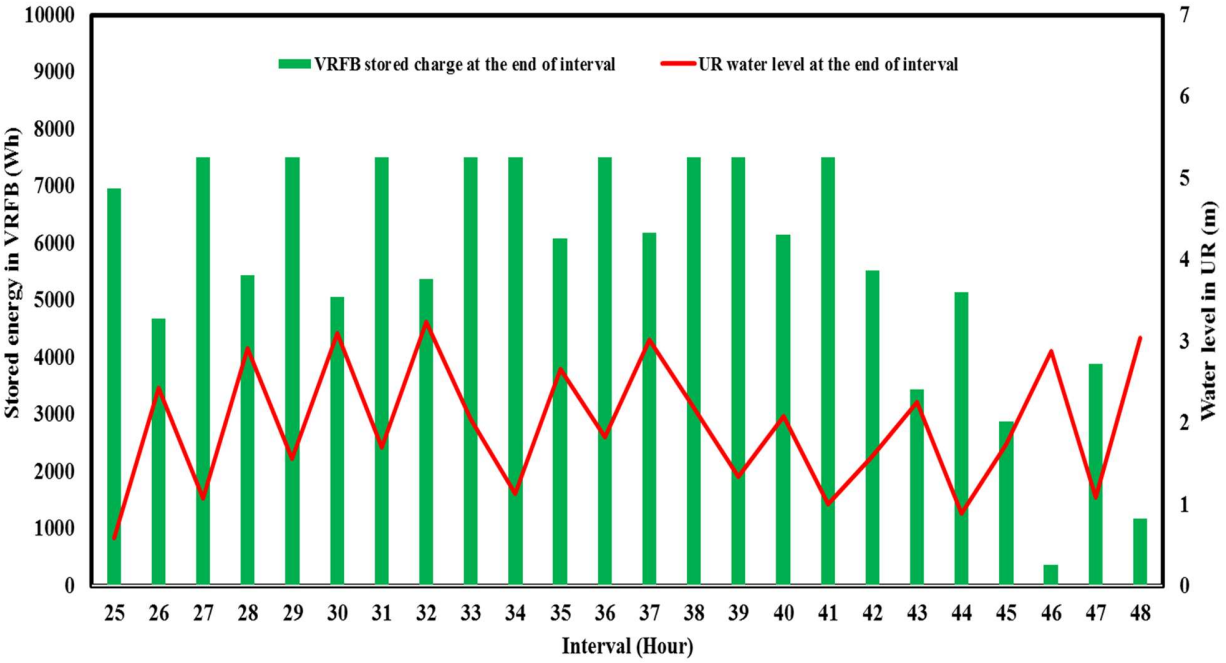

Figure 5.14. VRFB Stored Charge and UR Water Level at the end of Each Interval (Interval 25-48)

Figure 5.15 and Figure 5.16 shows the change in water level i.e. the amount of water pumped to UR through CP and released to generate electricity from UR at every slot of 48 intervals.

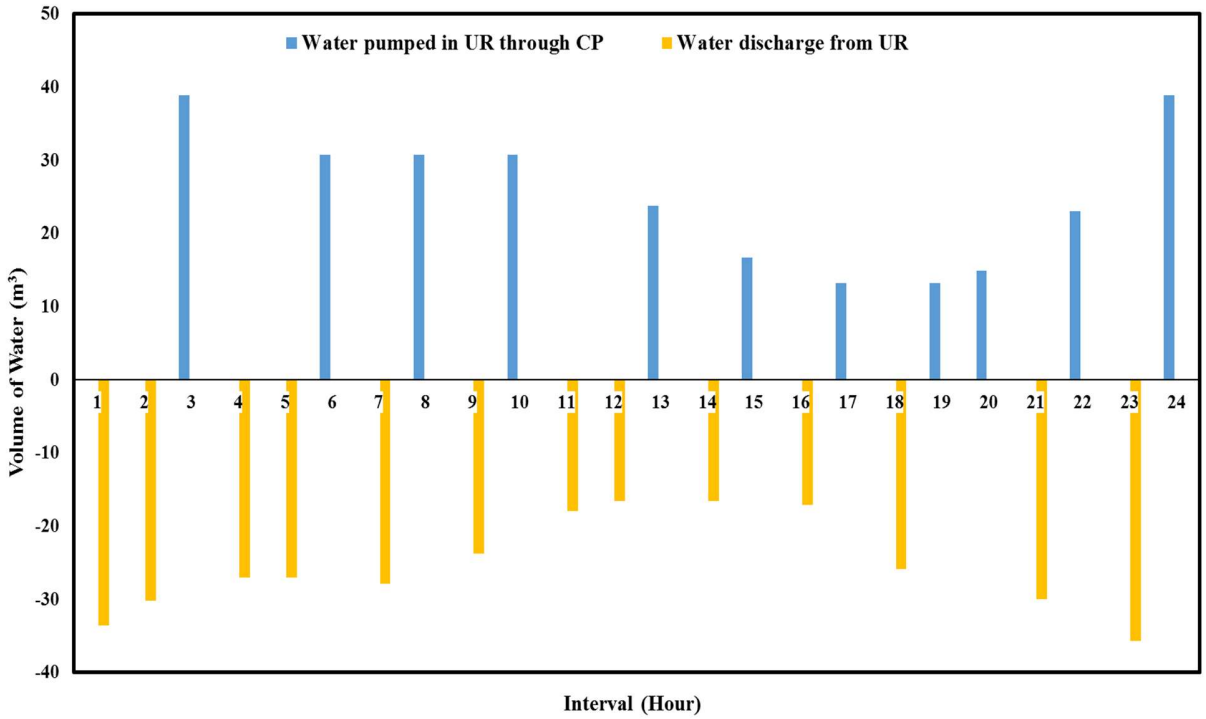

Figure 5.15. Water Pumped in UR and Discharge from UR throughout the day in Each Interval (Interval 1-24)

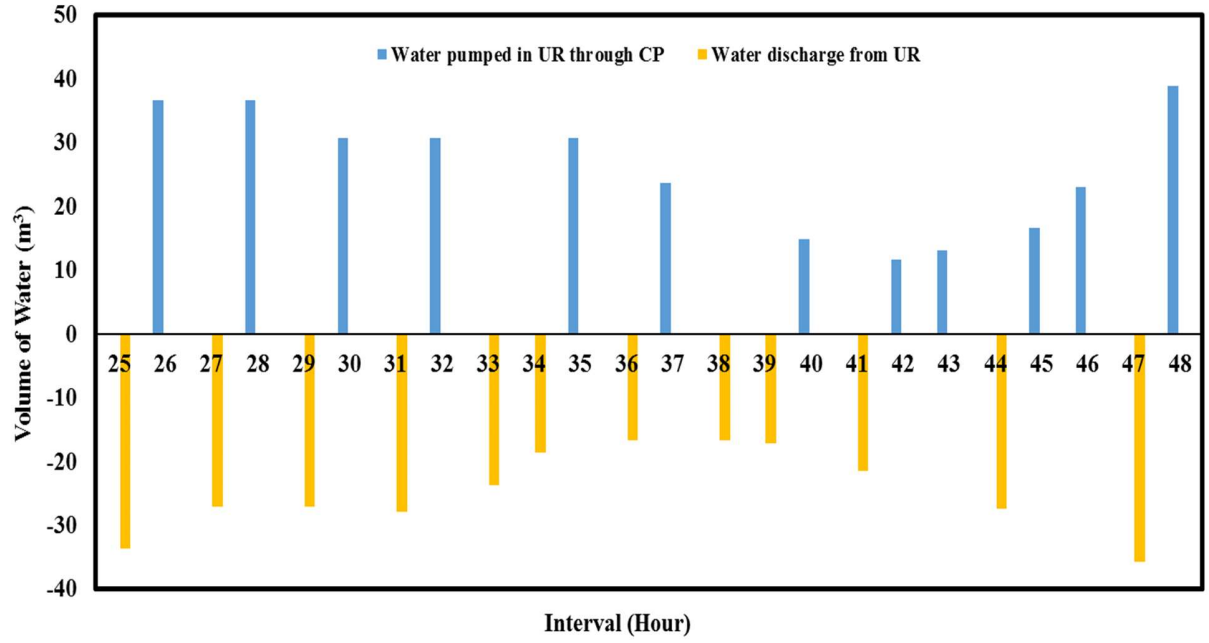

Figure 5.16. Water Pumped in UR and Discharge from UR throughout the day in Each Interval (Interval 25-48)

5.3.1. Voltage Stabilization of the Proposed DMWT – PSH – VRFB System

Figure 5.17 displays the output voltage of the proposed system across various intervals, demonstrating consistent and stable performance without any noticeable voltage deviation. This indicates that the proposed system is reliable and capable of maintaining a steady output voltage. The stability shown in Figure 5.17 reinforces the effectiveness of the system in meeting its intended objectives. Overall, the results presented in Figure 5.17 support the conclusion that the proposed system is stable and suitable for its intended application.

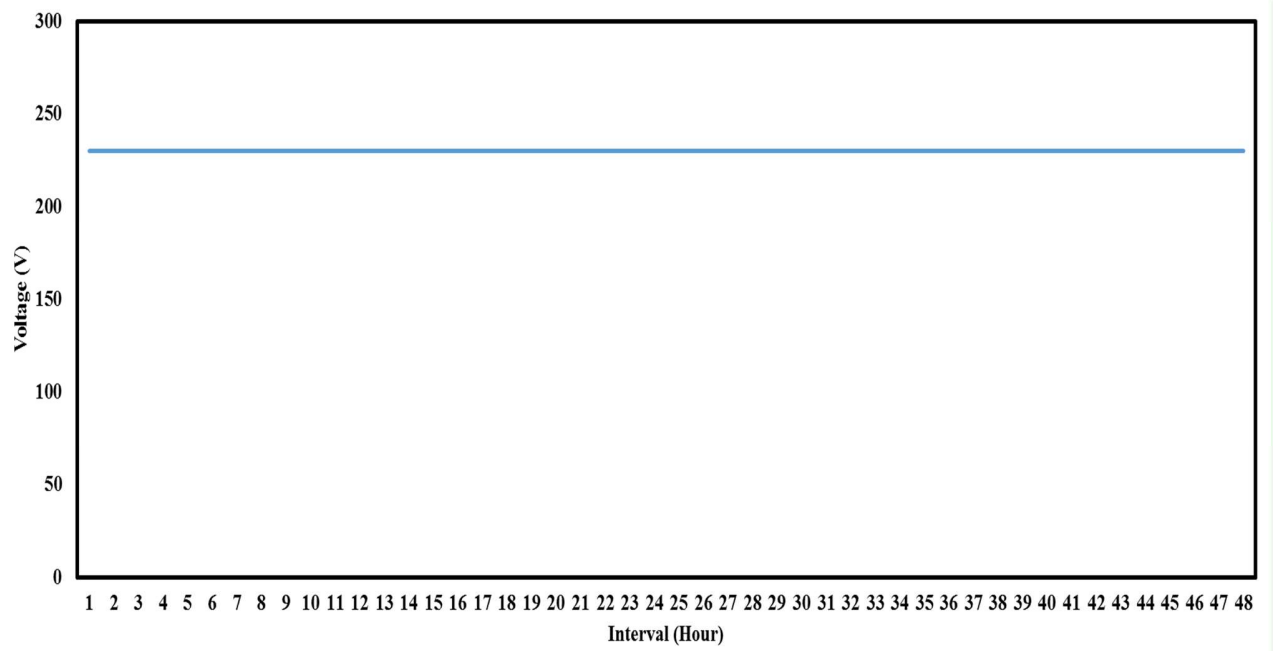

Figure 5.17. Output Voltage of the Proposed DMWT – PSH – VRFB System

5.4. Results of Operation of two mechanically driven Gravity Energy Storage Systems using one Wind Turbine

This section deals with the results generated from the simulation of the system, consisting of two mechanically driven GESSs by one WT, discussed in section 3.4. The wind turbine specification under consideration for the simulation of the proposed system in section 3.4 is similar to commercially available wind turbine Aeolos-H 5000 W wind turbine [174]. The rotor blade diameter is 6.4 meter, cut-in speed and rated wind speed are 3 m/s and 10 m/s respectively. The location of the microgrid is considered to be in Barmer, Rajasthan and the wind speed considered is the actual wind speed of the location dated 15th October, 2017 [105]. This wind turbine is considered due to its specifications which is actually in accordance with the wind speed of the considered location. A smaller wind turbine may not fulfill the proposed requirements or an incorporation of larger wind turbine in this microgrid may result in wastage of energy.

For the simulation purpose of the proposed system, two GESS of 8.0 kWh each, have been considered. The main objective for considering two number of GESS, is to ensure uninterrupted energy supply without incorporation of any conventional resources. The storage capacity considered as such; one GESS can supply the demand over a period of time when the other gets charged. This also ensures uninterrupted energy supply. A smaller capacity GESS may not fulfill this clause whereas a larger GESS may result in wastage of energy. Moreover, a larger GESS requires a larger height of the tunnel, which in turn requires higher mechanical power delivered from the wind turbine for charging and results in larger wind turbine, which finally indicates more wastage economically, technically and environmentally. At the beginning of the day, it is assumed that GESS 1 is fully charged and GESS 2 is fully discharged. Two GESSs considered here are identical in all aspects. Their suspended weights are made of steel with diameter of 4 meter and height of 2 meter each. Taking into consideration the dimensions and maximum energy storage capacity of GESS 1 and GESS 2, the underground vertical tunnel height of each GESS is calculated as 16.50 meter.

The proposed system is designed to be completely operated through wind resource to deliver uninterrupted energy at a constant voltage in an isolated microgrid. In this section, detailed discussion on system output for a loading pattern has been carried out. The system load for each interval is shown in Figure 5.18. The peak demand is considered as 2073 W, whereas the off-peak load demand is 949.44 W only. A day ahead operation is performed to validate the feasibility of the system. An entire day of operation is divided into 24 intervals of 1(One) hour each. Output of GESS 1 and GESS 2 are shown in Figure 5.19. It is to be observed that for each interval, energy

to the load is fully supplied by either GESS 1 or GESS 2. The proposed system can handle regular wind speed variation but any extreme fluctuation of wind speed for a long time may impact its operation capability.

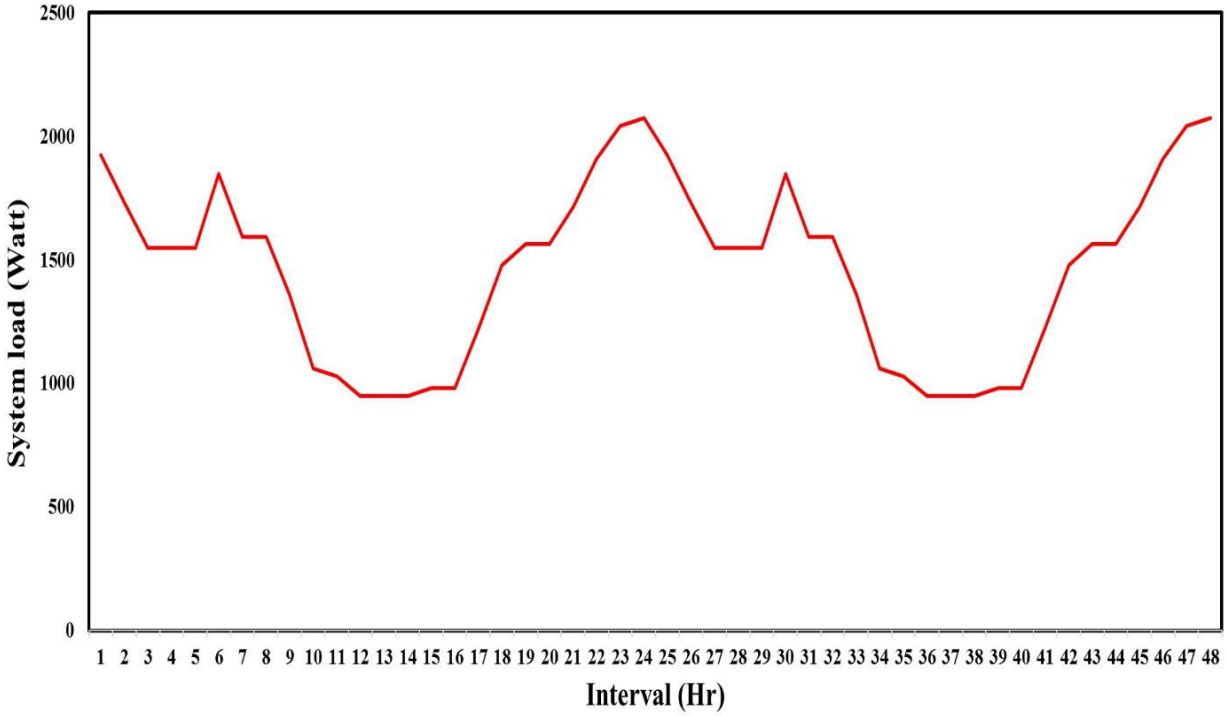

Figure 5.18. System Load per Interval in a Day Ahead Scenario

Energy generated from GESS 1 and GESS 2 in each interval for 24 hours has been depicted in Figure 5.19, which shows the supply of the entire load demand. As discussed in Section 3.4.3, until and unless GESS 1 is incapable of supplying the entire load of a particular interval, it continues to generate for consecutive intervals while GESS 2 continues to get charged or remains idle. Thus, the GESS 1 gets first priority while delivering the load.

At the starting of the day, GESS 1 starts supplying the energy requirement of the load and continues till 3rd interval (Mode 2). At the end of the 3rd interval its charge/stored energy drops to 9.74% *i.e.* 779.2 Wh, whereas GESS 2 gets fully charged by the end of the 3rd interval (as shown in Figure 5.20) Therefore, during the 4th interval, GESS 1 becomes incapable of supplying the full load, which enables the GESS 2 to supply the load demand. Thus, at the starting of the 4th interval, the mode of operation changes from Mode 2 to Mode 1 and GESS 2 starts supplying the system load while GESS 1 starts to get charged. At the end of 4th interval GESS 1 gets charged to 50.77% *i.e.* 4061.6 Wh (Figure 5.20), which is sufficient enough to supply the load of 5th interval. Again, the mode of operation changes and the system starts operating in Mode 2, enabling GESS 1 to supply the load of 5th interval (Figure 5.19) and GESS 2 to get charged. At the end of the 5th interval stored

energy in GESS 1 reduces to 1977.2 Wh and in GESS 2 stored energy increases to 8000Wh. In the 6th interval load demand goes 19.38% higher to 1848 Wh as compared to 5th interval load demand of 1548 Wh (Figure. 5.18). GESS 1 does not possess enough charge to supply the full load, thus, the mode changes from Mode 2 to Mode 1 and GESS 2 supplies the load. During 6th interval GESS 1 gets charged and stored energy reaches around 60 % *i.e.* 4656.6 Wh (Figure 5.20), which is enough to deliver the load of 7th and 8th interval (Figure 5.19) due to lower demand in those intervals. While at the end of 6th interval energy stored in GESS 2 reduces to 5433.6 Wh.

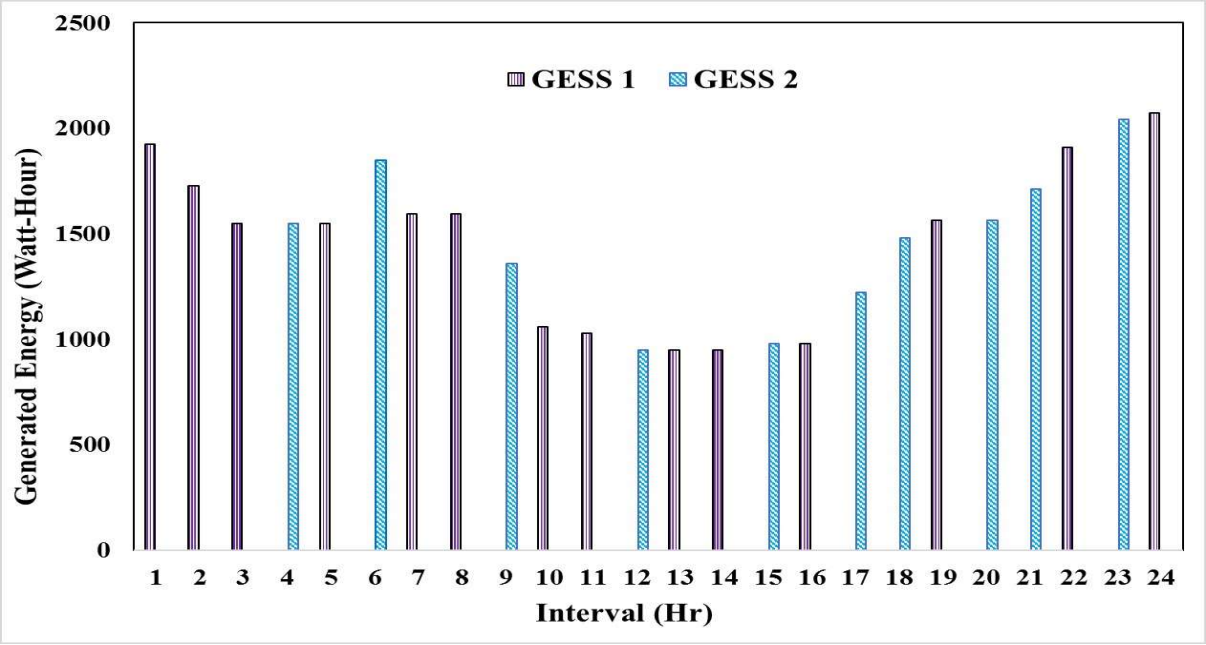

Figure 5.19. Generated Energy from GESS 1 and GESS 2 in Each Interval

As per the set operation strategy (refer to section 3.4.3), GESS 1 keeps on generating during 7th and 8th interval and refraining GESS 2 from charging during 8th interval as at the end of 7th interval GESS 2 gets fully charged. This same situation is also observed in 10th and 13th interval. This scenario has occurred due to comparatively lower energy demand and GESS 1 holding enough charge to deliver the energy demand during 10th – 11th and 13th – 14th interval.

At the end of 11th and 14th interval GESS 1 becomes almost fully discharged (Figure 5.20). Thus, in 12th and 15th interval GESS 2 supplies the load (Figure 5.19). The load in the 16th interval is again supplied through GESS 1.

However, due to low wind speed during 17th – 18th and 20th – 21st intervals, GESS 1 has to get charged for two consecutive intervals to possess enough charge to supply the full load of the 19th and 22nd intervals respectively.

At the end of the 24th interval it is observed that the GESS 2 holds around 40% of charge and is capable to supply during the 1st interval of the next day, while GESS 1 got almost discharged (Figure 5.20).

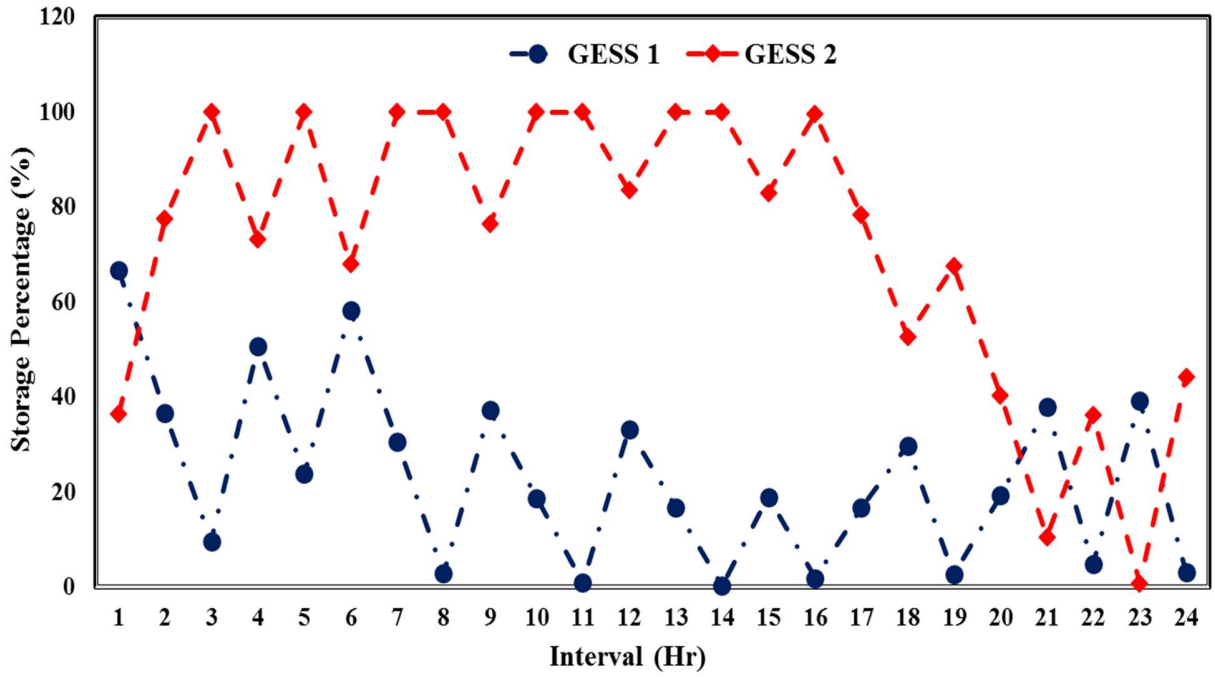

Figure 5.20. Stored Energy Percentage of GESS 1 And GESS 2 at the End of Each Intervals

During the day of operation, wind speed varies in different intervals resulting in different amount of energy available to charge the GESSs. The charging variations are depicted in Figure 5.21. Stored energy at starting of any interval and charging during any interval of GESS 1 and GESS 2 are presented in Figure 5.21 (a) and 5.21 (b) respectively. As discussed earlier, for 1st – 3rd interval, GESS 1 keeps on supplying the load and GESS 2 gets fully charged from fully discharged condition. In the 1st interval GESS 2 gets charged around 2918 Wh, whereas, due to higher wind speed, in the 2nd interval the GESS 2 stores 12.49% more energy than the previous interval. The lowest charging of 1044.31 Wh can be observed in the 18th interval (when the wind speed is 3.55 m/s), for GESS 1, which is around 70% lower than the highest energy available for charging during any interval, which is for GESS 2 at 24th interval. Although the wind speed (Figure A.1) is same in both the 3rd and 24th interval i.e. 5.3 m/s, but the charging of GESS 2 is much lower in the 3rd interval as GESS 2 gets fully charged after absorbing 1800.12 Wh of energy. Whereas, at the starting of 24th interval the charge of GESS 2 is 69.6 Wh only, therefore, the wind energy gets fully utilized by charging the GESS 2 by 43.44% (3475.12 Wh). Comparing Figure 5.21 (a) and 5.21 (b), it can be observed that, no charging took place at 8th interval, as GESS 2 is fully charged and GESS 1 is on generating mode. Similar scenario occurred in 11th and 14th interval. Interval number 25 shown in Figure. 5.21 (a) and 5.21 (b) is the stored energy of the respective GESS 1 and GESS 2 available for the 1st interval of the next day.

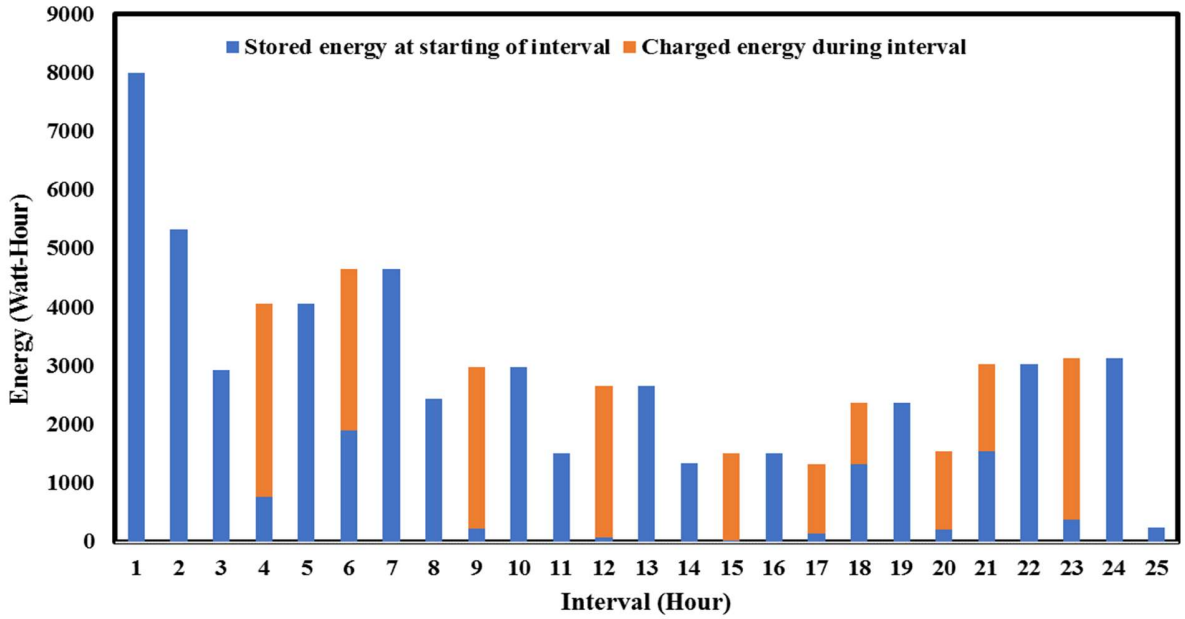

Figure 5.21 (a). Stored Energy at the Starting of Interval and Charged Energy During Interval in GESS 1 throughout the Day

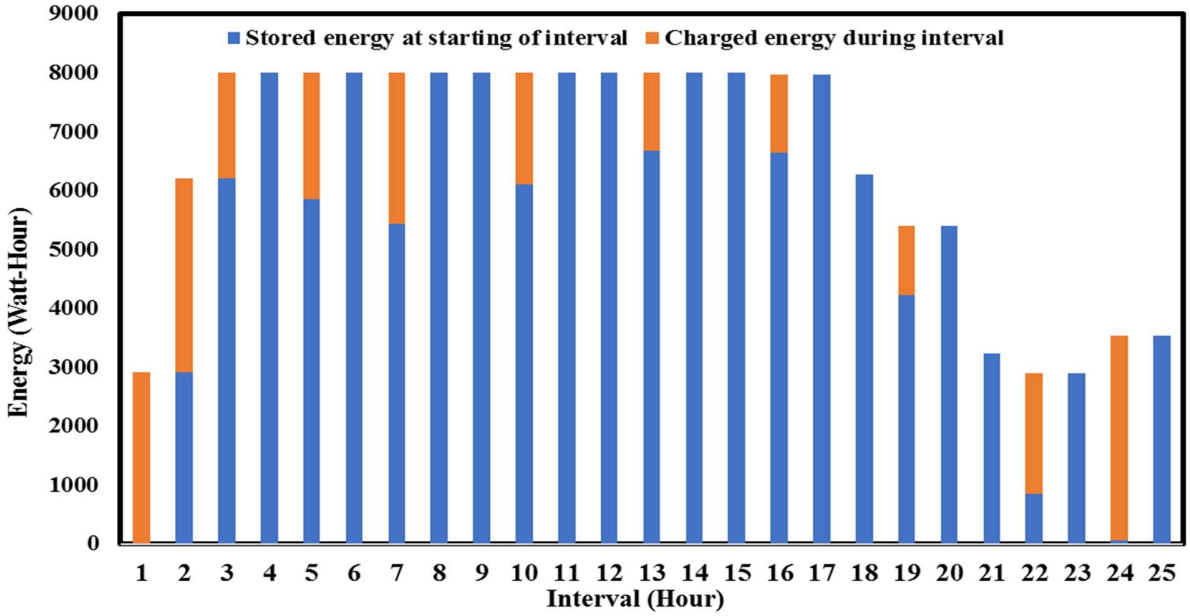

Figure 5.21 (b). Stored Energy at the Starting of Interval and Charged Energy During Interval in GESS 2 throughout The Day

Table 5.6 ECONOMIC ANALYSIS OF WIND TURBINE DRIVEN DUAL GESS SYSTEM

Total Load throughout a year	356017.92 kWh
GESS Cost for each one (80KW) [174, 175]	40000 $
Wind Turbine Cost (5kW) [173]	4117 $
Other Equipment cost (assumed) [176]	1051.46 $
Labour Cost [132]	2823.53 $ Per Year
Life Time	25 Years
Energy Charge	0.031 $/ kWh

Economic analysis of the operation strategy of two mechanically driven GESS using one wind turbine is depicted in Table 5.6. The unit energy cost analysis is performed taking into consideration of total serviceable energy of the microgrid throughout a year, GESS installation cost, wind turbine installation cost, other ancillary equipment cost, Salary of Labour and lifetime of the project. Ancillary equipment cost is assumed to be 25% of the total project cost and yearly salary is assumed as per industry standards.

The unit energy cost of the system is calculated to be 0.031$/kWh or Rs.2.6/kWh. The derived energy cost is much lower than the current cost of energy of the assumed location which is around Rs.7/kWh.

Moreover, the system is completely free from environmental damage, requires smaller installation area and does not affect the ecology of the geographical area.

Thus, it may be stated that the system is economical, pollution free, stable and safe for environment.

Further modification of the proposed system may result in better operation standards and can be operated autonomously, also more economical aspects will be investigated in the future work.

CHAPTER 6

6. Conclusion and Future Work

The researches undertaken throughout the course of PhD is solely dedicated to technically bring renewable-based electricity generation at par the electricity generated from thermal power plants, in terms of voltage stability and consistency.

In the first study, a self-sustainable microgrid with stable voltage has been designed for the backward areas of Assam utilizing the locally available renewable resources like hydro and wind. A Li-ion battery system has also been incorporated to maintain the stability and enhance the reliability of the system. The robustness of the system has also been examined by simulating the system under three different types of varying load and three different types of varying wind speed conditions.

Apart from only analyzing the technical feasibility of the proposed RE-based hybrid system, a techno-economic analysis has also been performed in the second study. Where the hybrid system consists of solar PV, biomass generator and GESS and simulated considering the real data of the state of Nagaland. These results of the analysis depict that along with being consistent, in terms of supply and voltage stability the generated electricity is also very cost-effective. The LCOE calculated from this hybrid system is found to be lower than the domestic tariff of the Nagaland, which strengthens the main focus of the undertaken researches throughout the PhD tenure.

In the third study, a novel system has been designed where a single wind turbine can operate in both mechanical mode and electrical mode to store energy in PSH and VRFB respectively. An innovative electromagnet-based mode changer assembly has also been designed to provide the mode changing operation of the wind turbine. Furthermore, it has been observed that the combined operation of Dual mode wind turbine – Pump Storage hydro – Vanadium redox flow battery hybrid system is able to provide uninterrupted and stable power supply.

In the fourth study, another novel idea has been introduced for the supply of uninterrupted electricity at stable voltage. Here, a single wind turbine has been used to charge and discharge two GESSs at the same time for continuous power supply with the help of a mode changer assembly. The design of mode changer assembly provided in this scheme has also been an innovative idea which is quite different from the third study. The system further depicts its cost effectiveness. The novel hybrid system is found to be able to supply electricity at Rs. 2.6/kWh which is much lower than the present electricity unit price of Rs. 7 of the considered location.

Therefore, it can be stated that if a renewable-based system can be designed properly, it can supply electricity at much lower than the thermal power generation both in terms of technicality and economy.

The novel designs provided for two hybrid systems comprising of – (i) Dual mode wind turbine – Pump storage hydro – Vanadium redox flow battery and (ii) Single Wind turbine – Two Gravity energy storage systems require further studies before practical executions, like the effects of incorporation of high starting current loads (water pump, air-conditioner etc.) in the system. From

the construction view-point, both the system requires an extensive study over the materials and equipment sizing. Furthermore, the systems require techno-economic optimizations to go for a pilot project followed by commercial applications.

Appendix

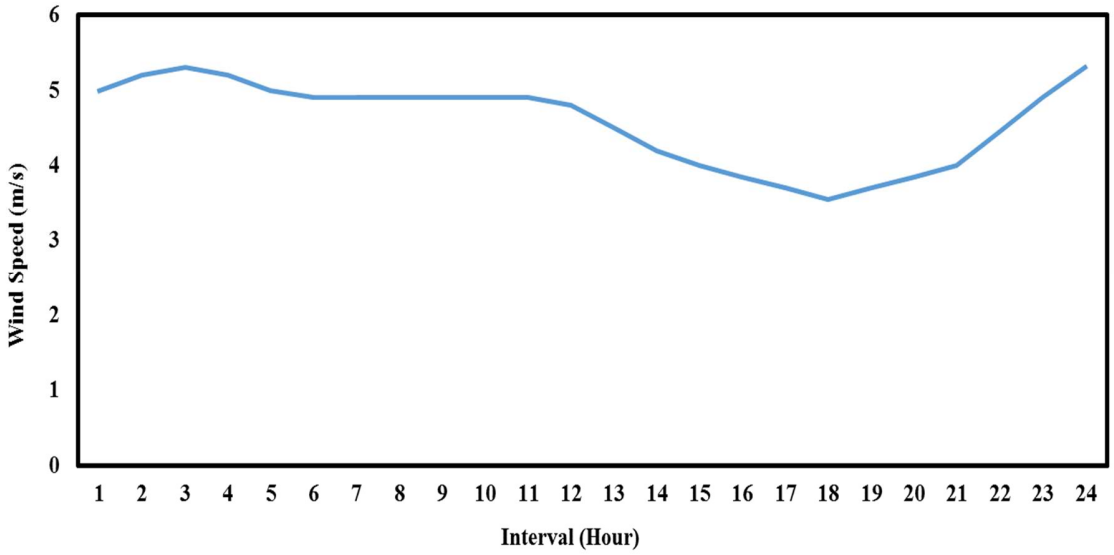

FIGURE A.1. HOURLY WIND SPEED OF 15TH OCTOBER 2017 [105]

Reference

[1] World Energy Outlook – 2018, International Energy Agency. https://www.iea.org/reports/world-energy-outlook-2018 [as on February 16, 2024]

[2] International Energy Agency. https://iea.blob.core.windows.net/assets/85b9fc1b-74a6-477e-8052-81bb0d821f4a/Coal_2018.pdf [as on February 16, 2024]

[3] Lakshmanan PK, Seetharaman AL. Paris Agreement on Climate Change and India. Journal of Climate Change. 2017 May 25;3(1). DOI: http://dx.doi.org/10.2139/ssrn.3048720

[4] Press Information Bureau. Government of India. https://pib.gov.in/newsite/printrelease.aspx?relid=174832 [as on February 19, 2024]

[5] Rathore A, Patidar NP. Reliability assessment using probabilistic modelling of pumped storage hydro plant with PV-Wind based standalone microgrid. International Journal of Electrical Power & Energy Systems. 2019 Mar 1;106:17-32. DOI: https://doi.org/10.1016/j.ijepes.2018.09.030

[6] Tudu B, Roy P, Kumar S, Pal D, Mandal KK, Chakraborty N. Techno-economic feasibility analysis of hybrid renewable energy system using improved version of particle swarm optimization. InInternational Conference on Swarm, Evolutionary, and Memetic Computing 2012 Dec 20 (pp. 116-123). *Springer*, Berlin, Heidelberg. DOI: 10.1007/978-3-642-35380-2_15

[7] US Department of Energy. Website: https://www.energy.gov/articles/how-microgrids-work [as on 15 December, 2021]

[8] Xiao, Jun, Linquan Bai, Fangxing Li, Haishen Liang, and Chengshan Wang. "Sizing of energy storage and diesel generators in an isolated microgrid using discrete Fourier transform (DFT)." *IEEE Transactions on Sustainable Energy* 5, no. 3 (2014): 907-916. DOI: 10.1109/TSTE.2014.2312328

[9] Krishnamurthy, Shashank, T. M. Jahns, and R. H. Lasseter. "The operation of diesel gensets in a CERTS microgrid." In *2008 IEEE Power and Energy Society General Meeting-Conversion and Delivery of Electrical Energy in the 21st Century*, pp. 1-8. IEEE, 2008. DOI: 10.1109/PES.2008.4596500

[10] Adaramola, Muyiwa S., Samuel S. Paul, and Olanrewaju M. Oyewola. "Assessment of decentralized hybrid PV solar-diesel power system for applications in Northern part of Nigeria." *Energy for Sustainable Development* 19 (2014): 72-82. DOI: https://doi.org/10.1016/j.esd.2013.12.007

[11] Ghenai, Chaouki, Tareq Salameh, Adel Merabet, and Abdul Kadir Hamid. "Modeling and optimization of hybrid solar-diesel-battery power system." In *2017 7th International Conference on Modeling, Simulation, and Applied Optimization (ICMSAO)*, pp. 1-5. IEEE, 2017. DOI: 10.1109/ICMSAO.2017.7934885

[12] Usman, Mohammad, Mohd Tauseef Khan, Ankur Singh Rana, and Sarwar Ali. "Techno-economic analysis of hybrid solar-diesel-grid connected power generation system." *Journal of Electrical Systems and Information Technology* 5, no. 3 (2018): 653-662. DOI: https://doi.org/10.1016/j.jesit.2017.06.002

[13] Mohammed, Ammar, Jagadeesh Pasupuleti, Tamer Khatib, and Wilfried Elmenreich. "A review of process and operational system control of hybrid photovoltaic/diesel generator systems." *Renewable and Sustainable Energy Reviews* 44 (2015): 436-446. DOI: https://doi.org/10.1016/j.rser.2014.12.035

[14] Chaudhary, Anil, Alex Huggett, Wai Kean Yap, and Vishy Karri. "Remote area hybrid solar-diesel power systems in Tropical Australia." *Energy Procedia* 57 (2014): 1485-1491. DOI: https://doi.org/10.1016/j.egypro.2014.10.140

[15] Wu, Baojia, Akbar Maleki, Fathollah Pourfayaz, and Marc A. Rosen. "Optimal design of stand-alone reverse osmosis desalination driven by a photovoltaic and diesel generator hybrid system." *Solar Energy* 163 (2018): 91-103. DOI: https://doi.org/10.1016/j.solener.2018.01.016

[16] Jeyaprabha, S. Berclin, and A. Immanuel Selvakumar. "Optimal sizing of photovoltaic/battery/diesel based hybrid system and optimal tilting of solar array using the artificial intelligence for remote houses in India." *Energy and Buildings* 96 (2015): 40-52. DOI: https://doi.org/10.1016/j.enbuild.2015.03.012

[17] Ameen, Ammar Mohammed, Jagadeesh Pasupuleti, and Tamer Khatib. "Simplified performance models of photovoltaic/diesel generator/battery system considering typical control strategies."

Energy Conversion and Management 99 (2015): 313-325. DOI: https://doi.org/10.1016/j.enconman.2015.04.024

[18] Ghenai, Chaouki, Adel Merabet, Tareq Salameh, and Erola Colon Pigem. "Grid-tied and stand-alone hybrid solar power system for desalination plant." *Desalination* 435 (2018): 172-180. DOI: https://doi.org/10.1016/j.desal.2017.10.044

[19] Lai, Chun Sing, and Malcolm D. McCulloch. "Levelized cost of electricity for solar photovoltaic and electrical energy storage." *Applied energy* 190 (2017): 191-203. DOI: https://doi.org/10.1016/j.apenergy.2016.12.153

[20] Akter, M. N., M. A. Mahmud, and Amanullah MT Oo. "Comprehensive economic evaluations of a residential building with solar photovoltaic and battery energy storage systems: An Australian case study." *Energy and Buildings* 138 (2017): 332-346. DOI: https://doi.org/10.1016/j.enbuild.2016.12.065

[21] Debnath, Dipankar, and Kishore Chatterjee. "Two-stage solar photovoltaic-based stand-alone scheme having battery as energy storage element for rural deployment." *IEEE Transactions on Industrial Electronics* 62, no. 7 (2014): 4148-4157. DOI: 10.1109/TIE.2014.2379584

[22] Fleischhacker, Andreas, Hans Auer, Georg Lettner, and Audun Botterud. "Sharing solar PV and energy storage in apartment buildings: resource allocation and pricing." *IEEE Transactions on Smart Grid* 10, no. 4 (2018): 3963-3973. DOI: 10.1109/TSG.2018.2844877

[23] Guo, Li, Zhouzi Yu, Chengshan Wang, Fangxing Li, Jean Schiettekatte, Jean-Claude Deslauriers, and Lingquan Bai. "Optimal design of battery energy storage system for a wind–diesel off-grid power system in a remote Canadian community." *IET Generation, Transmission & Distribution* 10, no. 3 (2016): 608-616. DOI: https://doi.org/10.1049/iet-gtd.2015.0190

[24] Sebastián, Rafael. "Application of a battery energy storage for frequency regulation and peak shaving in a wind diesel power system." *IET Generation, Transmission & Distribution* 10, no. 3 (2016): 764-770. DOI: https://doi.org/10.1049/iet-gtd.2015.0435

[25] Sebastián, Rafael. "Battery energy storage for increasing stability and reliability of an isolated Wind Diesel power system." *IET Renewable Power Generation* 11, no. 2 (2017): 296-303. DOI: 10.1049/iet-rpg.2016.0220

[26] Saad, Y., R. Younes, S. Abboudi, and A. Ilinca. "Hydro-pneumatic storage for wind-diesel electricity generation in remote sites." *Applied energy* 231 (2018): 1159-1178. DOI: https://doi.org/10.1016/j.apenergy.2018.09.090

[27] Nguyen-Hong, Nhung, Huy Nguyen-Duc, and Yosuke Nakanishi. "Optimal sizing of energy storage devices in isolated wind-diesel systems considering load growth uncertainty." *IEEE Transactions on Industry Applications* 54, no. 3 (2018): 1983-1991. DOI: 10.1109/TIA.2018.2802940

[28] Khalid, Muhammad, Ricardo P. Aguilera, Andrey V. Savkin, and Vassilios G. Agelidis. "On maximizing profit of wind-battery supported power station based on wind power and energy price forecasting." *Applied Energy* 211 (2018): 764-773. DOI: https://doi.org/10.1016/j.apenergy.2017.11.061

[29] Fathima, A. Hina, and Kaliannan Palanisamy. "Battery energy storage applications in wind integrated systems—a review." In *2014 International Conference on Smart Electric Grid (ISEG)*, pp. 1-8. IEEE, 2014. DOI: 10.1109/ISEG.2017.12005604

[30] Ibrahim, Hussein, Karim Belmokhtar, and Mazen Ghandour. "Investigation of usage of compressed air energy storage for power generation system improving-application in a microgrid integrating wind energy." *Energy Procedia* 73 (2015): 305-316. DOI: https://doi.org/10.1016/j.egypro.2015.07.694

[31] Zhang, Guotao, and Xinhua Wan. "A wind-hydrogen energy storage system model for massive wind energy curtailment." *International journal of hydrogen energy* 39, no. 3 (2014): 1243-1252. DOI: https://doi.org/10.1016/j.ijhydene.2013.11.003

[32] Alami, Abdul Hai, Kamilia Aokal, Jehad Abed, and Mohammad Alhemyari. "Low pressure, modular compressed air energy storage (CAES) system for wind energy storage applications." *Renewable Energy* 106 (2017): 201-211. DOI: https://doi.org/10.1016/j.renene.2017.01.002

[33] Mesbahi, Tedjani, Ahmed Ouari, Tarak Ghennam, El Madjid Berkouk, Nassim Rizoug, Nadhir Mesbahi, and Moudrik Meradji. "A stand-alone wind power supply with a Li-ion battery energy storage system." *Renewable and Sustainable Energy Reviews* 40 (2014): 204-213. DOI: https://doi.org/10.1016/j.rser.2014.07.180

[34] Nguyen, Cong-Long, Hong-Hee Lee, and Tae-Won Chun. "Cost-optimized battery capacity and short-term power dispatch control for wind farm." *IEEE Transactions on Industry Applications* 51, no. 1 (2014): 595-606. DOI: 10.1109/TIA.2014.2330073

[35] Luo, Fengji, Ke Meng, Zhao Yang Dong, Yu Zheng, Yingying Chen, and Kit Po Wong. "Coordinated operational planning for wind farm with battery energy storage system." *IEEE Transactions on Sustainable Energy* 6, no. 1 (2015): 253-262. DOI: 10.1109/TSTE.2014.2367550

[36] Rashid, Sumon, Shezan Rana, S. K. A. Shezan, Sayuti AB Karim, and Shamim Anower. "Optimized design of a hybrid PV-wind-diesel energy system for sustainable development at coastal areas in Bangladesh." *Environmental progress & sustainable energy* 36, no. 1 (2017): 297-304. DOI: https://doi.org/10.1002/ep.12496

[37] Olatomiwa, Lanre, Saad Mekhilef, AS Nazmul Huda, and Kamilu Sanusi. "Techno-economic analysis of hybrid PV–diesel–battery and PV–wind–diesel–battery power systems for mobile BTS: the way forward for rural development." *Energy Science & Engineering* 3, no. 4 (2015): 271-285. DOI: https://doi.org/10.1002/ese3.71

[38] Kusakana, Kanzumba. "Optimal scheduled power flow for distributed photovoltaic/wind/diesel generators with battery storage system." *IET Renewable Power Generation* 9, no. 8 (2015): 916-924. DOI: https://doi.org/10.1049/iet-rpg.2015.0027

[39] Bianchini, Alessandro, Niccolò Magnelli, Giovanni Ferrara, Ennio Antonio Carnevale, and Lorenzo Ferrari. "Optimization of a PV-wind-diesel hybrid system for a remote stand-alone application." *Energy Procedia* 81 (2015): 133-145. DOI: https://doi.org/10.1016/j.egypro.2015.12.068

[40] Spiru, Paraschiv, and Paraschiv Lizica-Simona. "Technical and economical analysis of a PV/wind/diesel hybrid power system for a remote area." *Energy Procedia* 147 (2018): 343-350. DOI: https://doi.org/10.1016/j.egypro.2018.07.102

[41] Maleki, Akbar, and Fathollah Pourfayaz. "Sizing of stand-alone photovoltaic/wind/diesel system with battery and fuel cell storage devices by harmony search algorithm." *Journal of Energy Storage* 2 (2015): 30-42. DOI: https://doi.org/10.1016/j.est.2015.05.006

[42] Diab, Fahd, Hai Lan, Lijun Zhang, and Salwa Ali. "An environmentally friendly factory in Egypt based on hybrid photovoltaic/wind/diesel/battery system." *Journal of Cleaner Production* 112 (2016): 3884-3894. DOI: https://doi.org/10.1016/j.jclepro.2015.07.008

[43] Shi, Bin, Wei Wu, and Liexiang Yan. "Size optimization of stand-alone PV/wind/diesel hybrid power generation systems." *Journal of the Taiwan Institute of Chemical Engineers* 73 (2017): 93-101. DOI: https://doi.org/10.1016/j.jtice.2016.07.047

[44] Dufo-López, Rodolfo, Iván R. Cristóbal-Monreal, and José M. Yusta. "Optimisation of PV-wind-diesel-battery stand-alone systems to minimise cost and maximise human development index and job creation." *Renewable Energy* 94 (2016): 280-293. DOI: https://doi.org/10.1016/j.renene.2016.03.065

[45] Mamaghani, Alireza Haghighat, Sebastian Alberto Avella Escandon, Behzad Najafi, Ali Shirazi, and Fabio Rinaldi. "Techno-economic feasibility of photovoltaic, wind, diesel and hybrid electrification systems for off-grid rural electrification in Colombia." *Renewable Energy* 97 (2016): 293-305. DOI: https://doi.org/10.1016/j.renene.2016.05.086

[46] Dufo-Lopez, Rodolfo, Ivan R. Cristobal-Monreal, and Jose M. Yusta. "Stochastic-heuristic methodology for the optimisation of components and control variables of PV-wind-diesel-battery stand-alone systems." *Renewable Energy* 99 (2016): 919-935. DOI: https://doi.org/10.1016/j.renene.2016.07.069

[47] Ramli, Makbul AM, H. R. E. H. Bouchekara, and Abdulsalam S. Alghamdi. "Optimal sizing of PV/wind/diesel hybrid microgrid system using multi-objective self-adaptive differential evolution algorithm." *Renewable energy* 121 (2018): 400-411. DOI: https://doi.org/10.1016/j.renene.2018.01.058

[48] Maatallah, Taher, Nahed Ghodhbane, and Sassi Ben Nasrallah. "Assessment viability for hybrid energy system (PV/wind/diesel) with storage in the northernmost city in Africa, Bizerte, Tunisia." *Renewable and Sustainable Energy Reviews* 59 (2016): 1639-1652. DOI: https://doi.org/10.1016/j.rser.2016.01.076

[49] Khan, Mohammad Junaid, Amit Kumar Yadav, and Lini Mathew. "Techno economic feasibility analysis of different combinations of PV-Wind-Diesel-Battery hybrid system for

telecommunication applications in different cities of Punjab, India." *Renewable and Sustainable Energy Reviews* 76 (2017): 577-607. DOI: https://doi.org/10.1016/j.rser.2017.03.076

[50] Hossain, Monowar, Saad Mekhilef, and Lanre Olatomiwa. "Performance evaluation of a stand-alone PV-wind-diesel-battery hybrid system feasible for a large resort center in South China Sea, Malaysia." *Sustainable cities and society* 28 (2017): 358-366. DOI: https://doi.org/10.1016/j.scs.2016.10.008

[51] Maleki, Akbar, and Alireza Askarzadeh. "Optimal sizing of a PV/wind/diesel system with battery storage for electrification to an off-grid remote region: A case study of Rafsanjan, Iran." *Sustainable Energy Technologies and Assessments* 7 (2014): 147-153. DOI: https://doi.org/10.1016/j.seta.2014.04.005

[52] Tazvinga, Henerica, Bing Zhu, and Xiaohua Xia. "Energy dispatch strategy for a photovoltaic–wind–diesel–battery hybrid power system." *Solar Energy* 108 (2014): 412-420. DOI: https://doi.org/10.1016/j.solener.2014.07.025

[53] Zhao, Jingyi, and Xiaofang Yuan. "Multi-objective optimization of stand-alone hybrid PV-wind-diesel-battery system using improved fruit fly optimization algorithm." *Soft Computing* 20, no. 7 (2016): 2841-2853. DOI: https://doi.org/10.1007/s00500-015-1685-6

[54] Kazem, Hussein A., Hamood AS Al-Badi, Ahmed S. Al Busaidi, and Miqdam T. Chaichan. "Optimum design and evaluation of hybrid solar/wind/diesel power system for Masirah Island." *Environment, Development and Sustainability* 19, no. 5 (2017): 1761-1778. DOI: https://doi.org/10.1007/s10668-016-9828-1

[55] Bouchebbat, Rochdi, and Sofiane Gherbi. "A novel optimal control and management strategy of stand-alone hybrid PV/wind/diesel power system." *Journal of Control, Automation and Electrical Systems* 28, no. 2 (2017): 284-296. DOI: https://doi.org/10.1007/s40313-016-0290-y

[56] Merabet, Adel, Khandker Tawfique Ahmed, Hussein Ibrahim, Rachid Beguenane, and Amer MYM Ghias. "Energy management and control system for laboratory scale microgrid based wind-PV-battery." *IEEE transactions on sustainable energy* 8, no. 1 (2016): 145-154. DOI: 10.1109/TSTE.2016.2587828

[57] Katsigiannis, Yiannis A., and Emmanuel S. Karapidakis. "Operation of wind-battery hybrid power stations in autonomous Greek islands." In *2017 52nd International Universities Power Engineering Conference (UPEC)*, pp. 1-5. IEEE, 2017. DOI: 10.1109/UPEC.2017.8231943

[58] Polinder H, Ferreira JA, Jensen BB, Abrahamsen AB, Atallah K, McMahon RA. Trends in wind turbine generator systems. IEEE Journal of emerging and selected topics in power electronics. 2013 Sep 5;1(3):174-85. DOI: 10.1109/JESTPE.2013.2280428

[59] Jureczko ME, Pawlak M, Mężyk A. Optimisation of wind turbine blades. Journal of materials processing technology. 2005 Aug 30;167(2-3):463-71. DOI: https://doi.org/10.1016/j.jmatprotec.2005.06.055

[60] Njiri JG, Söffker D. State-of-the-art in wind turbine control: Trends and challenges. Renewable and Sustainable Energy Reviews. 2016 Jul 1;60:377-93. DOI: https://doi.org/10.1016/j.rser.2016.01.110

[61] Hudedmani MG, Soppimath V, Jambotkar C. A study of materials for solar PV technology and challenges. European Journal of Applied Engineering and Scientific Research. 2017;5(1):1-3.

[62] Dhass AD, Kumar RS, Lakshmi P, Natarajan E, Arivarasan A. An investigation on performance analysis of different PV materials. Materials Today: Proceedings. 2020 Jan 1;22:330-4. DOI: https://doi.org/10.1016/j.matpr.2019.06.005

[63] Reddy VS, Kaushik SC, Ranjan KR, Tyagi SK. State-of-the-art of solar thermal power plants—A review. Renewable and Sustainable Energy Reviews. 2013 Nov 1;27:258-73. DOI: https://doi.org/10.1016/j.rser.2013.06.037

[64] Mondal M, Datta A. Energy transfer in hydrogen separation from syngas using pressure swing adsorption (PSA) process: A thermodynamic model. International Journal of Energy Research. 2017 Mar 10;41(3):448-58. DOI: https://doi.org/10.1002/er.3627

[65] Kougias PG, Angelidaki I. Biogas and its opportunities—A review. Frontiers of Environmental Science & Engineering. 2018 Jun;12:1-2. DOI: 10.1007/s11783-018-1037-8

[66] Encyclopedia Britannica. https://www.britannica.com/science/geothermal-energy [as on May 17, 2024]

[67] Moya D, Aldás C, Kaparaju P. Geothermal energy: Power plant technology and direct heat applications. Renewable and Sustainable Energy Reviews. 2018 Oct 1;94:889-901. DOI: https://doi.org/10.1016/j.rser.2018.06.047

[68] Chowdhury MS, Rahman KS, Selvanathan V, Nuthammachot N, Suklueng M, Mostafaeipour A, Habib A, Akhtaruzzaman M, Amin N, Techato K. Current trends and prospects of tidal energy technology. Environment, development and sustainability. 2021 Jun;23:8179-94. DOI: 10.1007/s10668-020-01013-4

[69] Johnstone CM, Pratt D, Clarke JA, Grant AD. A techno-economic analysis of tidal energy technology. Renewable Energy. 2013 Jan 1;49:101-6. DOI https://doi.org/10.1016/j.renene.2012.01.054

[70] Baker JN, Collinson A. Electrical energy storage at the turn of the millennium. Power Engineering Journal. 1999 Jun 1;13(3):107-12. DOI: 10.1049/pe:19990301

[71] Chen H, Cong TN, Yang W, Tan C, Li Y, Ding Y. Progress in electrical energy storage system: A critical review. Progress in natural science. 2009 Mar 10;19(3):291-312. DOI: https://doi.org/10.1016/j.pnsc.2008.07.014

[72] Dhundhara S, Verma YP, Williams A. Techno-economic analysis of the lithium-ion and lead-acid battery in microgrid systems. Energy conversion and management. 2018 Dec 1;177:122-42. DOI: https://doi.org/10.1016/j.enconman.2018.09.030

[73] Zhang X, Li Y, Skyllas-Kazacos M, Bao J. Optimal sizing of vanadium redox flow battery systems for residential applications based on battery electrochemical characteristics. Energies. 2016 Oct 22;9(10):857. DOI: https://doi.org/10.3390/en9100857

[74] Li X, Zhang H, Mai Z, Zhang H, Vankelecom I. Ion exchange membranes for vanadium redox flow battery (VRB) applications. Energy & Environmental Science. 2011;4(4):1147-60. DOI: https://doi.org/10.1039/C0EE00770F

[75] Wang H, Sheng L, Yasin G, Wang L, Xu H, He X. Reviewing the current status and development of polymer electrolytes for solid-state lithium batteries. Energy Storage Materials. 2020 Dec 1;33:188-215. DOI: https://doi.org/10.1016/j.ensm.2020.08.014

[76] Gravitricity [Online]. Available: https://www.gravitricity.com/ [as on April 28, 2022].

[77] Gravitypower, 2011. Gravity Power Module. Energy Storage. Grid-scale Energy Storage. Available at: http://www.gravitypower.net/. [as on December 23, 2021]

[78] Ibrahim H, Ilinca A, Perron J. Energy storage systems—Characteristics and comparisons. Renewable and sustainable energy reviews. 2008 Jun 1;12(5):1221-50. DOI: https://doi.org/10.1016/j.rser.2007.01.023

[79] Gupta, Ajai, R. P. Saini, and M. P. Sharma. "Steady-state modelling of hybrid energy system for off grid electrification of cluster of villages." Renewable Energy 35.2 (2010): 520-535. DOI : https://doi.org/10.1016/j.renene.2009.06.014

[80] Bahramara S, Moghaddam MP, Haghifam MR. Optimal planning of hybrid renewable energy systems using HOMER: A review. Renewable and Sustainable Energy Reviews. 2016 Sep 1;62:609-20. DOI: https://doi.org/10.1016/j.rser.2016.05.039

[81] Khan EU, Martin AR. Optimization of hybrid renewable energy polygeneration system with membrane distillation for rural households in Bangladesh. Energy. 2015 Dec 15;93:1116-27. DOI: https://doi.org/10.1016/j.energy.2015.09.109

[82] Reddy SS. Optimization of renewable energy resources in hybrid energy systems. Journal of Green Engineering. 2017 Jan 31;7(1):43-60. DOI: https://doi.org/10.13052/jge1904-4720.7123

[83] Momoh JA, Reddy SS. Review of optimization techniques for renewable energy resources. In2014 IEEE Symposium on Power Electronics and Machines for Wind and Water Applications 2014 Jul 24 (pp. 1-8). IEEE. DOI: 10.1109/PEMWA.2014.6912225

[84] Reddy SS. Optimal power flow with renewable energy resources including storage. Electrical Engineering. 2017 Jun 1;99(2):685-95. DOI: 10.1007/s00202-016-0402-5

[85] Reddy SS, Momoh JA. Realistic and transparent optimum scheduling strategy for hybrid power system. IEEE Transactions on Smart Grid. 2015 Mar 11;6(6):3114-25. DOI: 10.1109/TSG.2015.2406879

[86] Ahmad S, Alhaisoni MM, Naeem M, Ahmad A, Altaf M. Joint energy management and energy trading in residential microgrid system. IEEE Access. 2020 Jul 6;8:123334-46. DOI: 10.1109/ACCESS.2020.3007154

[87] Ahmad S, Naeem M, Ahmad A. Unified optimization model for energy management in sustainable smart power systems. International Transactions on Electrical Energy Systems. 2020 Apr;30(4):e12144. DOI: 10.1002/2050-7038.12144

[88] Ahmad H, Ahmad A, Ahmad S. Efficient energy management in a microgrid. In2018 International Conference on Power Generation Systems and Renewable Energy Technologies (PGSRET) 2018 Sep 10 (pp. 1-5). IEEE. DOI: 10.1109/PGSRET.2018.8685946

[89] Ahmad S, Naeem M, Ahmad A. Low complexity approach for energy management in residential buildings. International Transactions on Electrical Energy Systems. 2019 Jan;29(1):e2680. DOI: 10.1002/etep.2680

[90] Chen L, Chen H, Li Y, Li G, Yang J, Liu X, Xu Y, Ren L, Tang Y. SMES-battery energy storage system for the stabilization of a photovoltaic-based microgrid. IEEE Transactions on Applied Superconductivity. 2018 Jan 30;28(4):1-7. DOI: 10.1109/TASC.2018.2799544

[91] Ramli MA, Hiendro A, Twaha S. Economic analysis of PV/diesel hybrid system with flywheel energy storage. Renewable Energy. 2015 Jun 1;78:398-405. DOI: https://doi.org/10.1016/j.renene.2015.01.026

[92] Bogno B, Sawicki JP, Salame T, Aillerie M, Saint-Eve F, Hamandjoda O, Tibi B. Improvement of safety, longevity and performance of lead acid battery in off-grid PV systems. International Journal of Hydrogen Energy. 2017 Feb 2;42(5):3466-78. DOI: https://doi.org/10.1016/j.ijhydene.2016.12.011

[93] Ghorbanzadeh M, Astaneh M, Golzar F. Long-term degradation based analysis for lithium-ion batteries in off-grid wind-battery renewable energy systems. Energy. 2019 Jan 1;166:1194-206. DOI: https://doi.org/10.1016/j.energy.2018.10.120

[94] Bhattacharjee A, Saha H. Design and experimental validation of a generalised electrical equivalent model of Vanadium Redox Flow Battery for interfacing with renewable energy sources. Journal of Energy Storage. 2017 Oct 1;13:220-32. DOI: https://doi.org/10.1016/j.est.2017.07.016

[95] Ma T, Yang H, Lu L, Peng J. Technical feasibility study on a standalone hybrid solar-wind system with pumped hydro storage for a remote island in Hong Kong. Renewable energy. 2014 Sep 1;69:7-15. DOI: https://doi.org/10.1016/j.renene.2014.03.028

[96] Gravitricity: Gravity energy storage. DOI: https://www.gravitricity.com/#fast-long-life-energy-storage [as on March 04, 2020]

[97] Morstyn T, Chilcott M, McCulloch MD. Gravity energy storage with suspended weights for abandoned mine shafts. Applied Energy. 2019 Apr 1;239:201-6. DOI: https://doi.org/10.1016/j.apenergy.2019.01.226

[98] Sivakumar N, Das D, Padhy NP, Kumar AS, Bisoyi N. Status of pumped hydro-storage schemes and its future in India. Renewable and Sustainable Energy Reviews. 2013 Mar 1;19:208-13. DOI: https://doi.org/10.1016/j.rser.2012.11.001

[99] Deane JP, Gallachóir BÓ, McKeogh EJ. Techno-economic review of existing and new pumped hydro energy storage plant. Renewable and Sustainable Energy Reviews. 2010 May 1;14(4):1293-302. DOI: https://doi.org/10.1016/j.rser.2009.11.015

[100] Office of Energy Efficiency & Renewable Energy. Government of United States of America. https://www.energy.gov/eere/water/pumped-storage-hydropower [as on 05 August, 2020]

[101] Ma T, Yang H, Lu L. Feasibility study and economic analysis of pumped hydro storage and battery storage for a renewable energy powered island. Energy Conversion and Management. 2014 Mar 1; 79:387-97. DOI: https://doi.org/10.1016/j.enconman.2013.12.047

[102] Ma T, Yang H, Lu L, Peng J. Technical feasibility study on a standalone hybrid solar-wind system with pumped hydro storage for a remote island in Hong Kong. Renewable energy. 2014 Sep 1; 69:7-15. DOI: https://doi.org/10.1016/j.renene.2014.03.028

[103] Xu X, Hu W, Cao D, Huang Q, Chen C, Chen Z. Optimized sizing of a standalone PV-wind-hydropower station with pumped-storage installation hybrid energy system. Renewable Energy. 2020 Mar 1;147:1418-31. DOI: https://doi.org/10.1016/j.renene.2019.09.099

[104] Abdelshafy AM, Jurasz J, Hassan H, Mohamed AM. Optimized energy management strategy for grid connected double storage (pumped storage-battery) system powered by renewable energy resources. Energy. 2020 Feb 1;192:116615. DOI: https://doi.org/10.1016/j.energy.2019.116615

[105] Pali, Bahadur Singh, and Shelly Vadhera. "A novel pumped hydro-energy storage scheme with wind energy for power generation at constant voltage in rural areas." *Renewable energy* 127 (2018): 802-810. DOI: https://doi.org/10.1016/j.renene.2018.05.028

[106] Pali, Bahadur Singh, and Shelly Vadhera. "An innovative continuous power generation system comprising of wind energy along with pumped-hydro storage and open well." *IEEE Transactions on Sustainable Energy* 11, no. 1 (2018): 145-153. DOI: 10.1109/TSTE.2018.2886705

[107] Chandel SS, Naik MN, Chandel R. Review of solar photovoltaic water pumping system technology for irrigation and community drinking water supplies. Renewable and Sustainable Energy Reviews. 2015 Sep 1;49:1084-99. DOI: https://doi.org/10.1016/j.rser.2015.04.083

[108] Pali BS, Vadhera S. A novel solar photovoltaic system with pumped-water storage for continuous power at constant voltage. Energy conversion and management. 2019 Feb 1;181:133-42. DOI: https://doi.org/10.1016/j.enconman.2018.12.004

[109] Pali, Bahadur Singh, and Shelly Vadhera. "Uninterrupted sustainable power generation at constant voltage using solar photovoltaic with pumped storage." *Sustainable Energy Technologies and Assessments* 42 (2020): 100890. DOI: https://doi.org/10.1016/j.seta.2020.100890

[110] Khazali AH, Kalantar M. Optimal reactive power dispatch based on harmony search algorithm. International Journal of Electrical Power & Energy Systems. 2011 Mar 1;33(3):684-92. DOI: https://doi.org/10.1016/j.ijepes.2010.11.018

[111] Sulaiman MH, Mustaffa Z, Mohamed MR, Aliman O. Using the gray wolf optimizer for solving optimal reactive power dispatch problem. Applied Soft Computing. 2015 Jul 1;32:286-92. DOI: https://doi.org/10.1016/j.asoc.2015.03.041

[112] Khorsandi A, Alimardani A, Vahidi B, Hosseinian SH. Hybrid shuffled frog leaping algorithm and Nelder–Mead simplex search for optimal reactive power dispatch. IET generation, transmission & distribution. 2011 Feb 1;5(2):249-56. DOI: 10.1049/iet-gtd.2010.0256

[113] Shaw B, Mukherjee V, Ghoshal SP. Solution of reactive power dispatch of power systems by an opposition-based gravitational search algorithm. International Journal of Electrical Power & Energy Systems. 2014 Feb 1;55: 29-40. DOI: https://doi.org/10.1016/j.ijepes.2013.08.010

[114] Singh S, Kaushik SC. Optimal sizing of grid integrated hybrid PV-biomass energy system using artificial bee colony algorithm. IET Renewable Power Generation. 2016 May 1;10(5):642-50. DOI: 10.1049/iet-rpg.2015.0298

[115] Mirjalili S, Lewis A. The whale optimization algorithm. Advances in engineering software. 2016 May 1;95:51-67. DOI: https://doi.org/10.1016/j.advengsoft.2016.01.008

[116] Emrani A, Berrada A, Bakhouya M. Optimal sizing and deployment of gravity energy storage system in hybrid PV-Wind power plant. Renewable Energy. 2022 Jan 1;183:12-27. DOI: https://doi.org/10.1016/j.renene.2021.10.072

[117] Ameur A, Berrada A, Emrani A. Dynamic forecasting model of a hybrid photovoltaic/gravity energy storage system for residential applications. Energy and Buildings. 2022 Sep 15;271:112325. DOI: https://doi.org/10.1016/j.enbuild.2022.112325

[118] Mondal M, Mandal KK, Datta A. Solar PV driven hybrid gravity power module—Vanadium redox flow battery energy storage for an energy efficient multi-storied building. International Journal of Energy Research. 2022 Oct 25;46(13):18477-94. DOI: https://doi.org/10.1002/er.8460

[119] Tong W, Lu Z, Zhao H, Han M, Zhao G, Hunt JD. The structure and control strategies of hybrid solid gravity energy storage system. Journal of Energy Storage. 2023 Sep 1;67:107570. DOI: https://doi.org/10.1016/j.est.2023.107570

[120] Merei G, Berger C, Sauer DU. Optimization of an off-grid hybrid PV–Wind–Diesel system with different battery technologies using genetic algorithm. Solar Energy. 2013 Nov 1;97:460-73. DOI: https://doi.org/10.1016/j.solener.2013.08.016

[121] Khatib T, Ibrahim IA, Mohamed A. A review on sizing methodologies of photovoltaic array and storage battery in a standalone photovoltaic system. Energy Conversion and Management. 2016 Jul 15; 120:430-48. DOI : https://doi.org/10.1016/j.enconman.2016.05.011

[122] Hosseina M, Bathaee SM. Optimal scheduling for distribution network with redox flow battery storage. Energy conversion and management. 2016 Aug 1. DOI: https://doi.org/10.1016/j.enconman.2016.05.001

[123] Dhar P, Chakraborty N. A dual mode wind turbine operation with hybrid energy storage system for electricity generation at constant voltage in an islanded microgrid. International Journal of Energy Research. 2021 Oct 25;45(13):18885-902. DOI: https://doi.org/10.1002/er.6994

[124] DLLD Power. https://dlldpower.com/gd30kw-9m/ [as on February 03, 2019]

[125] https://en.wind-turbine-models.com/turbines/2593-ryse-energy-e-5-hawt [as on February 05, 2019]

[126] AT&C loss for the state of Nagaland. Government of Nagaland. DOI: https://www.uday.gov.in/MOU/MoU_Nagaland.pdf [as on April 10, 2020]

[127] Phek District. Government of Nagaland. DOI: https://phek.nic.in/document-category/census/ [as on April 10, 2020]

[128] Census of India 2011, Nagaland. DOI: https://cdn.s3waas.gov.in/s3109a0ca3bc27f3e96597370d5c8cf03d/uploads/2019/01/2019010281.pdf [as on April 15, 2020]

[129] Riffonneau Y, Bacha S, Barruel F, Ploix S. Optimal power flow management for grid connected PV systems with batteries. IEEE Transactions on sustainable energy. 2011 Feb 17;2(3):309-20. DOI: 10.1109/TSTE.2011.2114901.

[130] Biomass Portal, Ministry of New and Renewable Energy. https://biomasspower.gov.in/nagaland.php [as on April 09, 2020]

[131] Photovoltaic Geographical Information System, European Commission. DOI: https://re.jrc.ec.europa.eu/pvg_tools/en/tools.html#MR [as on April 10, 2020]

[132] Kenbrook Solar Private Limited (CIN : U74994HR2018PTC077516, Data available in Ministry of Corporate affairs Govt. of India), DOI: https://kenbrooksolar.com/system/50kw-solar-system-price [as on May 05, 2020]

[133] Thomas J, Ashok S, Jose TL. A pricing model for biomass-based electricity. Energy Sources, Part B: Economics, Planning, and Policy. 2015 Jan 2;10(1):103-10. DOI: https://doi.org/10.1080/15567249.2010.511513

[134] VDA wef. 1 Oct 2019, Chief Labour Commissioner (Central). DOI: https://clc.gov.in/clc/node/614 [as on December 20, 2020]

[135] Area Prices, Indian Energy Exchange. DOI: https://www.iexindia.com/marketdata/areaprice.aspx [as on December 20, 2020]

[136] Aeolos 10kW Wind Turbine : https://www.windturbinestar.com/10kwh-aeolos-wind-turbine.html [as on June 07, 2020]

[137] Suneco 3kW Hydro Turbine : https://www.micro-hydro-power.com/Micro-Hydro-Power-Single-Nozzle-XJ25-3.0DCT4-Z.htm [as on June 07, 2020]

[138] Choi J, Park WK, Lee IW. Application of vanadium redox flow battery to grid connected microgrid energy management. In 2016 IEEE International Conference on Renewable Energy Research and Applications (ICRERA) 2016 Nov 20 (pp. 903-906). IEEE. DOI:10.1109/ICRERA.2016.7884466

[139] Lei J, Gong Q. Operating strategy and optimal allocation of large-scale VRB energy storage system in active distribution networks for solar/wind power applications. IET Generation, Transmission & Distribution. 2017 Apr 25;11(9):2403-11. DOI: 0.1049/iet-gtd.2016.2076

[140] Ali US. Impedance source converter for photovoltaic stand-alone system with vanadium redox flow battery storage. Materials Today: Proceedings. 2018 Jan 1;5(1):241-7. DOI: https://doi.org/10.1016/j.matpr.2017.11.078

[141] Martínez M, Molina MG, Mercado PE. Optimal sizing method of vanadium redox flow battery to provide load frequency control in power systems with intermittent renewable generation. IET Renewable Power Generation. 2017 Sep 12;11(14):1804-11. DOI: 10.1049/iet-rpg.2016.0798

[142] Arani AK, Karami H, Gharehpetian GB, Hejazi MS. Review of Flywheel Energy Storage Systems structures and applications in power systems and microgrids. Renewable and Sustainable Energy Reviews. 2017 Mar 1;69:9-18. DOI: https://doi.org/10.1016/j.rser.2016.11.166

[143] Rathore A, Patidar NP. Reliability assessment using probabilistic modelling of pumped storage hydro plant with PV-Wind based standalone microgrid. International Journal of Electrical Power & Energy Systems. 2019 Mar 1;106:17-32. DOI: https://doi.org/10.1016/j.ijepes.2018.09.030

[144] Mousavi N, Kothapalli G, Habibi D, Das CK, Baniasadi A. A novel photovoltaic-pumped hydro storage microgrid applicable to rural areas. Applied Energy. 2020 Mar 15;262:114284. DOI: https://doi.org/10.1016/j.apenergy.2019.114284

[145] Vulusala G VS, Madichetty S. Application of superconducting magnetic energy storage in electrical power and energy systems: a review. International Journal of Energy Research. 2018 Feb;42(2):358-68. DOI: https://doi.org/10.1002/er.3773

[146] Inthamoussou FA, Pegueroles-Queralt J, Bianchi FD. Control of a supercapacitor energy storage system for microgrid applications. IEEE transactions on energy conversion. 2013 May 20;28(3):690-7. DOI: 10.1109/TEC.2013.2260752

[147] Nguyen TA, Crow ML, Elmore AC. Optimal sizing of a vanadium redox battery system for microgrid systems. IEEE transactions on sustainable energy. 2015 Apr 3;6(3):729-37. DOI: 10.1109/TSTE.2015.2404780

[148] Pradhan SK, Chakraborty B. Substrate materials and novel designs for bipolar lead-acid batteries: A review. Journal of Energy Storage. 2020 Dec 1;32:101764. DOI: https://doi.org/10.1016/j.est.2020.101764

[149] Kitagawa Y, Lin L, Fukui M. An analysis for cooling Li-ion battery modules. In2014 IEEE Fourth International Conference on Consumer Electronics Berlin (ICCE-Berlin) 2014 Sep 7 (pp. 233-237). IEEE. DOI: 10.1109/ICCE-Berlin.2014.7034313

[150] Baronti F, Zamboni W, Femia N, Rahimi-Eichi H, Roncella R, Rosi S, Saletti R, Chow MY. Parameter identification of Li-Po batteries in electric vehicles: A comparative study. In2013 IEEE International Symposium on Industrial Electronics 2013 May 28 (pp. 1-7). IEEE. DOI: 10.1109/ISIE.2013.6563887

[151] Yilanci A, Dincer I, Ozturk HK. A review on solar-hydrogen/fuel cell hybrid energy systems for stationary applications. Progress in energy and combustion science. 2009 Jun 1;35(3):231-44. DOI: https://doi.org/10.1016/j.pecs.2008.07.004

[152] Dincer I, Dost S, Li X. Performance analyses of sensible heat storage systems for thermal applications. International Journal of Energy Research. 1997 Oct 10;21(12):1157-71. DOI: https://doi.org/10.1002/(SICI)1099-114X(19971010)21:12<1157::AID-ER317>3.0.CO;2-N

[153] Elouali A, Kousksou T, El Rhafiki T, Hamdaoui S, Mahdaoui M, Allouhi A, Zeraouli Y. Physical models for packed bed: Sensible heat storage systems. Journal of Energy Storage. 2019 Jun 1;23:69-78. DOI: https://doi.org/10.1016/j.est.2019.03.004

[154] Korti AI, Tlemsani FZ. Experimental investigation of latent heat storage in a coil in PCM storage unit. Journal of Energy Storage. 2016 Feb 1;5:177-86. DOI: https://doi.org/10.1016/j.est.2015.12.010

[155] Aly KA, El-Lathy AR, Fouad MA. Enhancement of solidification rate of latent heat thermal energy storage using corrugated fins. Journal of Energy Storage. 2019 Aug 1;24:100785. DOI: https://doi.org/10.1016/j.est.2019.100785

[156] Bimbhra, Dr PS. Generalized theory of electrical machines. Khanna Publishers, 1996.

[157] Gharehchopogh FS, Gholizadeh H. A comprehensive survey: Whale Optimization Algorithm and its applications. Swarm and Evolutionary Computation. 2019 Aug 1;48:1-24. DOI: https://doi.org/10.1016/j.swevo.2019.03.004

[158] Rana N, Latiff MS, Abdulhamid SI, Chiroma H. Whale optimization algorithm: a systematic review of contemporary applications, modifications and developments. Neural Computing and Applications. 2020 Oct;32:16245-77. DOI: https://doi.org/10.1007/s00521-020-04849-z

[159] Nalcaci G, Ermis M. Selective harmonic elimination for three-phase voltage source inverters using whale optimizer algorithm. In2018 5th International Conference on Electrical and Electronic Engineering (ICEEE) 2018 May 3 (pp. 1-6). IEEE. DOI: 10.1109/ICEEE2.2018.8391290

[160] Mohamed F, Abdel-Nasser M, Mahmoud K, Kamel S. Economic dispatch using stochastic whale optimization algorithm. In2018 International Conference on Innovative Trends in Computer Engineering (ITCE) 2018 Feb 19 (pp. 19-24). IEEE. DOI: 10.1109/ITCE.2018.8316594

[161] Mahdad B. Improvement optimal power flow solution under loading margin stability using new partitioning whale algorithm. International Journal of Management Science and Engineering Management. 2019 Jan 2;14(1):64-77. DOI: https://doi.org/10.1080/17509653.2018.1488225

[162] Kumar A, Bhalla V, Kumar P, Bhardwaj T, Jangir N. Whale optimization algorithm for constrained economic load dispatch problems—a cost optimization. InAmbient Communications and Computer Systems: RACCCS 2017 2018 (pp. 353-366). Springer Singapore. DOI: https://doi.org/10.1007/978-981-10-7386-1_31

[163] Das S, Bhattacharya A, Chakraborty AK, Pandey V. Fixed head short-term hydrothermal scheduling using whale optimization algorithm considering the uncertainty of solar power. In2017 Ninth International Conference on Advanced Computing (ICoAC) 2017 Dec 14 (pp. 179-185). IEEE. DOI: 10.1109/ICoAC.2017.8441177

[164] Rosyadi A, Penangsang O, Soeprijanto A. Optimal filter placement and sizing in radial distribution system using whale optimization algorithm. In2017 international seminar on intelligent technology and its applications (ISITIA) 2017 Aug 28 (pp. 87-92). IEEE. DOI: 10.1109/ISITIA.2017.8124060

[165] Marimuthu A, Gnanambal K, Priyanka R. Optimal allocation and sizing of DG in a radial distribution system using whale optimization algorithm. In2017 International Conference on Innovations in Green Energy and Healthcare Technologies (IGEHT) 2017 Mar 16 (pp. 1-5). IEEE. DOI: 10.1109/IGEHT.2017.8093979

[166] Neagu BC, Ivanov O, Gavrilaş M. Voltage profile improvement in distribution networks using the whale optimization algorithm. In2017 9th International Conference on Electronics, Computers and Artificial Intelligence (ECAI) 2017 Jun 29 (pp. 1-6). IEEE. DOI: 10.1109/ECAI.2017.8166465

[167] Prakash DB, Lakshminarayana C. Optimal siting of capacitors in radial distribution network using whale optimization algorithm. Alexandria Engineering Journal. 2017 Dec 1;56(4):499-509. DOI: https://doi.org/10.1016/j.aej.2016.10.002

[168] Sahu PR, Hota PK, Panda S. Power system stability enhancement by fractional order multi input SSSC based controller employing whale optimization algorithm. Journal of Electrical Systems and Information Technology. 2018 Dec 1;5(3):326-36. DOI: https://doi.org/10.1016/j.jesit.2018.02.008

[169] Touma HJ. Study of the economic dispatch problem on IEEE 30-bus system using whale optimization algorithm. International Journal of Engineering Technology and Sciences. 2016 Jun 30;3(1):11-8. DOI: https://doi.org/10.15282/ijets.5.2016.1.2.1041

[170] Ben oualid Medani K, Sayah S, Bekrar A. Whale optimization algorithm based optimal reactive power dispatch: A case study of the Algerian power system. Electric Power Systems Research. 2018 Oct 1;163:696-705. DOI: https://doi.org/10.1016/j.epsr.2017.09.001

[171] Goldbogen JA, Friedlaender AS, Calambokidis J, Mckenna MF, Simon M, Nowacek DP. Integrative approaches to the study of baleen whale diving behavior, feeding performance, and foraging ecology. BioScience. 2013 Feb 1;63(2):90-100. DOI: https://doi.org/10.1525/bio.2013.63.2.5

[172] Growth in Electricity Generation Vis-A-Vis Demand, Ministry of Power. DOI: https://powermin.nic.in/sites/default/files/uploads/RS31072017_Eng.pdf [as on April 24, 2020]

[173] Electricity Tariff, Department of Power Nagaland. DOI: https://www.dopn.gov.in/irj/go/km/docs/internet/NAGALAND/Pages/Tariff.html [as on April 26, 2020]

[174] Aeolos-H 3000 W wind turbine specification. Website: https://www.windturbinestar.com/3kwh-aeolos-wind-turbine.html [as on July 11, 2020]

[173] 5KW Wind Turbine Price. Website: https://www.indiamart.com/proddetail/windistar-5000-5kw-wind-turbine-25532425533.html?srsltid=AfmBOork_J0E-sBcHSW-jsQjHelSvpb8kG0FDr3ULpIAHbpw9HGzufD8 [as on July 15, 2025]

[174] Franklin, Miles, Peter Fraenkel, Chris Yendell, and Ruth Apps. "Gravity energy storage systems." In *Storing Energy*, pp. 91-116. Elsevier, 2022. DOI: https://doi.org/10.1016/B978-0-12-824510-1.00023-4

[175] Gravitricity Gravity-based Energy Storage Demonstrator, NS Energy. Website: https://www.nsenergybusiness.com/projects/gravitricity-gravity-based-energy-storage-demonstrator/#:~:text=Gravitricity%20is%20piloting%20a%20250kW,%C2%A31m%20($1.25m). [as on September 22, 2020]

[176] Balance of Solar PV Systems (BOS). Greentech Renewables. Website: https://www.greentechrenewables.com/article/balance-solar-pv-systems-bos?utm_source=chatgpt.com [as on July 15, 2025]